TARGETING BRAF AND NF1 MUTATIONS IN GLIOMA

A Dissertation

Presented to the Faculty of the Weill Cornell Graduate School

of Medical Sciences

in Partial Fulfillment of the Requirements for the Degree of

Doctor of Philosophy

By

Michael Chad Kaufmann

May 2016

TARGETING BRAF AND NF1 MUTATIONS IN GLIOMA

Michael Chad Kaufmann, Ph.D.

Cornell University 2016

Gliomas are responsible for a disproportionate share of cancer-related morbidity and mortality, despite being less common than other cancers, so treatments for glioma patients are a serious unmet need. About 3% of gliomas harbor either constitutively activating point mutations or fusions in the gene BRAF which activate the BRAF-MEK-ERK pathway. Because there are specific inhibitors for this pathway available, in this work we interrogated the underling biology of the sensitivity of BRAF-mutant gliomas to these inhibitors. We identified cell lines with BRAF mutations and showed that BRAF-V600E gliomas are dependent on BRAF signaling and MEK kinase activity for tumor maintenance. Next we showed that the monomeric BRAF inhibitor vemurafenib is able to inhibit mutant-BRAF signaling in glioma, However, this inhibition is transient, and ERK phosphorylation quickly rebounds. This ERK rebound is associated with incomplete inhibition of Cyclin D1 and lack of growth suppression. We then sought to identify possible candidate RTKs that were upregulated by relief of ERK-dependent feedback and might reactivate ERK signaling. We found that ERBB family members and their activity were upregulated. However, we also found that EGFR and HER2 kinase activity does not appear to be necessary in order to induce ERK rebound. We then looked into the role of negative feedback on RAS signaling and showed that vemurafenib relieves negative feedback on RAS signaling, leading to increases in RAS-GTP and the induction of a vemurafenib insensitive state. However,

drugs that target the RAF dimers that are a product of increased RAS-GTP are able potently suppress ERK rebound, Cyclin D1 expression, and achieve greater growth suppression. Finally, we tried to understand the role of the RAS-GAP NF1 in GBM. We established and biochemically validated an inducible NF1 expression system and examined its biological role. Interestingly, NF1 expression is not growth suppressive in all NF1-deficient cell lines. Despite this, NF1-deficient cell lines appear to maintain a MEK dependency that can be therapeutically targeted with a MEK inhibitor, even though NF1 reconstitution has little direct effect on MEK and ERK signaling. Together, this works describes alterations at two different nodes of the MAP-Kinase pathway and their therapeutic relevance.

BIOGRAPHICAL SKETCH

Michael Chad Kaufmann was born early in his life in Arkansas City, KS to his parents Leo and Stacia. The oldest of three children, including Kristin and Stephanie, he spent most of his formative years in Houston, TX, with brief bouts in Ponca City, OK, and Denver, CO. Michael showed an early interest in science, eschewing Saturday morning cartoons for the Weather Channel, much to his sisters' annoyance. After falling love with molecular biology in his AP Biology class in high school, he decided to pursue his Bachelors in Biochemistry and Molecular Biology at Boston University. Three years later, touched by the loss of his grandfather to Lou Gehrig's Disease, he entered his first job at The ALS Therapy Development Institute in Cambridge, MA where he devoted his time and research to uncovering and developing treatments for ALS. He then worked at the Belfer Institute of Applied Cancer Science at the Dana-Farber Cancer Institute in Boston, MA where he worked to identify therapeutic targets and early drug candidates for cancer. This exposure to the world of drug development inspired him to pursue his Ph.D. in pharmacology at the Weill Cornell Graduate School of Medical Sciences under the supervision of his mentor Dr. Ingo Mellinghoff at the Sloan Kettering Institute. There he performed his doctoral research on inhibitors of signal transduction in glioma. Michael is the proud caretaker of his (almost too large) dog Charlie and his cat Bip in his (definitely too small) NYC apartment. In his free time, he enjoys ordering take out when he should be cooking, gaming when he should be cycling around Central Park, and drinking wine while debating politics with his friends on weeknights when he should be better at adulting.

With so much love to my parents,

who told me to "shoot for the moon"

all while knowing I might land far away.

ACKNOWLEDGMENTS

I first want to thank my thesis mentor Dr. Ingo Mellinghoff. Dr. Mellinghoff taught me how to think critically about my work both in and outside of the lab, and his questions, guidance, and support throughout my time here have helped me grow into the scientist I am today. Dr. Mellinghoff strives to do so much good for the world through his work in science and medicine, and to have been part of that is an honor. I know that the time I spent with him will be evident throughout all of my future professional endeavors.

I also want to thank the other faculty at Sloan Kettering who have offered their expert advice and support. My thesis work would not have been possible without Dr. Neal Rosen, who practically wrote the textbook on BRAF, as well as Dr. Yueming Li, who served on both my thesis committee and as my Pharmacology Program Director. Finally, I also want to thank Dr. Diane Felsen, whom I rotated with when I was yet a baby grad student, for her advice then as well as for serving on my examining committee now, along with Dr. Sarat Chandarlapaty.

Also important to me have been the lab members, both past and present, who I've worked with. Dr. Owen Clark, Dr. Paolo Codega, Dr. Christian Grommes, Wan-Ying Hsieh (thank you for not graduating before me), Dr. Donna Nichol, Dr. Dan Rohle, Dr. Milan Chheda, Dr. Barbara Oldrini, and Dr. Igor Vivanco have all offered invaluable scientific advice and entertaining lunchtime ruminations, which I am both grateful for and will sorely miss. Special thanks go to our lab manager and technician Carl Campos, who keeps our lab running in tip-top shape, as well as to Mike Chen and Derek Schartz for their help. I also want to thank our collaborator, Dr. Zhan Yao, for his advice and guidance in my project. More special thanks goes to our lab administrator Bridget King. Without her, I would still probably be trying to schedule my defense.

Finally, I want to thank all of my family, friends, fellow grad students, and loved ones past and present. This has not been an easy road, but your support throughout my Ph.D.—be it with conversation, cocktails, or Charlie walks—have made it possible, and for that I am eternally grateful.

I also want to acknowledge the generations of gay scientists who came before me. The world they faced was a much different place, but they blazed a trail through their own tribulations, both scientific and personal, so that I can proudly be who and where I am today.

TABLE OF CONTENTS

LIST OF FIGURES

CHAPTER 1: INTRODUCTION

PART 1 – Cancer and glioma

Cancer is a collective term for a group of related diseases that, on a simplified level, are commonly defined by uncontrolled cellular proliferation. Hanahan and Weinberg defined "hallmarks of cancer" that cells collect as they progress from a normal, non-neoplastic state to become tumorigenic and cancerous (Hanahan and Weinberg 2011). The six primary hallmarks are:

1. sustained proliferative signaling;
2. the evasion of growth suppressive signaling;
3. activating invasive and metastatic programs;
4. circumventing normal programs of senescence to achieve replicative immortality;
5. inducing angiogenesis, the formation of blood vessels to feed tumors;
6. and resisting cell death.

Though benign tumors can arise in nearly any tissue type of the body and can possess many of these traits, a growth must achieve all of these hallmarks to progress to a frank cancer.

Tumors of the central nervous system, collectively known as "malignant gliomas," are a heterogeneous mix of tumors that occur within the tissues of the brain or spinal cord. Despite being relatively uncommon, totaling approximately 22,500 cases worldwide, they are a disproportionate cause of cancer-related morbidity and mortality (Wen and Kesari 2008). The majority of gliomas (estimated to be about 60 to 70%) are glioblastomas, with the remainder split between anaplastic astrocytomas (about 10

to 15%), and anaplastic oligodendrogliomas and anaplastic oligoastrocytomas (also about 10%-15%). While almost all gliomas fall into these categories, there are still many other rare types of gliomas that still occur with some frequency.

Since the 1950s, neurologists have worked to devise a universal classification system for tumors of the central nervous system (Ringertz 1950). The World Health Organization's (WHO) classification system was first codified in 1980 (Zülch 1980) and last updated in 2007 (Louis et al. 2007). According to the WHO classification system, tumors are classified based on their anatomical location within the CNS and according to their histopathological features. From there, tumors are assigned to one of four grades, from Grade I (low proliferative potential, not malignant) to grade IV (highly proliferative and invasive, most malignant).

Grade I and II tumors are known as low-grade glioma, while grade III and IV tumor are known as high-grade gliomas (Louis et al. 2007). Low grade gliomas are very diverse. Some, like pilocytic astrocytoma (discussed below) are highly circumscribed and indolent. Others are more diffuse and infiltrative, and tend to be difficult to resect. Prognosis in low grade gliomas is also diverse, as some tumors will remain stable for even fifteen years, while others will progress to higher grade gliomas within a matter of months.

The symptoms that arise from most gliomas share a common etiology. As physical space inside the cranium is limited, gliomas induce symptoms by placing pressure on normal brain tissue, thereby impairing normal brain function, leading to seizures, headache, and other neurological symptoms like memory loss, personality change, confusion, speech problems. If tumors occur in critical areas, these symptoms can be quite severe and life threatening, even if the tumor itself is not highly malignant. Because higher grade tumors grow so much quicker and are more invasive and

malignant, they tend to result in morbidity and mortality on a much more accelerated time scale than in lower grade gliomas.

Pilocytic astrocytoma (PA) is a grade I glioma that is typically indolent and whose tumor borders are very well circumscribed that most frequently occurs in young children. Although surgical treatment can be curative, if tumors occur in surgically inaccessible locations or recur following resection, they can be associated with morbidity and mortality. Patients with mutations in the neurofibromin 1 (*NF1*) gene are at increased risk for PA as well as for optic pathway gliomas, a tumor of the cellular sheaths of the optic nerves. Of note, is is thought that neurofibromin (NF1), the protein product of the *NF1* gene, is thought to control the RAS-ERK signaling pathway (discussed in greater detail later). Interestingly, activating point mutations or gene fusions of the BRAF or RAF1 genes are also frequently occur in PA, and the RAF genes are integral members of the RAS-ERK pathway, underscoring the importance of this signaling pathway in the pathogenesis of the disease.

The most common primary brain tumor is glioblastoma (GBM), a grade IV tumor. GBM most frequently occurs in patients over the age of 50. Originally, high grade gliomas like GBM were aggressively treated with surgical resection to the fullest extent possible and ionizing radiation. However, these therapies remain mostly ineffective. Because GBM is highly invasive, surgical resection is invariably incomplete, leading to a regrowth of the original tumor (then diagnosed as recurrent GBM). In 2005, a Phase III clinical trial showed a clear benefit to adding the nitrosourea alkylating agent temozolomide (TMZ), resulting in significantly longer overall survival and progression-free survival (Stupp et al. 2005). Despite this important advance, overall median survival for newly diagnosed GBM remains at 12-18 months and is still nearly universally fatal (Cloughesy et al. 2014). Indeed, GBM is resistant to most other standard cytotoxic chemotherapeutic agents, and frequent

alterations can often lead to de novo resistance to temozolomide (TMZ), currently the only FDA approved chemotherapy for GBM. Shortly after TMZ was added to the standard of care in GBM, it was demonstrated that the *MGMT* gene promoter, which is typically epigenetically silenced, can lead to de novo resistance to TMZ when active (Hegi et al. 2005).

Before 2008, knowledge of these such molecular alterations was fragmentary, but included dysregulation of growth factor signaling through mutation and activation of receptor tyrosine kinases (RTKs), frequent activation of the phosphatidylinositol-3-OH kinase (PI3K) pathway, and inactivation of the Rb and p53 tumor suppressor pathways. Without a unified approach to the frequency, co-occurrence, or mutual exclusivity of these alterations and because of the lack of therapeutic options available, GBM was selected as for the pilot project of The Cancer Genome Atlas (TCGA). The aim of TCGA was to catalog the genomic alterations present in cancer genes across many samples of a given type of cancer.

The results of the TCGA project confirmed the dysregulation of these pathways, but revealed that they occurred for diverse and often different reasons. Indeed, the PI3K pathway could be hyperactivated through somatic mutation of PI3K genes (like *PIK3CA*), deletion of PTEN, amplification of AKT genes, or somatic mutation of FOXO genes, transcriptional effectors of the PI3K pathway (Cancer Genome Atlas Research Network 2008). 80-90% of the tumors surveyed had some recorded mutation in the RB, TP53, and RTK pathways and these pathway alterations tended to be highly mutually exclusive. Despite being treated as one disease in the clinic, this suggested that GBM might actually be able to be further subclassified.

The next TCGA project in GBM included transcriptomic analysis of tumors in addition to the genomic analysis performed in the pilot project (Verhaak et al. 2010). Gene expression profiling and hierarchical classification of the resulting data showed

that GBM could be broadly classified into one of four subtypes, each of which was typified by a different genomic alteration. Following the addition of genome-wide methylation data, GBM is now classified into one of six molecular subgroups (Sturm et al., 2012). The first two subtypes are pediatric GBMs associated with two mutations in the histone gene *H3F3A* (encoding histone H3.3). The third subgroup, termed proneural, is characterized by point mutation in the isocitrate dehydrogenase 1 (*IDH1*) gene. This subgroup most frequently manifests in young adults whose IDH1 mutated tumors progressed from grade II or II gliomas. The fourth group, termed "RTK I" includes tumors with alterations in platelet derived growth factor α (*PDGFRA*) and a proneural expression pattern. The fifth, termed "RTK II" or classical, is characterized by frequent epidermal growth factor receptor (*EGFR*) gene amplification. The sixth, termed mesenchymal, is defined by loss of *NF1* function through mutation or deletion.

Of note, in the subtypes identified by Verhaak (classical, neural, proneural, and mesenchymal), aggressive treatment resulted in better overall survival in the classical and mesenchymal subgroups, while it was less effective in the neural subgroup, and had no effect on the proneural subgroup. This suggested that clinicians could spare patients from a chemotherapeutic regimen that would be both unsuccessful and detrimental to quality of life.

As the TCGA expanded beyond GBM to other cancer types, the catalogue of genomic alterations found in tumors became ever more complex. As scientists and clinicians observed that tumors could harbor even hundreds or thousands of mutations and chromosomal aberrations, the field began to fear that it might be impossible to use this data to guide therapeutic decisions. However, preclinical experiments showed that despite possessing a constellation of genomic alterations, many tumors were in fact exquisitely dependent on a single oncogene, a phenomenon termed oncogene addiction (Weinstein and Joe 2008). One of the earliest examples of the therapeutic

exploitation of oncogene addiction was the development of the drug imatinib (Gleevec).

After clinicians observed that over 90% of chronic myeloid leukemias possessed a chromosomal translocation between the *BCR* and *ABL* kinase genes (BCR-ABL) resulting in a constitutively active ABL kinase that was both necessary and sufficient for leukemogenesis (Daley et al. 1990). Hypothesizing that one might be able to inhibited the kinase activity of the dysregulated ABL kinase with a small molecule, Novartis developed the drug imatinib (brand name Gleevec.) The pivotal Phase III clinical trial recorded an almost 90% response rate, and most importantly, was very well tolerated, as the drug carried none of the typical side effects of cytotoxic chemotherapeutic regimens (O'Brien et al. 2003) in a disease that was universally fatal within months following diagnosis.

Quickly following imatinib was the introduction of trastuzumab (brand name Herceptin) which targeted human epidermal growth factor receptor type 2 (HER2) which was highly overexpressed in a subset of breast cancers (Eiermann, 2001). In trastuzumab's pivotal Phase III trial, the response rate was raised from 32% to 49% when compared to standard of care chemotherapy, a major milestone in the treatment of a disease that used to have dismal survival prospects.

These early trials establish proof of concept for the development of molecularly targeted therapeutics, and researchers, drug makers, and clinicians quickly ramped up efforts to find "druggable" alterations. EGFR is one of the most frequently altered genes in GBM, with high level copy amplification (2008), activating point mutations in the extracellular domain (Vivanco et al., 2012), and deletions of exon 2-7 in the extracellular domain (a specific mutation known as *EGFRvIII*). Despite impressive response rates and success in EGFR mutant lung cancers (Lynch et al., 2004), EGFR inhibitors have failed to achieve much success in GBM. (Mellinghoff et al., 2005).

showed that in clinical trials of the EGFR inhibitor erlotinib or gefitinib, only patients that expressed EGFRvIII and had intact copies of phosphatase and tensin homologue deleted in chromosome 10 (PTEN) had demonstrable responses.

PART 2 – Signal transduction

The cells of all multicellular organisms require the means to communicate with each other in order to coordinate information about proliferation, metabolism, and differentiation across the whole of the organism. This process is known as "signal transduction." Signal transduction has several major steps that can be generalized across many pathways and purposes (Hendrickson, 2005). As a cell determines that it needs to communicate some piece of information, that cell must first synthesize, and then release a "signal." That signal, which can be molecules including amino acids or peptides or metabolic products, must then be transported to a target cell. That cell must then detect the presence of that signal, usually through a receptor protein. The receptor-signal complex then triggers a change in the target cell. Finally, once it has served its purpose, the signal must then be removed to terminate the cellular response.

Cellular signaling in multicellular organisms is classified by the distance that the signal travels. Endocrine signals travel over long distances to distant cells while paracrine signaling acts on nearby or adjacent cells. Some cells also signal to themselves, a process termed autocrine signaling (Hendrickson, 2005).

A receptor protein exhibits a fit, or affinity, for certain signals, or ligands. This means that receptors tend only to transmit signals when bound by specific ligands. After doing so, receptors then undergo a conformational change that start a chain of reactions to propagate the signal through the cell in order to effect change. These reactions typically move through so-called second messengers, which amplify the

signal and help to specify the specific action the cell should take in response to the ligand (McCormick and Baillie, 2014).

Receptors are classified based on their location. Some ligands, especially those that are highly lipophilic, readily diffuse across the cell's plasma membrane and bind to intracellular receptor proteins (Hendrickson, 2005). These ligand-receptor complexes then translocate to the nucleus and act as transcription factors to cause transcriptional changes. Other ligands which are more hydrophilic cannot diffuse across the plasma membrane and bind to receptor proteins that are embedded within it (transmembrane receptors). These transmembrane receptors fall into three categories. G-protein coupled receptors (GPCRs) use a G protein that is released from the signal-receptor complex which then modulates second messengers. Ion-channel receptors change conformation following ligand binding to permit the flow of charged ions along their concentration gradients and change cellular potential. The final category are receptors with intrinsic enzymatic activities, such as receptor tyrosine kinases (RTKs).

Following stimulation of a receptor, cells often employ a "second messenger." Second messengers are typically small molecular weight molecules generated through enzymatic activity (such as cyclic adenosine monophosphate, cAMP) or are stored inside the cell and released (such as Ca^{2+} ions). Second messengers are usually generated locally, resulting in an increase in their concentration. The elevated local concentration of these second messengers can trigger a diverse array of cellular activities, but they mainly serve to amplify a local message, and propagate it through the cell to eventually effect the change that the original signal was intended for. Indeed, as individual steps in signaling cascades are often enzymatic in nature, each one can increase the size of the signal by orders of magnitude, allowing very small inputs to effect great change in both individual cells as well as across the many tissues

of an organism. They also are free to diffuse throughout the cytosol of the cell where they can then effect changes in geographically distant regions of the cell.

Finally, the signal must be removed in order to keep it from perpetually signaling. This can be done through several means. Small molecular components of the signaling process, such as peptides or second messenger molecules like cAMP can be degraded by enzymes specific to those molecules. Activated receptors are subject to dephosphorylation by phosphatases as well as to ubiquitination and subsequent targeting of the receptor to the proteasome for degradation.

Kinases are a diverse group of proteins, of which there are thought to be 500 members of in the human genome (Zhang et al., 2009). The primary role of a kinase is to catalyze the enzymatic transfer of a phosphate group from the donor molecule adenosine triphosphate (ATP) to a recipient protein. Charged phosphate groups carry a formal charge of negative two, and when covalently attached to proteins, induce structural changes through affecting hydrogen bonding networks and changing the conformation of protein-interaction surfaces. These conformational changes can affect the activity of the recipient protein, thereby activating or inactivating it, or modulating its activity to some degree.

The active site of kinases, known as the ATP binding site, is located between two "lobes," a N-terminal lobe with of a β-sheet and a single α-helix, and a mostly α-helical C-terminal lobe, connected by a linker region (Endicott et al., 2012). The C-terminal lobe contains the "activation segment" which contains a highly conserved DFG motif (where each letter refers to the single letter amino acid abbreviations) that chelates a Mg^{2+} ion when in the active formation which in turn positions a molecule of ATP for optimal catalysis. The activation segment is often phosphorylated in order to promote the active conformation of the kinase. In the inactive conformation, the

activation segment becomes disordered and often turns its phenylalanine towards the ATP binding site to block it.

Substrate recognition and specificity employ two different types of interactions. The first is the recognition of the individual kinase's consensus motif in its preferred substrate. Although kinase domains are largely structurally conserved, they differ at key amino acid residues in the ATP binding pocket in order to guide the specificity of the kinase protein as a whole. These differences, discussed in greater detail below, are key to the discovery and synthesis of small molecular inhibitors of kinase activity. The second type of interaction that guides kinase specificity is mediated through diverse protein association and docking of more distal domains in both the kinase protein and its substrates.

Humans possess the genes for 52 different RTKs, which include the aforementioned EGFR and HER2 (Lemmon and Schlessinger, 2010). RTKs are share a common structure with an extracellular, ligand-sensing domain, a single-pass helical transmembrane domain, and a cytoplasmic region that contains a tyrosine kinase domain along with more regulatory regions. RTKs also share a common activation and signaling mechanism. Canonically, RTKs are expressed as inactive monomers at the cell surface whose dimerization and subsequent activation are induced by ligand binding at the extracellular domain. However, it has become clear that some RTKs, like the insulin receptor, are actually expressed as constitutive heterodimeric complexes that remain inactive until ligand binding (Ward et al., 2007).

Upon receptor dimerization or ligand activation of pre-existing oligomers, the kinase domain of one receptor typically phosphorylates the kinase domain of the other oligomer to activate it. The diversity of RTKs however is also reflected in the diversity of their dimerization and activation processes, and here the case of the insulin receptor is described. When in its inactive, non-ligand bound state, Y1162 of one kinase

activation segment of insulin receptor projects into the active site of its own kinase domain, as if poised to be phosphorylated, thereby blocking access to ATP and the kinase substrate (Endicott et al., 2012). When activated by insulin, conformational changes induce the kinase domain of one oligomer to *trans*-phosphorylate the other domain, thereby relieving its *cis*-autoinhibition.

The primary substrates of RTKs are the *trans*-phosphorylation of each other on several sites. The kinase domain often contains several tyrosines that drastically change the enzymatic activity of the kinase (Lemmon and Schlessinger, 2010). Typically, the phosphorylation of these sites occurs in a precise order that each increase kinase activity. Next, "secondary" tyrosines are phosphorylated that act as docking sites to recruit other signaling molecules, forming assembly scaffolds responsible for carrying out further downstream signaling processes. Proteins that bind these phosphotyrosine motifs contain either Src homology-2 (SH2) domains or phosphotyrosine-binding (PTB) domains. These proteins are either directly recruited or indirectly associate through other proteins that become phosphorylated as part of the signaling cascade. Finally, in some RTKs, a tertiary set of tyrosines become phosphorylated that maximize the kinase activity of the kinase domain. RTKs can also contain a divesr array of other association domains that control the recruitment of proteins to the cell membrane through pleckstrin homology (PH) domains or to other proteins through domains like SH3 and PDZ domains.

The differential presence and quantity of these domains is largely responsible for dictating the role of the RTK and its associated partners in downstream signaling. For instance, some RTKs will become differentially transphosphorylated under certain conditions and recruit different signaling complexes with altered signaling capabilities (Eck et al., 1996). Indeed, the signaling output from RTKs and their signaling network is less a linear pathway and more of a complex set of integrated nodes carefully

regulated by feedback. While this systems level approach to signaling pathways and networks has only recently begun to be mapped with the advent of gene expression arrays and phosphoproteomic tools, it has been long known that the exact same signaling components can be used to different effect. Short duration activation of the EGFR receptor with its ligand EGF in PC12 cells leads to proliferation, largely by stimulating the Mitogen Activated Kinase Pathway (MAPK). However, by overexpressing the EGFR receptor in these cells, EGF stimulation leads to more prolonged MAPK activation, followed by neurite outgrowth and cellular differentiation (Santos et al., 2007).

Therefore, signal transduction through a more contemporary lens holds that signaling processes resemble an "hourglass" structure (Citri and Yarden, 2006). On top, the input layer is made up of many input RTKs and their diverse ligands which can result in a variety of strengths and durations of signaling. From there, these inputs move into a "conserved core processes" node where the input signals move through non-receptor kinase activity (including the MAPK pathway), phosphoinositide signaling (such as the PI3K pathway), small GTPase cycles (like RAS, discussed later), and the addition and removal of ubiquitin moieties (which can both regulate the activity of proteins and target them for degradation at the proteasome). These signals are then "read out" by a diverse output layer, resulting in transcriptional changes, cytoskeletal rearrangements, or other changes in cell-intrinsic properties. Most important to the systems level approach to signaling are the feedback mechanisms employed by the core processes that carefully regulate their activity.

On some level, almost all signaling processes employ feedback in order to fine tune their magnitude and duration. Furthermore, the conserved processes also employ feedback between the many pathways as well, which is known as pathway crosstalk

(Citri and Yarden, 2006). Pathway crosstalk is important to signal transduction since so many different signaling processes employ the very same signaling machinery. On a general level, there are several kinds of feedback loops (Kolch et al., 2015). The first is positive feedback, where the product of a pathway further stimulates an earlier step, increasing the magnitude of signaling through the pathway. This is analogous to holding down the accelerator on a car. On its own, a positive feedback loop can result in runaway perpetual signaling, so they are used by cells in order to force commitments, such as progressing through the cell cycle after the restriction point, the point at which a cell commits to complete the cell cycle. Positive feedback adds robustness to signaling, especially in situations when signaling noise might complicate cell-fate decision that require commitment. It also allows a cell to react to very low abundance signals, amplifying them to biologically active levels.

The second type is negative feedback, where the output of a pathway inhibits an earlier step, essentially attenuating signaling through the pathway up to completely turning it off. This is analogous to pressing on the brake of a car, slowing it down, and given enough time and force, eventually bringing it to a halt. In general negative feedback adds robustness to signal transduction, smoothing noise and sudden perturbations (Nguyen and Kholodenko, 2015). Depending on the strength and duration of both input signal and of the feedback, negative feedback can convert oscillating signals to a smooth input. Both positive and negative feedback loops work in tandem to order to translate signaling network dynamics into cell-intrinsic decisions in response to signals. Interestingly, many of the genes that regulate this feedback are often tumor suppressors or oncogenes, demonstrating their importance in cancer pathogenesis.

PART 3 – The RAS-ERK pathway components

One of the most well described "core conserved" pathways is the RAS-mitogen activated protein kinase cascade (RAS-MAPK). It is composed of several proteins and successively activate each other in turn, culminating in many cellular actions including growth, proliferation, differentiation, senescence, and migration (Santarpia et al., 2012). Its constituent members are the small GTPase KRAS, NRAS and HRAS (collectively referred to as RAS), the serine/threonine kinases c-Raf, ARAF, and BRAF (collectively referred to as RAF), MEK1 and MEK2 (named for **M**APK/**E**RK **K**inase, collectively referred to as MEK), and ERK1 and ERK2 (**e**xtracellular signal **r**egulated **k**inases, collectively referred to as ERK).

RAS was originally identified as gene components of tumor causing viruses in mice starting in the 1960s (Santarpia et al., 2012). Eventually, three different isoforms of Ras were identified, the first two named after their discoverers—HRAS, for Jennifer **H**arvey (Harvey, 1964); KRAS, for Werner **K**irsten (Kirsten et al., 1970)—while the third, NRAS, was identified in **n**euroblastoma cells. Several seminal papers of this era identified mutations in *RAS* genes as causative, transforming oncogenes in human cancer. Eventually, sequencing of the *RAS* genes in human tumors demonstrated that up to a third of tumors harbored an activation mutation of RAS. With this, the field rapidly set out to understand RAS biology.

The three human *RAS* genes code for four highly related protein products, namely HRAS, NRAS, KRAS4A and KRAS4B, which are alternative splicing products of the *KRAS* gene (Takashima and Faller, 2013). RAS is a small GTPase that acts as molecular switch, alternating between an inactive GDP-bound state and an active GTP-bound state. This processes, while thermodynamically favorable, are highly inefficient, so they are largely controlled by the presence of external factors. When

activated by guanine exchange factors (GEFs), RAS releases bound GDP and binds GTP, which is found at a higher intracellular concentration. When bound by GTP, active RAS can then bind and activate downstream effector pathways. As a GTPase, RAS has an intrinsic hydrolytic activity. However, this enzymatic activity is greatly catalyzed by the enzymatic stimulation by GTPase activation proteins (GAPs). GAPs stimulate the hydrolysis of bound GTP, converting it to GSP and inactivating RAS.

The proper functioning of RAS requires a certain set of posttranslational modifications in order for proper functioning. RAS is decorated with a farnesyl tail (a modified fatty acid) that is necessary for the localization of RAS to the inner leaflet of the cellular membrane (Takashima and Faller, 2013). This localization is important because GEFs are often activated by signaling receptors, like RTKs, which are also located in the cell membrane. As described before, ligand binding to RTKS leads to transautophosphorylation and the nucleation of phosphorylated binding sites for adaptor proteins. For EGFR, the protein GRB2 binds these sites through its SH3 domain, which in turn recruits SOS, through its SH2 domain. SOS then acts a GEF, stimulating the activation of RAS and allowing it to engage its downstream effector pathways.

RAS has several parallel effector pathways, many of which also have been independently implicated in cancer. All of these effectors possess a RAS binding domain (RBD) that associated with active GTP-bound RAS. The most well described of these pathways include the MAPK pathway, the PI3K pathway, RAC, RALGDS, and phospholipase Cε (PLCε) (Downward, 2003). Activated RAS binds the catalytic subunit of PI3-Kinase which recruits it to the cell membrane and activates its lipid kinase activity, generating the second messenger PIP_3 in the plasma membrane. Downstream of PIP_3 activation, the protein kinases Akt and PDK1 are activated, which activate several anti-apoptotic pathways. RALGDS, itself also a small GTPase,

is activated when active RAS binds RALGDS's exchange factors. RALGDS signaling inactivates the FORKHEAD family of transcription factors, which promote cell cycle arrest and are also proapoptoic. PLCε also has a RAS-binding domain, and links RAS signaling with protein kinase C (PKC) and Ca^{2+} mobilization.

The MAPK pathways are well studied signaling cascades that transduce a variety of growth, proliferation, differentiation, developmental, and stress signals from membrane bound receptors to a namesake transcription factor (Zhang and Liu, 2002). There are currently four known MAPK pathways— ERK, JNK, p38 and BMK— although there are possibly more, as many MAPK genes have been identified through homology searches, though their specific functions have yet to be elucidated. All MAPK pathways share a common structure, where a MAP-Kinase Kinase Kinase (MAP-KKK) phosphorylates and activates a MAP Kinase Kinase (MAP-KK) which in turn phosphorylates and activates a terminal MAP kinase (MAP-K). The best characterized of these pathways is the RAS-RAF-MEK-ERK (shortened to RAS-ERK) pathway.

The RAF family of genes is composed of CRAF (*RAF1*, also known as c-Raf and RAF1), ARAF (*ARAF*), and BRAF (*BRAF*). CRAF was originally identified as a proto-oncogene through induced mutagenesis experiments that invariably revealed N-terminal truncations or rearrangements but an intact kinase domain (Stanton et al., 1989). After the identification of the closely related isoforms ARAF and BRAF, research from many groups identified similar physiological roles of MEK and ERK, and eventually the field converged on a consensus view of the core RAS-ERK pathway (Lavoie and Therrien, 2015).

KSR is the prototypical RAS-ERK scaffold. In addition to optimizing the proximity and orientation of RAS-ERK signaling modules, KSR can also prevent pathway crosstalk by anchoring or sequestering RAS-ERK modules from other

MAPK modules, preventing crosstalk (Ramos, 2008). The stoichiometry of scaffolds to MAPK modules also affects the ability of the pathway to signal. At too low of concentrations, the scaffolds fail to bring signaling components together and signaling is hindered. At too high of concentrations, MAPK modules bind different scaffolds and individually and again, signaling is impaired. Thus, cells can regulate the levels of scaffolds in order to tune ERK signaling. Indeed, KSR protein levels are regulated by the E3 ubiquitin ligase IMP1. While KSR is the most characterized scaffold, many others have been shows to bind RAS-ERK signaling modules which aids in context specific signaling.

The N-terminal region of RAF contacts and inhibits the kinase domain in inactive RAF (Cutler et al., 1998; Rajakulendran et al., 2009). CRAF is also repressed by phosphorylation of S259 (BRAF has a homologous S365 site) by Akt and protein kinase A (PKA). When phosphorylated, these residues are bound by 14-3-3, holding RAF in an inactive conformation. When dephosphorylated by PP2A, 14-3-3 is released and RAF can become activated. Active GTP-bound RAS recruits RAF to the plasma membrane, binding to RAF's RAS-binding domain. RAF then forms dimers with other RAF molecules, forming both homodimers and heterodimers. This dimerization is necessary for normal RAF function, as the BRAF-R509H mutation, located in the interface of the two RAF molecules, impedes both BRAF dimerization and activity (Rajakulendran et al., 2009). CRAF is then further activated by phosphorylation of S338 and Y441 (S299 on ARAF, S445 on BRAF) which is necessary for maximal RAF kinase activity for subsequent MEK binding (Lito et al., 2013). In addition to these phosphorylations, RAF must also either homo-dimerize or hetero-dimerize in order to become fully signaling competent.

However, S445 in BRAF is constitutively phosphorylated and together with a phosomimetic D445 (Y441 on CRAF) is thought to explain BRAF's higher basal

activity. Phosphorylation of the activation loop is also required for RAF activity, though detection of these sites is technically difficult to detect through both phosphoproteomic and crystallographic techniques (Lavoie and Therrien, 2015). The net result is that BRAF is "charged" for activity, and requires only RAS-dependent recruitment to the plasma membrane, while ARAF and CRAF first require a constellation of phosphorylation events and plasma membrane recruitment in order to become signaling competent.

The next step in the RAS-ERK cascade is the activation of the MAP-KK MEK1 and MEK2 (Shaul and Seger, 2007). While the RAF isoforms are the best studied and most widely accepted MEK activators, there is evidence that several other MAPKKKs are capable of activating MEK, including COT (MAP3K8) (Caunt et al., 2015; Johannessen et al., 2010). While MEK1 and MEK2 are 85% homologous. MEK must be recruited to RAF, either directly, or through scaffolding proteins like KSR1 and KSR2 (**k**inase **s**uppressor of **R**AS, which resemble RAF but harbor inactivating mutations in their kinase domains) which are thought to recruit, orient, and stabilize the components of the RAS-ERK signaling module. RAF then phosphorylates the activation loop of MEK1 at S218 and MEK2 at S222, leading to their activation. While all three RAF family members have been shown to possess the capability to phosphorylate MEK, BRAF is the predominate isoform responsible for activing MEK. For instance, depleting normal brain of BRAF led to 96% reduction of MEK phosphorylation (Moodie et al., 1994). MEK is also phosphorylated at other residues to modulate its activity, including phosphorylation of S298 on MEK1 by p21-activating kinase (PAK1) which increases activated MEK's kinase activity. Although referred to collectively, MEK1 and MEK 2 have been shown to mediate specific and non-redundant roles in certain contexts (Skarpen et al., 2008). For instance, *Mek2*$^{-/-}$

mice develop normally, while *Mek1*$^{-/-}$ mice results in embryonic lethality at E10.5 due to placental defects.

Another class of scaffolds that deserves special mention as negative regulators of RAS-ERK signaling are the Raf kinase inhibitor proteins (RKIPs). RKIP binds RAF and MEK, but prevents their activation (Ramos, 2008). When RAS activates RAF, RKIP releases RAF and MEK, resulting in pathway activation. Consistent with activating the RAS-ERK pathway, RKIP is downregulated in various tumor types.

MEK is a dual specificity kinase, and can phosphorylate both the tyrosine and threonine residues of its only validated substrate, the MAP-Kinase ERK. Indeed, MEK's exquisite specificity for only ERK makes it a discriminatory gate in the RAS-ERK pathway. In its inactive conformation, MEK binds inactive ERK, primarily retaining it in the cytoplasm. When activated, MEK phosphorylates and releases ERK. MEK activates ERK1 (also known as p44) at T202 and Y204 as well as and ERK2 (p42) at T185 and Y187 (Roberts and Der, 2007). Upon dual phosphorylation, ERK's serine/threonine kinase activity is activated, and ERK phosphorylates a whole host of substrates including transcription factors, other kinases and phosphatases cytoskeletal proteins, scaffolds, RTKs and intracellular signaling molecules, as well and many others. ERK is further phosphorylated on S244 and S246 (ERK2 numbering) are important for importin7 binding and nuclear translocation, although the specific kinase (or kinases) responsible for these sits have yet to be fully elucidated (Wainstein and Seger, 2016). Although referred to collectively, it is important to note that ERK1 and ERK2 are not entirely redundant, similar to MEK1 and MEK2. For instance, *Erk2*$^{-/-}$ mice are embrypnic lethal by E8.5, while *Erk1*$^{-/-}$ mice are appear relatively normal (Ramos, 2008).

ERK localization plays a substantial role in its regulation and activity. At rest, ERK is predominantly located in the cytoplasm bound to anchoring and scaffolding

proteins through its the common docking (CD) domain (Wainstein and Seger, 2016). When phosphorylated and activated, ERK is released and shuttled to other locations in the cell. Most activated ERK goes to the nucleus, but a portion also is shuttled to various organelles and membranes.

Most recent estimates are that ERK has over 250 distinct substrates, split approximately equally between the nucleus and extra-nuclear locations (Wainstein and Seger, 2016). ERK phosphorylates many cytoplasmic substrates, but can also translocate into the nucleus where it can phosphorylate many other substrates, especially transcription factors (Shaul and Seger, 2007). Substrates of note include the transcription factors c-Fos and Elk1, which are activated by ERK phosphorylation, and drive proliferation, as do the vast majority of nuclear ERK substrates (Cargnello and Roux, 2011). Continuous ERK activity is also necessary and sufficient for Cyclin D1 transcription, which is required to pass the restriction point and G_1/S-phase checkpoint. Elk-1, and the ETS family ERK also amplifies its own signal by activating the family of kinases known as the MAPK-activated protein kinase (MAPKAPKs), including the cytoplasmic kinase p90RSK (Romeo et al., 2012). The RSK family of kinases phosphorylate their own diverse set of substrates that control proliferation, growth, migration, and survival.

Just as important as the mechanisms of RAS-ERK pathway activation are the mechanisms by which the pathway is ultimately downregulated. As mentioned before, RAS is principally inactivated by GAPs which stimulate RAS's intrinsic GTPase activity, hydrolyzing bound GTP to GDP and blocking RAS's ability to bind to and activate its various effector pathways. One of the best studied RAS GTPases is the protein neurofibromin 1 (NF1). Interestingly, NF1 is commonly mutated or deleted in various cancer types, causing spurious RAS activation.

RAF, MEK, and ERK inactivation is firstly mediated by the dephosphorylation of the activating phosphoresidues by various phosphatases. On RAF, only the direct dephosphorylation of S338 by protein phosphatase 5 (PP%) has been described, but dephosphorylation of either site in MEK or ERK is sufficient to deactivate them (Lavoie and Therrien, 2015). There are several phosphatases that control the activity MAP kinase family members (MPKs, for MAP kinase phosphatases), and they are classified based on their preference for dephosphorylating tyrosine, serine/threonine, or both tyrosine and threonine (a family known as dual specificity phosphatases, or DUSPs) (Roskoski, 2012).

Perhaps the most significant method of negative regulation in the RAS-ERK pathway is the negative feedback exerted by ERK across almost every component of the RAS-ERK in order to limit stimulation of the pathway under physiologic conditions (Lito et al., 2013). ERK phosphorylates EGFR at T669 in order to simulate receptor turnover. ERK (as well as p90RSK) also phosphorylate SOS1 on several sites, preventing ligand-bound RTKs from activating RAS. ERK also has recently been shown to phosphorylate NF1 which is thought to regulate its stability in response to growth factor stimulation. ERK also phosphorylates CRAF on many residues including S29, S43, S289, S96, S301, and S642 which act in concert to decrease CRAF kinase activity. Phosphorylation of S43 can also be carried about by PKA which hinders RAS-RAF association. ERK also phosphorylates MEK1 at T212 and T292 in order to inhibit its activity and prevent further activation by PAK1.

In addition to its direct kinase activity, ERK also causes the transcriptional upregulation of many genes that, in turn, also inhibit activation of the RAS-ERK pathway. Active phospho-ERK directly induces the upregulation of the transcription of several DUSPs, which then dephosphorylate the tyrosine and threonine residues on ERK in order to deactivate it (Kidger and Keyse, 2016). There are three families of

DUSPs: DUSP1, DUSP2, DUSP4, and DUSP5 dephosphorylate nuclear ERK; DUSP3, DUSP7, and DUSP9 dephosphorylate cytoplasmic ERK; DUSP8, DUSP10, and DUSP16 act on other MAP kinases (like p38 and JUNK) instead of ERK, and not considered here any further. All of the DUSPs share a highly homologous structure of a non-catalytic and regulatory N-terminal domain and a catalytic C-terminal tail. Nuclear DUSPs contain a nuclear localization signal (NLS) while cytoplasmic DUSPs contain a nuclear export signal (NES). ERK has also been shown to phosphorylate DUSP1 which induces its degradation, underscoring the multi-layered and even reciprocal regulation of ERK and the DUSPs (Brondello et al., 1997) and perhaps helps determine the duration and intensity of ERK signaling following differing types and magnitudes of pathway activation.

Dysregulation of the DUSPs is thought to play a role in many tumor types. DUSP6, the first ERK-selective DUSP to be identified is not mutated at any significant rate in any tumor type. However, in pancreatic tumors, of which 90% harbor activating RAS mutations, DUSP6 transcription was consistently lowered, often through epigenetic silencing of the DUSP6 promoter (Furukawa et al., 2003). Furthermore, in lung cancer, about 17% of tumors surveyed demonstrated loss of heterozygosity at the DUSP6 locus and a concomitant decrease in DUSP6 expression, underscoring the important escaping (or disabling) the physiological pressure of ERK's own negative feedback (Okudela et al., 2009).

Another class of inducible negative regulators of the RAS-ERK pathway are the Sprouty family of genes (*SPRY*). SPRY proteins are phosphorylated on an N-terminal tyrosine which can serve as a docking site for GRB2 (through its SH2 domain), thereby sequestering GRB2 away from SOS and RTKs at the cell membrane (Hanafusa et al., 2002; Lito et al., 2013). Furthermore, mutations in the protein SPRED (transcriptionally upregulated by ERK) which is also a member of the SPRY

family, have been shown to prevent NF1 from associating with RAS at the cell membrane (Stowe et al., 2012). These mutations were found in patients with a RAS-opathy, a collection syndromes associated with overactive RAS-ERK signaling.

With an understanding of the negative feedback and feed-forward mechanisms in the RAS-ERK pathway, it helps to consider the example of pathway activation in the context of PC12 cells again. By modulating individual components of the RAS-ERK pathway with RNAi such as ERK's DUSP or MEK's phosphatase, Santos et al. observed that EGF stimulation resulted in only negative feedback and therefore transient ERK activation (Santos et al., 2007). Conversely, following NGF stimulation, ERK output was sustained and only positive, reinforcing feedback was observed to CRAF via protein kinase C (PKC). By activating PKC with phorbol-12-myristate-13-acetate (PMA) in conjunction with EGF, the authors achieved sustained ERK activation resembling NGF activation. This demonstrates that altering levels of feedback proteins and their activity can alter systems level ERK activity.

Part 4 – RAS-ERK signaling in cancer

While dysregulation of RAS-ERK signaling had been noted for a long time in the cancer research community, the landmark finding in 2002 by Davies et al. described mutations in *BRAF* in several different tumor types (Davies et al., 2002). Using a panel of cell lines, most with matched normal blood for comparison, the group noted mutations in BRAF in "59% [of] melanomas, 18% [of] colorectal cancers, 11% [of] gliomas, 3% [of] lung cancers, 9% [of] sarcomas, 4% [of] ovarian carcinomas, 2% [of] breast cancers and 14% [of] liver cancers," establishing recurrent somatic mutation of *BRAF*. Interestingly, the authors noted that the cancer types in which

BRAF mutations most frequently occurred were also types which frequently harbored mutations in the *RAS* genes, underscoring the important of the RAS-ERK pathway to these cancer types. Of the tumor types surveyed with *BRAF* mutations, 89% harbored a mutation within the activation loop of BRAF. Of those, 92% were a single amino acid substitution at valine 600, most often to glutamic acid (V600E) and less frequently to several other amino acids.

Since 2002, numerous genome-wide sequencing studies, including those done through the TCGA project, have established the rate of BRAF mutation at around 50-60% in malignant melanoma, 30-50% in thyroid, 10% in colorectal, 100% on hairy cell leukemia, and about 3% in lung and glioma each (Samatar and Poulikakos, 2014). Indeed, most recent counts find that nearly all mutations in BRAF occur in the kinase domain, 98.4% occur at V600 (of which 97.8% are V600E) (Lavoie and Therrien, 2015). Genome-wide surveys have identified very few mutations in CRAF, and even fewer in ARAF, KSR1, and KSR2, of whose importance has very to be identified in any significant manner (Forbes et al., 2011).

After identifying the recurrent mutations in BRAF, Davies et al. expressed cDNAs for BRAF harboring the various mutations they had observed in order to ascertain their oncogenic potential (Davies et al., 2002). BRAF-V600E had a much higher elevated in vitro kinase rate than wild-type BRAF and was also able to induce transformation of NIH-3T3 cells. Confirmation of the oncogenic role of BRAF-V600E came from the introduction of BRAF-V600E alleles into transgenic animals. Mice and zebrafish with a BRAF-V600E allele expressed in a melanocyte tissue-specific manner displayed senescent melanocytic masses as well as highly invasive tumors (Mercer et al., 2005; Patton et al., 2005). Indeed, mutations in BRAF have also been identified in many RAS-opathies (Rauen, 2013). These patients also often display a

predisposition to various malignancies as well, underscoring the role mutations in BRAF play in pathogenic RAS-ERK signaling.

The mechanistic and oncogenic role of BRAF in cancer derives from two important observations. The first is that BRAF is "primed" to signal. Recall that ARAF and CRAF require five different phosphorylations in order to become completely signaling competent, while BRAF only has four of these conserved sites and has a phosphomimetic aspartic acid at CRAF-Y341/BRAF-D448 (Wellbrock et al., 2004). Moreover, the CRAF-S338/BRAF-S445 site is constitutively phosphorylated in BRAF. This "priming" shows while a single amino acid substitution is sufficient for oncogenic activation, while CRAF and ARAF would require several more activating mutations, and likely explaining their relative scarcity in cancer.

The second important observation derives from a crystallographic model of wild type BRAF and BRAF-V600E bound with a first generation RAF inhibitor (Wan et al., 2004). From this model which assumes that inhibitor-bound BRAF mimics ATP-bound BRAF, mutations in the activation segment of BRAF (for example, BRAF-V600E) destabilize the hydophobic interactions of valine 600 with the phenyl 468 which hold it in an inactive conformation. Substituting valine 600 with a larger and charged side chain breaks the interaction, frees the activation loops and eliminates the need for its phosphorylation, and allows BRAF to fold into an active conformation. Other models propose that hydrophobic interactions between the G-loop and the DFG motif/P-loop of the activation segment are primarily responsible for holding BRAF in an inactive conformation (Lito et al., 2013).

As mentioned previously, RAF signaling requires hetero- or homo-dimerization in order to become fully signaling competent (Cutler et al., 1998; Rajakulendran et al., 2009). The BRAF-R509H mutation prevents the dimerization of BRAF, and attenuates the growth advantage in RAS-mutant cells (Hatzivassiliou et al., 2010).

Furthermore, the p61-BRAF mutation results in the loss of exons 4-8 of BRAF, leading to the constitutive dimerization of BRAF, even in the absence of activated RAS-GTP, and its oncogenic signaling to ERK (Poulikakos et al., 2011).

Following the discovery and conformation of the role of BRAF-V600E across many types of cancer, it was proposed that as a kinase, BRAF might be a druggable therapeutic target using ATP-competitive compounds (Tuveson et al., 2003). For instance, conditional expression and ablation of a BRAF-V600E allele with an shRNA resulted in inducible growth and regression of melanoma models (Hoeflich et al., 2006). The most pivotal evidence for the therapeutic potential of inhibiting mutant-BRAF was the discovery the BRAF-V600E oncogene in diverse tissue types was highly predictive of sensitivity to MEK inhibitors relative to RAS-mutant cell (whose sensitivey to MEK inhibition was more varied) or wild-type cells (Solit et al., 2006).

Indeed, there was much pharmaceutical interest in developing CRAF inhibitors initially, primarily based on their role as RAS effectors, including the development and approval of the drug sorafenib. Sorafenib's approval was based on its efficacy in renal and liver cancers, and considering the relative lack of RAS-ERK mutations in these tumor types, the current consensus is that sorafenib's efficacy is largely derived from its "off-target" inhibition of vascular endothelial growth factor receptor (VEGFR) family kinases (Bollag et al., 2012). Indeed, sorafenib was relatively ineffective in melanoma trials with unselected patient populations, which is unsurprising considering that sorafenib preferentially inhibits CRAF and only weakly binds mutant-BRAF.

The first mutant-BRAF selective inhibitor to receive FDA approval was vemurafenib (PLX4032, Zelboraf; Genentech/Plexxikon) in 2011 (Bollag et al., 2010, 2012; Tsai et al., 2008). Vemurafenib was propelled through the approval process by its striking response rate in mutant-BRAF selected patients with a "confirmed best

overall response rate of >50% and median progression-free survival of approximately 7 months" in Phase I and II trials comparted to a historical response rate to decarbazine, a cytotoxic chemotherapeutic agent, of <10% and 2 months (Bollag et al., 2012; Flaherty et al., 2010; Sosman et al., 2012). In fact, vemurafenib showed such promise in its Phase I and II trials that the FDA instructed that exposure to the control arm should be minimized out of ethical concerns (Chapman et al., 2011). Vemurafenib was approved in less than 5 years, an almost unheard of period in oncology (Bollag et al., 2012).

In biochemical assays, vemurafenib had a slightly higher affinity to mutant BRAF over wild type BRAF. However, in call-based assay, vemurafenib inhibited ERK signaling and associated proliferation in a highly BRAF-V00E selective manner, and demonstrated no effect in RAS-driven tumors (Joseph et al., 2010). This was initially a curious result considering that RAF is a key effector of RAS-ERK signaling. Several landmark works elucidated the mechanisms for these observations. The first evidence in 1999 was that an early CRAF inhibitor seemed to fail to block ERK phosphorylation despite being an effective inhibitor in in vitro studies (Hall-Jackson et al., 1999). This observation was underappreciated at the time though due to the lack of a market for RAF inhibitors. Another piece of evidence was the understanding of RAS-RAF signaling dynamics, and the observation that RAS-driven RAF dimer formation is required under physiological conditions in order for RAF to signal to ERK (Rajakulendran et al., 2009).

A further curious result was the occurrence of benign, but debilitating cutaneous squamous-cell carcinomas and keratoacanthomas in 15-30% of patients treated with first generation RAF inhibitors. Another landmark paper showed that the tumors in these patients harbored activating RAS mutations in approximate 60% of cases (Su et al., 2012). This finding initially worried the field, fearing that either vemurafenib or

RAF inhibition in general might be carcinogenic. This worry was dispelled by elegant studies that showed that kinase dead BRAF (kd-BRAF) cooperates with mutant-RAS in the presence of a RAF inhibitor to drive kd-BRAF/CRAF dimer formation, CRAF activation, and ultimately signaling to ERK, demonstrating that RAF pathway inhibition itself was not the cause of the secondary tumor formation (Heidorn et al., 2010).

These results finally coalesced around a unified view of RAF inhibitors in a pair of papers published in *Nature* by a team of scientists at Genetech (Hatzivassiliou et al., 2010) and the Rosen lab at the Memorial Sloan Kettering Cancer Center (Poulikakos et al., 2010). Hatzivassiliou et al measured the sensitivity of a panel of BRAF-V600E, RAS-mutant, and RAS/RAF-wild type cell lines to ATP competitive RAF inhibitors and MEK inhibitors (Hatzivassiliou et al., 2010). While all of the cell lines were quite sensitive to the MEK inhibitor PD0325901 (PD-901), only the BRAF-V600E cells lines demonstrated an exquisite sensitivity to the RAF inhibitors, including vemurafenib, while the RAS-mutant and RAS/RAF-wild type cell lines were all insensitive. They further demonstrated that in the context of mutant-RAS, RAF inhibitor binding to RAF results in the formation of RAS-dependent BRAF-CRAF dimers, membrane localization, and interaction with RAS-GTP.

Poulikakos et al. started with a very similar observation: while ATP-competitive RAF kinase inhibitors indeed block ERK phosphorylation in mutant-BRAF contexts, they paradoxically stimulate ERK signaling above baseline in BRAF-wildtype/RAS-mutant contexts that eventually becomes inhibited at much higher drug concentrations (Poulikakos et al., 2010). Using elegant chemical genetic experiments, Poulikakos demonstrated that vemurafenib binding to the ATP site of one protomer of a BRAF-BRAF or BRAF-CRAF dimer inhibits that promoter and then transactivates the other promoter in the presense of mutant-RAS, though the effect was much more significant

in CRAF containing dimers. In both studies though, so-called BRAF inhibitors failed to inhibit wild-type BRAF or CRAF. Also, in the presence of high-levels of RAS-GTP (induced through expression of a mutant-RAS allele), vemurafenib failed to inhibit BRAF-V600E signaling, though in both cases signaling was sensitive to a MEK inhibitor. These observations also showed significant clinical meaning. While RAF inhibitors would be expected to inhibit RAF-ERK signaling in tumor cells with BRAF-V600E, they would not in normal cells in the rest of a patient's body (or they would induce signaling, causing the cutaneous squamous-cell carcinomas and keratoacanthomas observed in some patients), suggesting that RAF inhibitors would have a much wider therapeutic index than would MEK inhibitors, which would inhibit MEK across all tissues in a patient. This would allow RAF inhibitors to be administered at high doses and more durably suppress ERK signaling. Indeed, complete suppression of ERK signaling is necessary to receive full therapeutic benefit from any drug designed to inhibit ERK signaling (Bollag et al., 2010). Because of the broad tissue activity of MEK inhibitors, administration of these drugs is often limited by their toxicities, leading to lower observed clinical efficacy.

The Rosen lab further showed that while RTK-activated tumors and BRAF-V600E tumors both demonstrate similar levels of activated ERK, only the BRAF-V600E cells were dependent on that ERK signaling (Pratilas et al., 2009). Indeed, using gene expression arrays, the group demonstrated that feedback inhibition in RTK-activated tumors attenuated ERK output (as measured by transcriptional output of ERK-dependent genes) while BRAF-V600E tumors appeared to be insensitive, ad in fact, appeared to be able to evade ERK-dependent feedback inhibition.

How RAF was able to evade this ERK dependent feedback then became an area of intense study. While observing RAF mutations that were acquired during vemurafenib treatment, Poulikakos found a BRAF mutant with an in-frame deletion of exons 4-8,

termed p61-BRAF-V600E (Poulikakos et al., 2011). While this truncated BRAF isoform was insensitive to vemurafenib, p61-BRAF-V600E which was engineered to co-express the dimer-breaking R509H mutant (p61-BRAF-V600E/R509H) rendered the mutant sensitive to vemurafenib, underscoring the importance of BRAF monomers to RAF inhibitiors.

One more important finding about ATP-competitive RAF inhibitors also came from the Rosen lab. Yao et al. used the ATP competitive RAF inhibitor LGX818, which has as extremely low pharmacokinetic off-rate and remains bound to RAF even after washing, to demonstrate that cells expressing mutant-RAS required much higher concentrations of first generation RAF inhibitors to bind the second protomer of RAF dimers that was required for the first protomer, establishing that RAF dimers demonstrate a negative cooperativity in addition to their RAS-dependent transactivity (Yao et al., 2015b). This phenomenon was irrespective of the RAF inhibitor used.

Lito et al. showed in a later study that negative feedback from active ERK to the RTKs themselves, as well as their signaling apparatus (SOS, Grb2, loss of Sprouty and DUSPs) indeed suppressed RTK signaling upstream of BRAF-V600E, leading to low RAS-GTP levels (Lito et al., 2012). Without sufficient levels of RAS-GTP, RAF fails to form dimers. However, BRAF-V600E signals effectively as a monomer, allowing it to evade the powerful feedback of its oncogenic signaling. Lito further showed that following long term vemurafenib treatment, RAS-GTP levels became slightly elevated, presumably leading to the formation of RAF-inhibitor insensitive dimers.

The source of this RAS-activation is hypothesized to come from various sources. Perhaps the primary driver is the loss of feedback inhibition of RTK components (SPRY2, SOS) (Lito et al., 2012). One hypothesized observation of would be that RTK-ligand stimulation of non-RAF inhibitor treated cells would activate their cognate receptors, but fail to activate downstream signaling. Indeed, non-vemurafenib

treated melanoma cells when treated with EFGF or NRG-1 activated EGFR and HER2 respectively, but failed to induce downstream signaling. Treatment with vemurafenib relieved the negative feedback on these receptors and restored their ability to signal.

Secondly, stromal secretion of RTK ligands has also been implicated in resistance to RAF inhibitor treatment. In a pair of papers co-published in Nature in 2012, two groups demonstrated that ligand secretion of hepatocyte growth factor (HGF) and the activation of its receptor MET led to RAF inhibitor resistance (Straussman et al., 2012; Wilson et al., 2012). While not directly demonstrated in the papers, presumably RTK activation would lead to RAS activation and an increase in RAS-GTP. Indeed, a similar secrotome experiment by Lito et al. confirmed the ability of secreted ligands to attenuate the effect of RAF inhibitors (Lito et al., 2012). Considering these papers together though, ligand secretion alone would likely be necessary, but not sufficient, to induce RAF inhibitor resistance (Lito et al., 2012). Resistance would also require RAF inhibitor treatment itself in order to relieve negative feedback on the RTK signaling apparatus in order to restore "signalability" to the ligand activated receptors.

Another mechanism of RAS-GTP level elevation comes from ERK-dependent transcriptional activity. Treatment with vemurafenib has also been shown to relieve active ERK-dependent repression of RTK ligand transcriptions. For example, when mutant-BRAF thyroid cells were treated with vemurafenib, transcription and autocrine secretion of the HER3 ligand neuregulin-1 (NRG1) was observed along with the activation of its receptor (Montero-Conde et al., 2013).

Ultimately, these observations were synthesized into what became known as the "RAF inhibitor paradox" (Samatar and Poulikakos, 2014). While first generation RAF inhibitors showed relatively similar in vitro potencies to various RAF isoforms, in vivo they inhibit ERK signaling in a strictly BRAF-V600E-dependent manner, and in fact stimulate ERK signaling in RAS-mutant cells. This is due to active RAS-

dependent RAF-dimerization, in which context RAF inhibitors transactivate the non-drug bound protomer and induce a negative cooperativity that limits the ability of the drug to inhibit its target effectively. Indeed, any context which induces RAF dimerization—for example, RAS activation (Hatzivassiliou et al., 2010; Poulikakos et al., 2010), N-terminal regulatory truncations of RAF (Poulikakos et al., 2011; Stanton et al., 1989)—would be expected to lead to RAF inhibitor insensitivity.

Indeed, this can be further contextualized into a view of tumor adaption to RAF inhibitor resistance (Lito et al., 2013). Initially low levels of RAS-GTP in BRAF-V600E mutant cells are due to the strong negative feedback of the constitutively high levels of activated ERK on RTKs, their signaling adaptor proteins (SPRY proteins, GRB2 and SOS phosphorylation), and on the MEK and ERK itself (including direct inhibitory phosphorylations and expression of DUSPs). This feedback inhibition prevents the signaling of RTKs, even in the presence of their activated ligands. The feedback also means that BRAF-V600E exists predominantly as a monomer that is sensitive to vemurafenib. Following RAF inhibitor treatment, RAF is inhibited along with ERK signaling, leading to a loss of feedback inhibition. RTKs in cells in this state can then be stimulated by ligands, leading to a strong increase in RAS-GTP levels. Elevated RAS-GTP levels lead to RAF dimerization and loss of RAF inhibitor binding. This leads to an increase in ERK signaling, restoring some amount ERK-dependent feedback. The cells will eventually reach a new steady state with both RTK-ligand sensitivity, some ERK activity, and relatively low drug sensitivity.

While most of the discussion to this point has been of BRAF-V600E in the context of melanoma, as mentioned earlier, BRAF-V600E mutations are also found in many other tumor types. However, in striking contrast to melanoma, RAF inhibition appears to be far less effective is most other tumor types. Indeed, a recent basket trial which enrolled all patients with BRAF-V600 mutations in various non-melanoma

cancer types demonstrated heterogeneous responses to vemurafenib treatment (Hyman et al., 2015). In BRAF-V600 non-small cell lung cancer (NSCLC), objective responses were observed in 40% of patients while no (0%) of responses were observed in a cohort of colorectal cancer (CRC) patients.

The relative insensitivity of BRAF-V600E positive CRC has been an area of intense study since shortly after the discovery of BRAF mutations. Approximately 10% of CRC patients harbor a BRAF alteration (Cancer Genome Atlas Network, 2012). Whereas BRAF-V600E positive melanoma patients demonstrate an almost 50% partial response rate to vemurafenib (Chapman et al., 2011), only 5 of 19 BRAF-V600E positive colorectal cancer (CRC) patients demonstrated a partial response in a Phase I trial (Kopetz et al., 2010). Indeed, patients with mutant-BRAF positive tumors exhibited a 70% increase in mortality over those with wild type BRAF (Van Cutsem et al., 2011).

Preclinical evaluation of BRAF-V600E CRC models demonstrated that vemurafenib could be added to several different approved treatment modalities, including the chemotherapies capecitabine and irinotecan, the anti-angiogenic antibody bevacizumab, or EGFR inhibitors cetuximab and erlotinib, to various amounts of positive benefit(Yang et al., 2012), but no mechanistic basis for these observations were uncovered.

Two studies in 2012 implicated EGFR as a key mediator of resistance to vemurafenib in CRC (Corcoran et al., 2012; Prahallad et al., 2012). A key observation is that while vemurafenib is able to durably suppress most ERK activation in the context of melanoma with only minimal tumor adaptation (Lito et al., 2013), ERK inhibition is only transient in CRC and quickly rebounds with 24 to 48 hours to 25-50% of original levels (Corcoran et al., 2012). Corcoran et al. also observed that vemurafenib relieved negative feedback on EGFR in CRC cell lines, leading to an

increase in RAS-GTP and RAF dimer formation, leading to relative vemurafenib insensitivity (Corcoran et al., 2012). Treating cells with an EGFR inhibitor with vemurafenib abrogated the increase in RAS-GTP and prevented the rebound in activated ERK. Similarly, Prahallad et al. observed that loss of ERK activity also results in a loss of CDC25C activity, a phosphatase responsible for dephosphorylating and deactivating EGFR, potentially leading to aberrantly activated EGFR (Prahallad et al., 2012).

BRAF is also commonly mutated in papillary thyroid carcinomas (Cancer Genome Atlas Research Network, 2014). In the thyroid context, vemurafenib was also unable to durable suppress ERK signaling. The mechanism observed in thyroid cancers was that loss of ERK negative feedback led to a depression of neuregulin-1 (*NRG1*) expression, a ligand that specifically activates the RTK HER3, as well as HER3 total receptor levels (Montero-Conde et al., 2013). This potent combination of permissive RTK signaling again leads to RAF dimerization and vemurafenib insensitivity.

In both of these cases, it is important to note that before vemurafenib treatment, ERK activity is insensitive to negative feedback and is largely only under the control of mutant-BRAF. Following drug treatment with vemurafenib, ERK activity then becomes dependent not only on mutant-BRAF but also on RTKs, RAS-GTP levels, and the induction of RAF dimers.

Part 5 – Drugs targeting the RAS-ERK pathway

The landscape of RAF inhibitors in preclinical development are quickly diversifying, though only two, vemurafenib and dabrafenib (Tafinlar; GSK)(Hauschild et al., 2012), are FDA approved in the setting of metastatic melanoma with BRAF-V600 mutations. Vemurafenib and dabrafenib and structurally distinct from one other,

but both are ATP-competitive and have similar pharmacodynamic profiles in that they induce paradoxical activation (via induced dimerization and transactivation) (Uehling and Harris, 2015). Many other RAF inhibitors are in clinical and preclinical development. Encorafenib (LGX818, Novartis/Array) binds in a similar manner as vemurafenib and dabrafenib but is possibly the most selective of the RAF inhibitiors described to date and also binds much more tightly with a disassociation half-life of over 24-hours (Uehling and Harris, 2015). Encorafenib still displays similar paradoxical activation, though its side-effect profile shows that it might be better tolerated due to the lower doses required.

Together, these drugs are "first-generation" RAF inhibitors that derive most of their clinical benefit in the BRAF-V600 contexts as they activate ERK signaling in the BRAF-wild type setting. A newer generation of drugs have been designed to avoid paradoxical activation (Arora et al., 2015). This class of drugs has been termed "paradox breakers." Several of these paradox breaking drugs have recently been introduced, and some have even entered into clinical trials (Uehling and Harris, 2015). One of the best described of these BRAF-mutant selective paradox breakers is PLX8394 (Plexxikon) (Zhang et al., 2015) in that it demonstrates some selectivity for mutant-BRAF over wild type RAF alleles, is able to inhibit mutant-BRAF signaling, yet ultimately fails to induce RAF signaling in the RAS-mutant/RAF wildtype context. Of note in glioma, a preclinical version of PLX8934 (PLX PB-3) was able to inhibit a constitutively active BRAF dimer where the N-terminal regulatory region of BRAF is translocated in frame with a portion of the *KIAA1549* gene (known as BRAF:KIAA1549) (Sievert et al., 2013). This fusion was shown to constitutively dimerize, which would be expected to make it insensitive to vemurafenib, which was demonstrated. However, PLX PB-3 was able to inhibit fusion BRAF signaling while vemurafenib paradoxically activated it. Another of these compounds is PLX7904

(Plexxikon) which failed to elicit ERK activation is RAS-mutant/RAF wildtype cells and was also shown to inhibit mutant-BRAF in melanoma cells that were resistant to vemurafenib due to acquiring a mutant NRAS allele, leading to RAS activation and RAF dimerization (Le et al., 2013). The drug failed to inhibit ERK activation in the NRAS-mutant/RAF-wildtype setting however. The observation the PLX7904 is able to inhibit the growth of NRAS-mutant/BRAF-mutant cells but not NRAS-mutant/RAF-wildtype suggests that the drug binds to mutant-RAF in mutant-BRAF/CRAF dimers, inhibits the mutant-BRAF protomer, but most importantly, fails to transactivate the CRAF protomer.

The drug TAK-632 (Takeda) (Nakamura et al., 2013) showed reduced paradoxical activation relative to vemurafenib. At low concentrations TAK-632 modestly induced MEK and ERK activation, but as the concentration increased, the drug inducted the formation of BRAF/CRAF heterodimers, but completely inhibited RAF kinase activity (as measured by MEK and ERK activation). The drug also demonstrated a very low off rate and remained bound which is the most likely reason for durable dimer inhibition.

The drug BGB-659 (Beigene, Millennium Pharmaceuticals) is another such paradox breaker (Gould et al., 2011). The drug binds both sites of BRAF dimers with similar affinities. BGB-659 inhibits mutant-BRAF signaling from V600E monomers and dimers (p61-BRAF-V600E) at similar concentrations (Yao et al., 2015b). In addition, the drug has paradoxical activating activity in the wild-type RAF and wild-type RAS context, which suggests that the drug should inhibit mutant BRAF signaling while sparing wild-type RAF signaling in other tissues of the body, widening its therapeutic window.

Some newer drugs are the pan-RAF inhibitors. These drugs are potent towards all RAF isoforms (ARAF, BRAF, and CRAF), including both mutant (V600) and wild-

type. The recently described drug LY3009120 is one such compound (Peng et al., 2015). Similar to TAK-632, LY3009120 induces both BRAF/CRAF heterodimerization and BRAF/BRAF homodimerization, yet effectively inhibits RAF kinase activity. LY3009120 also inhibits ERK signaling in RAS-mutant cells (0.384-1.17 μM), though at higher concentrations than what is required in mutant-BRAF cells (0.010-0.446 μM). Consistent with an ability to block RAF signaling in a RAS-mutant context, these drugs would be expected to have a narrower therapeutic window than vemurafenib or BGB-659 though they are tolerated in vivo and are able to induce tumor regression in both BRAF-V600E and KRAS mutant xenograft models.

Part 6 – BRAF mutations in tumor types other than melanoma

Although much research has been conducted to understand BRAF mutations in melanoma, CRC, and thyroid tumors, less is known about how BRAF mutations function in glioma. While about 3% of Grade IV GBM harbor the canonical BRAF-V600E mutation, other gliomas have different BRAF mutations. In low grade gliomas (especially pilocytic astrocytoma,) BRAF fusions, including the BRAF:KIAA1549 fusion are a defining hallmark genetic lesion (Sievert et al., 2013). In these fusions, the N-terminal region of BRAF (and sometimes CRAF) is lost, leading to the constitutive dimerization and kinase activity. Indeed, these RAF fusions have been demonstrated to undergo paradoxical activation by vemurafenib.

Less is known about the sensitivity of BRAF-V600E mutations in glioma. Work by the James group have shown in preclinical experiments that these tumors are dependent on BRAF for proliferation using short-hairpins to known down BRAF expression (Nicolaides et al., 2011). Also, vemurafenib can inhibit mutant BRAF signaling in the cells as well. Indeed, vemurafenib extended survival in mice bearing

intracranial xenografts of BRAF-V600E glioma cell lines by approximately a week (median survival was extended from 20 days in vehicle treated mice to 27 in vemurafenib treated mice).

The James group has also explored if combining vemurafenib with other treatment regiments might be able to augment their efficacy. Indeed, they showed that BRAF mutations cooperate with *CDKN2A* loss to induce the formation of high grade gliomas in transgenic mouse models (Huillard et al., 2012), consistent with reports that constitutively active alleles of BRAF alone tend to cause oncogene induced senescence and require a second mutation for oncogenic bypass (Michaloglou et al., 2005). These tumors also responded to both BRAF inhibition with vemurafenib and CDK4/6 inhibition with PD-0332991 as monotherapies. Combination therapy provided an additive (as opposed to a synergistic) effect. An additive positive benefit has also been observed when BRAF-mutant gliomas were treated with radiation and a low dose of vemurafenib, although the group failed to establish a mechanistic basis (Dasgupta et al., 2015).

Although the evidence that vemurafenib treatment is beneficial in BRAF-mutant glioma seems to be relatively well established, its efficacy in comparison to other BRAF-mutant tumors is less well understood. A survey of case reports in all types of gliomas with BRAF-V600E mutations has found that of 28 cases of various histology, most patients at best achieved stable disease or a partial response (Preusser et al., 2016). In a basket trial which enrolled patients with non-melanoma tumors with BRAF-V600E mutations, a similarly varied response was observed, with two of five patients progressing, and two of five achieving a partial response (Hyman et al., 2015).

Why exactly BRAF-V600E gliomas seem to be relatively insensitive to BRAF inhibitors is also relatively not well known. The James group has suggested that EGFR becomes feedback reactivated following BRAF inhibition though ERK-mediated loss

of expression of the EGFR inhibiting phosphatase PTPN9 (Yao et al., 2015a), ultimately preventing durable pathway suppression. This would be consistent with the mechanisms observed in CRC and thyroid tumors (Corcoran et al., 2012; Montero-Conde et al., 2013; Prahallad et al., 2012). While the president for such a mechanism existing in glioma is possible, the data the group presented are inconclusive. While neratinib (also known as HKI-272) is a potent EGFR inhibitor, it also inhibits the entire ERBB family of proteins, as well as a whole suite of other kinases (Fabian et al., 2005). While the in vivo data showed a 10% increase in the median survival time over either drug as a monotherapy, most of the other data the presented fail to demonstrate an additive effect between the drugs beyond the efficacy of each drug as a mono-therapy. Indeed, neratinib alone as a monotherapy shows efficacy in most of their assays, despite the fact that the authors' model posits that EGFR must be feedback reactivated by vemurafenib first.

CHAPTER 2: BRAF-V600E GLIOMA IS GENETICALLY DEPENDENT ON MUTANT BRAF

Introduction

Traditionally cancer patients in the clinic have received very similar treatments for their tumors. These treatments, like ionizing radiation and cytotoxic chemotherapy, are usually very toxic. However, following the advent of high throughput DNA sequencing in recent years, determining which genes are mutated in a given patient's tumor has become more routine. This information has begun to inform decisions as to which treatments parents might benefit from based on the specific mutations found within their tumors.

Gliomas, a general term for tumors of the central nervous system, account for a disproportionate amount of morbidity and mortality, despite being relatively more uncommon that other tumor types. However, few treatments available for glioma patients, who are typically treated with bulk surgical resection, radiation, and chemotherapy. However, if clinicians knew more about which mutations these patients' tumors harbored, they might be able to use more effective and less toxic tailored drugs.

For instance, various mutations found in human cancer can activate the RAS-RAF-MEK-ERK (RAS-ERK) signaling pathway, and there are several drugs designed to inhibit oncogenic RAS-ERK signaling. The RAS family of genes are the most commonly mutated in all cancers, found in approximately one-third of all tumors (Samatar and Poulikakos, 2014). However, while mutations in RAS do occur in glioblastoma (GBM), they are vanishingly rare (Knobbe et al., 2004).

While RAS activates the protein RAF, activating mutations in the *BRAF* gene are also found in approximately 8% of all tumors. These mutations are most common in melanoma where they make up approximately 50% of sequenced tumors. BRAF-mutant melanoma is highly addicted to mutant-BRAF signaling to MEK and ERK (Samatar et al.,, 2012). Specific inhibitors of MEK and ERK signaling in BRAF-mutant melanoma result in profound responses, leading to dramatic tumor shrinkage.

Several reports that surveyed the frequency of RAF mutations in gliomas have suggested that BRAF is recurrently mutated (Horbinski 2014). The frequency of these mutations varies based of the histology of the tumor type. Therefore, we sought to verify the frequency of BRAF alterations in gliomas and determine if they are similarly dependent on mutant-BRAF signaling like in melanoma.

Results

We initially sought to verify and summarize the frequency of BRAF alterations in gliomas based on databases of mutations in gliomas whose DNA has been sequenced.

A

	BRAF histology					
BRAF alteration	**PA**	**PMA**	**PXA**	**GG**	**DA**	**HGG**
B–K fusion	66.6 %	50.0 %	0.0 %	21.2 %	11.9 %	0.0 %
V600E	5.7 %	7.7 %	73.8 %	19.2 %	9.7 %	13.1 %

B

	Total tumors analyzed	BRAF Mutations		BRAF Fusions	BRAF Amplification
		V600	Other		
IMPACT	**462**	4	6	4	9
TCGA	**273**	5	1	0	0
Total	**735**	9	7		9
	3.5%	**1.2%**	**1.1%**	**0.5%**	**1.2%**

Figure 2-1. Frequency of BRAF alterations in adult human glioma. Shown is the frequency of human glioma samples harboring a BRAF missense mutations, fusion, or gene amplifications. (A) Frequency of BRAF-V600E and BRAF:KIAA1549 fusions as compiled by Horbinski C, *J Neuropathol Exp Neurol*. 2013. **(B)** The numbers are from two different datasets. The Cancer Genome Atlas (TCGA) only includes patients with glioblatoma (WHO grade IV), whereas the MSKCC in-house sequencing database (IMPACT) includes glioblastoma and lower grade (WHO grade II/III) gliomas. B-K – *BRAF:KIAA1549*; PA - pilocytic astrocytoma; PMA - pilomyxoid astrocytoma; PXA - pleomorphic xanthoastrocytoma; GG - ganglioglioma; DA - grade II diffuse astrocytoma; HGG = high-grade glioma (grade III and IV).

We first looked at a literature review of BRAF mutations in gliomas (**Figure 2-1A**). Horbinski complied the total frequency of BRAF-V600E mutations from various

references as of 2013, comprising over 700 tumors of various histologies (Horbinski, 2013). In these tumors, BRAF-V600E mutations were found most frequently in PXA (~74%), GG (~20%), and HGG (~13%). BRAF:KIAA1549 fusions were most commonly found in PA (~66%) and PMA (~50%). Interestingly, thiese BRAF fusions were never found in HGG. They were exclusively confined to lower grade tumors.

Because literature resources can over-report the frequency of mutations, we looked at a more unbiased approach to determining the frequencies of BRAF alterations. To do so, we analyzed the results of the IMPACT database (**Figure 2-1B**). Tumors from patients treated at Memorial Sloan Kettering are submitted for IMPACT testing, which sequences a panel of cancer related genes, including *BRAF*. These patients include lower grade glioma (WHO Grade I and II) as well has higher grade gliomas (WHO Grade III and IV) of various histologies. Of 462 analyzed gliomas, 10 point mutations were recorded, of which 4 were BRAF-V600E.

There were 4 recorded BRAF fusions. Two tumors had in-frame *BRAF:KIAA1549* mutations, while single reports of *BRAF:CCDC6* and *BRAF:FAM131B* were recorded. Finally, 9 patients had BRAF copy number gain. Next, we looked at the set of Grade IV glioblastoma tumors analyzed by the TCGA project. Of these 273 tumors, 5 had V600E mutations, while 1 patient had a mutation elsewhere.

Overall, this suggests that BRAF is indeed recurrently mutated in gliomas. The most common mutation in BRAF is the canonical BRAF-V600E mutation, although this mutation only appears to be mutatured at a frequency at around 1% of tumors. BRAF fusions are very common in lower grade tumors like PA and PMA where they make up substantial proportions of the populations of these tumors. Indeed, BRAF fusions are considered diagnostically indicative of PA in the clinic. While the proportion of BRAF-V600E mutations appears to be slightly higher as calculated by

Horbinski, this is likely because literature resources are biased towards finding and describing these mutations. Similarly, IMPACT and TCGA are more unbiased in which tumors are analyzed. However, the boas of IMPACT testing towards including lower grade gliomas is revealed in the frequency of BRAF fusions detected.

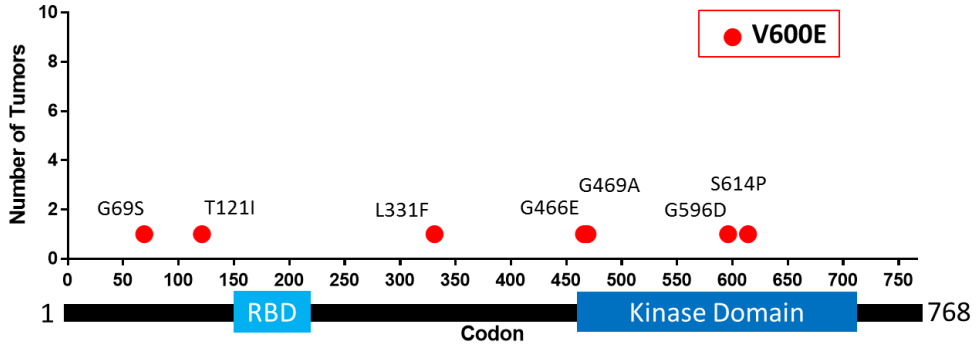

Figure 2-2. Localization of *BRAF* mutations in glioma. Shown are all mutations identified in the TCGA and IMPACT dataset. The most common mutation observed is a hotspot valine to glutamate mutation at codon 600.

We next mapped the missense mutations reported by IMPACT testing and in the TCGA data set of tumors (**Figure 2-2**). By far the most frequent mutation was the canonical BRAF-V600E mutation in the kinase domain on BRAF. Interestingly, of the 539 tumors in the IMPACT data set with BRAF mutations (out of a total 9235 tumors), only the G446, G469A, and G596D mutations were reported in tumors of any other type. All other BRAF mutations were unique to glioma in the IMPACT database. However, some of these mutations, like S614, have been described in melanoma by others (Chiappetta).

The G466, G469, and G596 mutations are also recurrent hotspots that are mutated both within and across tumor types, as measured by Chang (Chang et al., 2016), though at lower frequencies much lower than V600E. These mutations have

been functionalized. Mutations at G469 greatly stimulate BRAF activity and are insensitive to vemurafenib (Yao et al., 2015b). Mutations at G466 and G596 actually have impaired kinase activity than wild type BRAF, but induce oncogene MEK signaling through increased dimerization and activation with CRAF(Kamata et al., 2010).

From this, we conclude that while V600E is the most common mutational hotspot in glioma, other mutations recurrently found in other tumor types suggest that BRAF activation is a common feature of all of these tumor types.

		BRAF
BRAF mut.	AM38	**V600E** 227/228 98%
	DBTRG	**V600E** 91/287 31%
	NMCG1	**V600E** 300/531 56%
	KG1C	**V600E** 257/518 49%

		BRAF
BRAF wild type	8MBGA	-
	A172	-
	A204	-
	A431	-
	GBM39	-
	M059K	-
	OSU1123	-
	OSU326	-
	OSU528	-
	OSU83	-
	SW1783	-
	T98G	-
	TS516	-
	TS543	-
	TS561	-
	TS565	-
	TS590	-
	TS596	-
	TS600	-
	TS603	-
	TS608	-
	TS616	-
	TS676	-
	TS725	-
	TS753	-
	TS885	-
	TS905	-
	U251	-
	U87MG	-

Figure 2-3. Identification of four human glioblastoma cell lines with BRAF mutations. Shown are DNA sequencing results from 33 human glioma cell lines. Genomic DNA was isolated from 33 glioma cell lines and then sequenced on an Ilumina MiSeq next generation sequencing instrument to a depth of ~200-500 reads.

We next sought to identify cell lines with the BRAF-V600E mutation that we could use to study BRAF signaling. We isolated genomic DNA from a panel of human glioma cell clines and used high throughput DNA sequencing. By sequencing to a depth of 200-500 reads, we could determine if BRAF-V600E mutations were present and their allelic frequencies.

We found four cell lines with BRAF-V600E mutations: AM38, DBTRG, NMCG1, and KG1C (**Figure 2-3**). All 4 cell lines had a BRAF c.1799 T>A transversion resulting in a valine 600 to glutamic acid mutation. Of the total 228 sequencing reads for AM38, 98% were mutant, indicating that AM38 has a homozygous BRAF mutation. All other cell lines had about a 50% allelic frequency of BRAF-V600E, indicating that they possessed both a wildtype and mutant copy of BRAF. The allelic frequency for DBTRG was 31%, possibly suggesting aneuploidy at the BRAF locus. Nevertheless, there were sufficient reads of the BRAF-V600E allele to conclude that they had at least one copy of the BRAF-V600E allele.

The other 29 cell lines we sequenced were all wildtype for BRAF across their entire coding sequences.

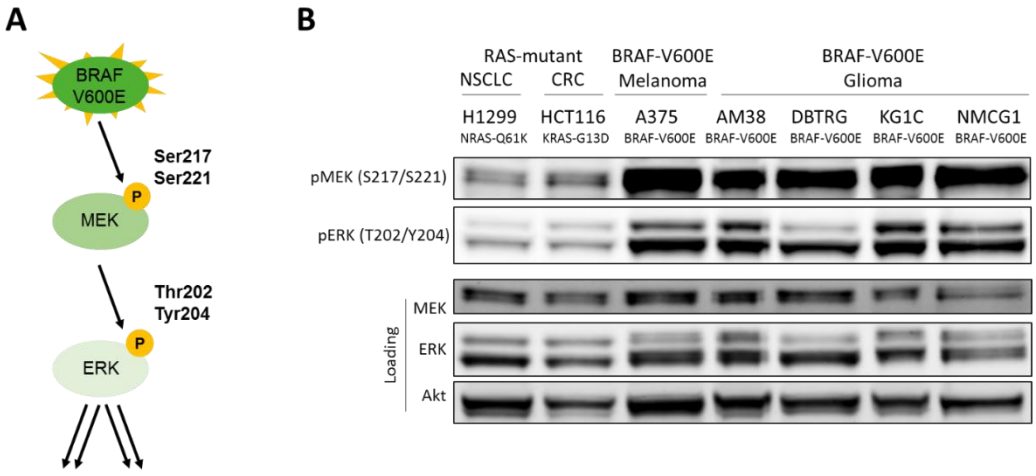

Figure 2-4. BRAF-V600E mutant glioma cell lines have high levels of phosphorylated MEK and ERK protein. (A) Simplified depiction of BRAF pathway signaling. **(B)** Immunoblot of whole cell lysates from seven different human cancer cell lines with RAS or BRAF-V600E mutations. The name of the cell line and mutation is indicated above each lane. were subjected to immunoblot analysis for the indicated proteins. NSCLC – Non-small cell lung cancer; CRC – colorectal cancer.

After identifying 4 cell lines with BRAF-V600E mutations, we next sought to determine if mutant-BRAF signals similarly in glioma and melanoma. We compared the four BRAF-mutant glioma cell lines to two RAS-mutant cell lines—the non-small cell lung cancer cell line H1299 and the colorectal cell line HCT116—as well as the BRAF-mutant melanoma cell line A375.

H1299 and HCT116 both had activated MEK and ERK signaling as determined by immunoblot for phosphorylation of MEK at S217 and S221 (pMEK), and of ERK at T202 and Y204 (pERK) (**Figure 2-4**). However, they had much lower

levels of pMEK and pERK than both BRAF-mutant A375 and the BRAF-mutant glioma cell lines, which uniformly possessed very high levels of pMEK and pERK.

The observation that the RAS-mutant cell lines have lower levels of pMEK and pERK despite having constitutively active RAS is consistent with the model that although RAS mutations are constitutively activating, they are sensitive to ERK-dependent feedback inhibition of components of RAS and RAF signaling(Pratilas et al., 2009). Conversely, BRAF-V600E is insensitive to this feedback and therefore has much higher levels of pERK and pMEK.

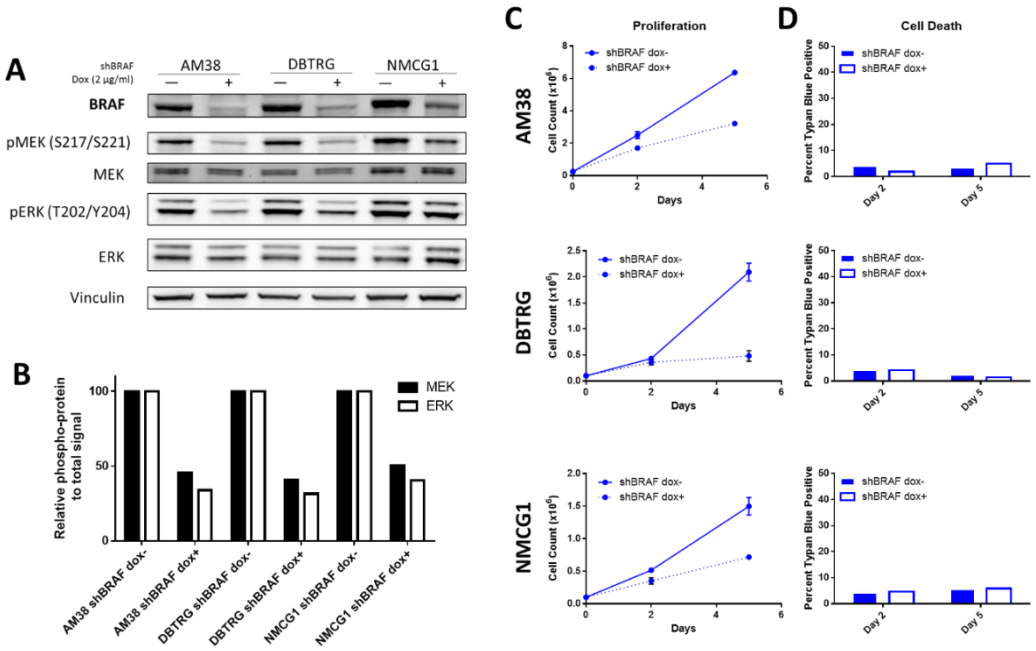

Figure 2-5. Knockdown of BRAF impairs growth of BRAF-V600E mutant glioma cell lines. (A) Immunoblot of whole cell lysates from BRAF-V600E glioma cell lines which were engineered to stably express a doxycycline inducible *BRAF* shRNA cassette and were treated with vehicle (lanes 1,3,5) or doxycycline (2 µg/ml) (lanes 2,4,6) for three days prior to lysis. **(B)** Graph of the relative signal intensity of pERK to total ERK or pMEK to total MEK for the immunoblot in (1-5A) **(C)** Effect of doxycycline induced BRAF knockdown on the growth and induction of cell death of BRAF-V600E glioma cell lines. Cells stably expressing a doxycycline inducible shRNA vector to BRAF were grown in vehicle or doxycycline (2 µg/ml) and the number of viable cells were counted in a trypan blue exclusion assay after the indicated number of days.

After determining that mutant-BRAF results in high pMEK and pERK signaling, as it does in melanoma, we next wanted to determine if BRAF-mutant glioma is dependent on constitutive BRAF signaling for proliferation. To do so, we knocked down BRAF protein by generating BRAF-mutant glioma cells lines which stably express a doxycycline inducible shRNA to *BRAF*. Treating these cells with doxycycline knocked down BRAF protein in all three cell lines (**Figure 2-5A**).

BRAF knockdown also resulted in concomitant decreases in pERK and pMEK signaling. This doxycycline induced decrease in pMEK and pERK, quantitated in **1-5B**, was greater than 50% of the vehicle treated cells in all cell lines. This indicates that lowering the amount of BRAF-V600E protein effectively decreases signaling flux through the pathway.

ERK signaling has many biological roles, but one of its primary outputs is stimulation of cellular proliferation. Therefore, we next asked if BRAF knockdown could inhibit the proliferation of BRAF-mutant glioma cells. To do so, we plated the BRAF-mutant glioma cell lines into doxycycline or vehicle for three days to deplete them of BRAF protein, then plated them in replicates and counted the number of viable cells at 2 and 5 days post-plating. Doxycycline induction of BRAF knockdown significantly decreased proliferation in all three cell lines (Figure 2-**5C**). DBTRG cells were the most sensitive to BRAF knockdown and were almost completely growth arrested. While BRAF knockdown caused a significant decrease in proliferation, it did not affect cell viability as measured in a trypan blue exclusion assay. We observed no induction of cell death above background in all three cell lines (**Figure 2-D**). This is consistent with the main phenotypic output of ERK signaling affecting proliferation and cell growth rather than survival and apoptosis. This confirms that BRAF-mutant glioma cells are dependent on BRAF-V600E for both MEK and ERK signaling as well as for tumor maintenance, but not for cell survival.

Under physiological conditions, either RAS-GTP dependent heterodimerization (for example, BRAF/CRAF) or homodimzerization (for example, BRAF/BRAF) of RAF proteins is required for RAF signaling (Lavoie and Therrien, 2015). However, in BRAF-mutant tumors, BRAF is thought to signal as a monomer because high levels of ERK-dependent feedback prevent the accumulation of sufficient levels of RAS-GTP to cause the formation RAF dimers, leaving BRAF in a predominantly monomeric state. To confirm the hypothesis that CRAF is dispensable for BRAF-mutant signaling in BRAF-mutant glioma, we knocked down CRAF protein by generating BRAF-mutant glioma cells lines which stably express a doxycycline inducible shRNA to *RAF1*.

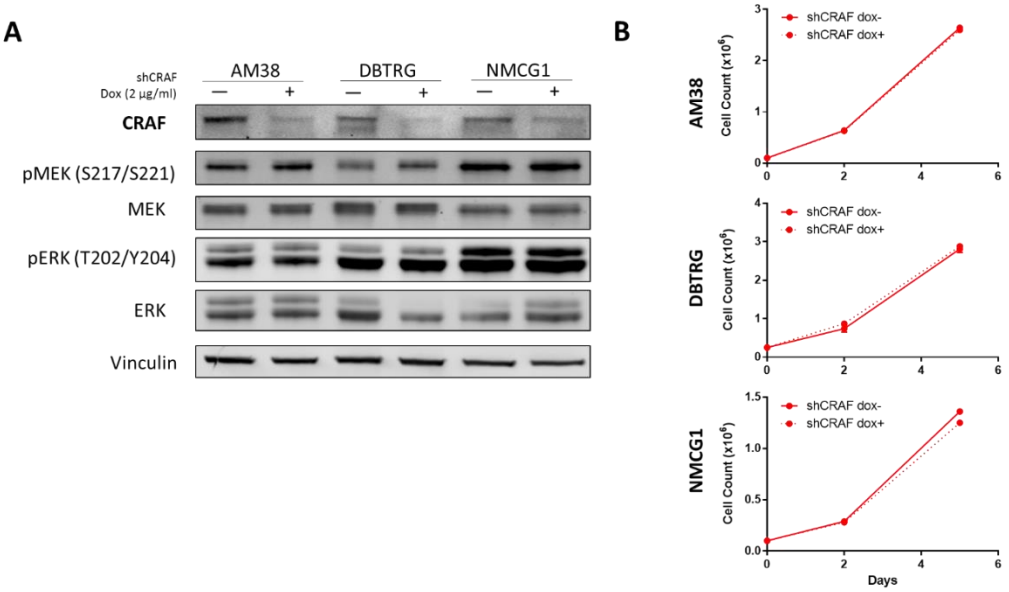

Figure 2-6. CRAF knockdown does not reduce MEK/ERK activity or growth of BRAF-V600E mutant glioma cells (A) Immunoblot of whole cell lysates from BRAF-V600E glioma cell lines which were engineered to stably express a doxycycline inducible *RAF1* (CRAF) shRNA cassette and were treated with vehicle (lanes 1,3,5) or doxycycline (2 µg/ml) (lanes 2,4,6) for three days prior to lysis. **(B)** Effect of doxycycline induced CRAF knockdown on the growth BRAF-V600E glioma cell lines. Cells stably expressing a doxycycline inducible shRNA vector to BRAF were grown in vehicle or doxycycline (2 µg/ml) and the number of viable cells were counted in a trypan blue exclusion assay after the indicated number of days.

Doxycycline induced CRAF knockdown was effective in all three BRAF-mutant cell lines tested (**Figure 2-6A**). However, in contrast to BRAF knockdown, CRAF knockdown resulted in no perturbation of pMEK and pERK signaling. Furthermore, CRAF knockdown also had no effect on the proliferation of the three BRAF-mutant cell lines (**Figure 2-B**). This is consistent with current models of BRAF signaling, suggesting that CRAF is not a necessary heterodimerization partner for

mutant-BRAF nor do CRAF/CRAF homodimers play a significant role in MEK/ERK signaling in mutant-BRAF tumors.

BRAF phosphorylated and activates its only known substrates MEK1 and MEK2 to transduce its signal. To confirm the role of MEK-ERK signaling in mutant-BRAF glioma we employed the highly potent and selective allosteric MEK inhibitor trametinib. Trametinib binds to a site adjacent to the MEK kinase domain and rapidly inhibits its kinase activity.

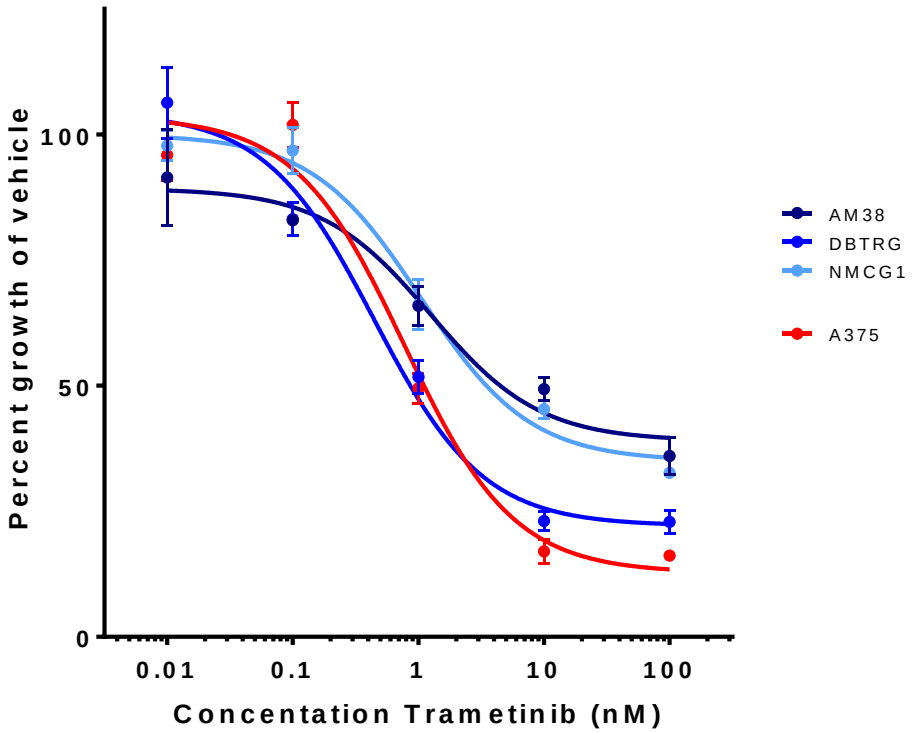

	A375	DBTRG	AM38	NMCG1
IC50	0.7709	0.4427	1.258	1.044

Figure 2-7. MEK kinase activity is required for proliferation of BRAF-V600E glioma. BRAF-mutant glioma cell lines were plated in various doses of trametinib for 5 days, then counted in a trypan blue exclusion assay. Normalized cell counts were plotted and the resulting growth inhibition curves plotted in Prism Graphpad. Immunoblots of each cell line treated with trametinib are shown.

Trametinib significantly inhibits the proliferation of all three mutant-BRAF glioma cell lines, with IC50s ranging between 0.5 and 1.5 nM trametinib, similar to the IC50 of the BRAF-mutant cell line A375 (**Figure 2-7**). This inhibition of proliferation indicates that MEK kinase activity is necessary to BRAF-mutant tumors, confirming the role of MEK in transducing activated BRAF signaling. This activity is

further consistent with trametinib being FDA approved for the treatment of BRAF-mutant metastatic melanoma where it has achieved quite some success.

Discussion

While BRAF mutations are not as common in glioma as they are in other tumor types like melanoma, it is important to understand their biology. BRAF-V600E mutations directly drive MEK/ERK signaling in glioma. We demonstrated this by showing that they have high levels of pMEK and pERK and further demonstrated that knockdown of BRAF protein lowers signaling through MEK and ERK by using a shRNA to *BRAF*. Finally, we showed that MEK kinase activity is required for the proliferation of BRAF-mutant melanoma. Inhibited MEK kinase activity with an inhibitor potently slows the proliferation of BRAF-mutant glioma like it does in BRAF-mutant melanoma.

While much work has been devoted specifically to understanding BRAF-V600E mutations in many tumor types, it is interesting to think of the other BRAF mutations that occur in gliomas. The fact that other highly activating BRAF mutations, like the G469 mutation, and the CRAF activating G466 and G596 mutations occur suggests that activated BRAF signaling is likely important to certain gliomas outside of the V600E context specifically.

Furthermore, some BRAF mutations are found at at higher frequencies than BRAF-V600E to the point that they are even considered diagnostic in some cases. This further suggests that when mutationally activated, BRAF likely plays a significant role in many types of gliomas. Its possible that being able to understand its biology in the V600E context will help us to understand it in other contexts.

CHAPTER 3: EFFECTS OF VEMURAFENIB IN BRAF-MUTANT GLIOMA.

Introduction

After the discovery of the V600E mutation in melanoma, several groups set out to validate it as a therapeutic target. Following studies that BRAF-V600E mutant cell lines were highly sensitive to genetic ablation of BRAF and the creation of genetic engineered mouse models of mutant-BRAF driven cancers, the pharmaceutical industry set out to identify selective inhibitors of BRAF.

The first of these drugs to be FDA approved was the drug vemurafenib, approved in 2011 for BRAF-V600E mutant metastatic melanoma. In vitro, vemurafenib showed a slight selectivity for mutant-BRAF over wild-type BRAF. In vivo, the drug potently inhibited utant-BRAF signaling, extinguishing pMEK and pERK signaling, and leading to dramtic reductions in tumor volume. However, the drug only inhibited mutant-BRAF signaling. In fact, the drug hyperactivated wild-type BRAF signaling in cells with activated RAS, a phenomenon known as the RAF-inhibitor paradox.

BRAF inhibitors have been tested in various tumor types. In fact, a current type of clinical trial known as a “basket trial” enrolls a patient with any tumor type provided that he or she has a given mutation. While responses to vemurafenib and similar drugs has been quite dramatic in melanoma, the response in other tumor types has been more heterogeneous. Therefore, we first sought to describe the acute and long term biochemical and biological response of BRAF-mutant glioma to vemurafenib in order to help us understand whether or not this drug might be effective.

Results

We first treated BRAF-mutant glioma cells with a range of doses of vemurafenib encompassing the typical IC50 of a BRAF-mutant cell line (**Figure 3-1A**). At higher doses (10 μM) of vemurafenib, pMEK and pERK are completely inhibited. As the concentration of vemurafenib decreases, pMEK and pERK increase. From the immunoblot, we estimate that the IC50 of pMEK and pERK inhibition is between 100 and 1000 nM vemurafenib. We plotted the inhibition curves of pERK in response to vemurafenib and confirmed that the IC50s fall between 100 and 200 nM vemurafenib.

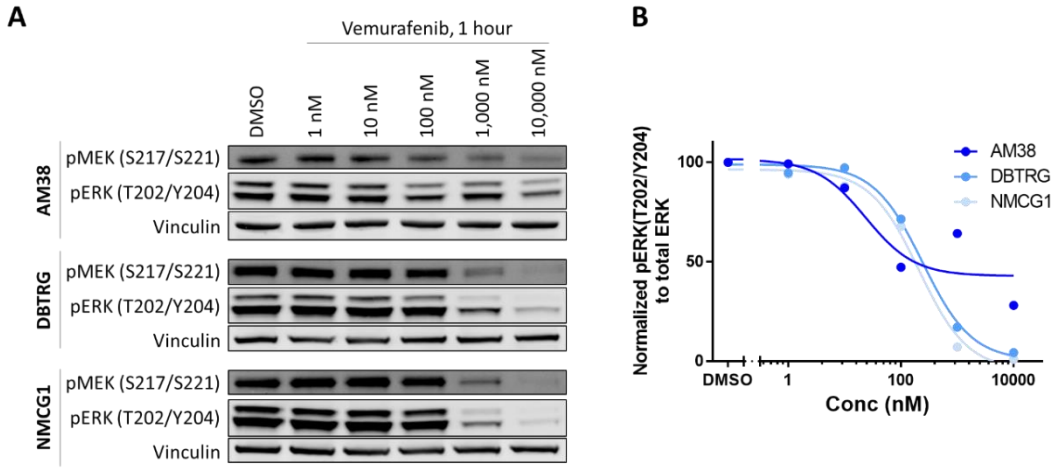

Figure 3-1. Biochemical effects of short-term (1 hour) treatment of BRAF-V600E GBM cells with vemurafenib. (A) Immunoblot of whole cell lysates from BRAF-mutant glioma cell lines treated with vemurafenib for 1 hour. **(B)** Relative signal intensity of phosphorylated ERK to total ERK from (2-1A) was calculated and the resulting inhibition curve plotted in GraphPad Prism.

Interestingly, AM38 appears to have some residual pMEK and pERK even at the highest doses of vemurafenib (**Figure 3-1A**). Three cell lines express relatively

similar levels of total BRAF protein (**see Figure 3-5A**). However, the BRAF antibody does not distinguish between wildtype and mutant BRAF protein. AM38 has a homozygous BRAF-V600E mutation (**see Figure 3-3**), so while the BRAF signal for DBTRG and NMCG1 is split between mutant and wildtype-BRAF, the entire BRAF signal for AM38 must be all mutant-BRAF. High levels of mutant-BRAF protein can induce the formation of BRAF-V600E homodimers (Shi et al., 2012). Vemurafenib only inhibits monomeric mutant-BRAF, so we hypothesize that the residual signal in AM38 is due to the formation of some BRAF-mutant homodimers that become transactivated in the presence of vemurafenib.

After confirming that vemurafenib can effectively inhibit BRAF-V600E in BRAF-mutant glioma, we next sought to compare the acute IC50 for pERK inhibition with that of a panel of BRAF-mutant melanoma lines to determine if mutant BRAF protein could be similarly inhibited in both tumor types. Using a more granular dilution series of vemurafenib, we treated a panel of BRAF-mutant glioma and melanoma cell lines for one hour and then visualized the amount of pERK and total ERK protein using an immuno-infrared assay (**Figure 3-2A**). The IC50 for pERK visually appears to be very similar in all three cell lines of each type.

We then calculated the signal intensity of pERK and total ERK in each well and plotted the resulting inhibition curves to determine the IC50 for vemurafenib induced pERK inhibition. The IC50s for all the cells lines were almost identical, falling between the range of 80-180 nM vemurafenib for BRAF-mutant glioma and 80 and 110 nM for BRAF-mutant melanoma. AM38 again had a slightly higher IC50 and the greatest amount of residual pERK. We again hypothesize that this is due to the formation of a small amount of vemurafenib-insensitive mutant-BRAF homodimers for the above mentioned reasons.

From this data we conclude that there are no significant differences between the biochemical identities of the BRAF-V600E protein in BRAF-mutant glioma and in BRAF-mutant melanoma, as it can be inhibited by vemurafenib at very similar concentrations.

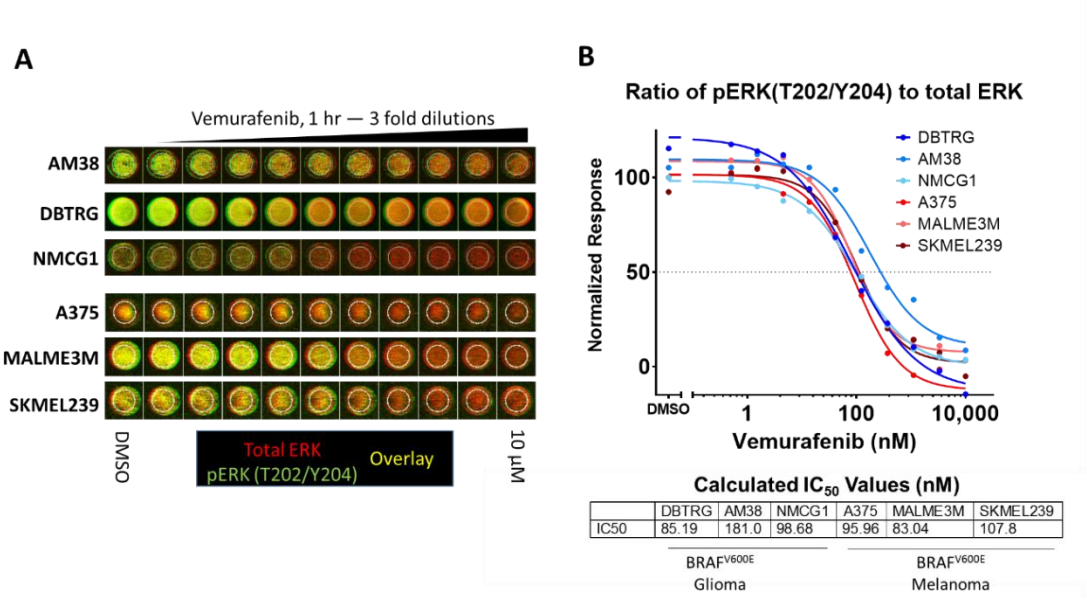

Figure 3-2. Comparison of short term (1 hour) vemurafenib IC50s between BRAF-V600E glioblastoma and melanoma cell lines. Shown are data from an immuno-infrared assay. (A) BRAF-mutant glioma and melanoma cells were treated with 3-fold dilutions of vemurafenib for 1 hour, fixed and permeabilized, then stained with IR-dye conjugated antibodies to total ERK (red) and phosphorylated-ERK (green). Representative images are shown. **(B)** Relative signal intensity of phosphorylated ERK to total ERK from (2-2A) in each well was calculated and the resulting inhibition curve plotted and IC50 calculated in GraphPad Prism. Error bars have been omitted for clarity.

After confirming that vemurafenib is able to inhibit mutant-BRAF signaling in BRAF-mutant glioma after one hour of treatment, we next asked whether vemurafenib continued to inhibit mutant-BRAF signaling over a longer period of treatment. We used 2 μM vemurafenib, a dose that inhibits most pMEK and pERK after one hour of treatment (**Figure 3-3A**). After confirming near complete inhibition of pMEK and pERK after one hour of treatment with vemurafenib, we then compared it to the level of pERK inhibition after 48 hours of treatment. We observed that pERK levels rebounded after 48 hours of vemurafenib treatment. Quantifying the pERK to total ERK signal revealed that this rebound was between 25-70% of the original pERK signal (**Figure 3-3B**).

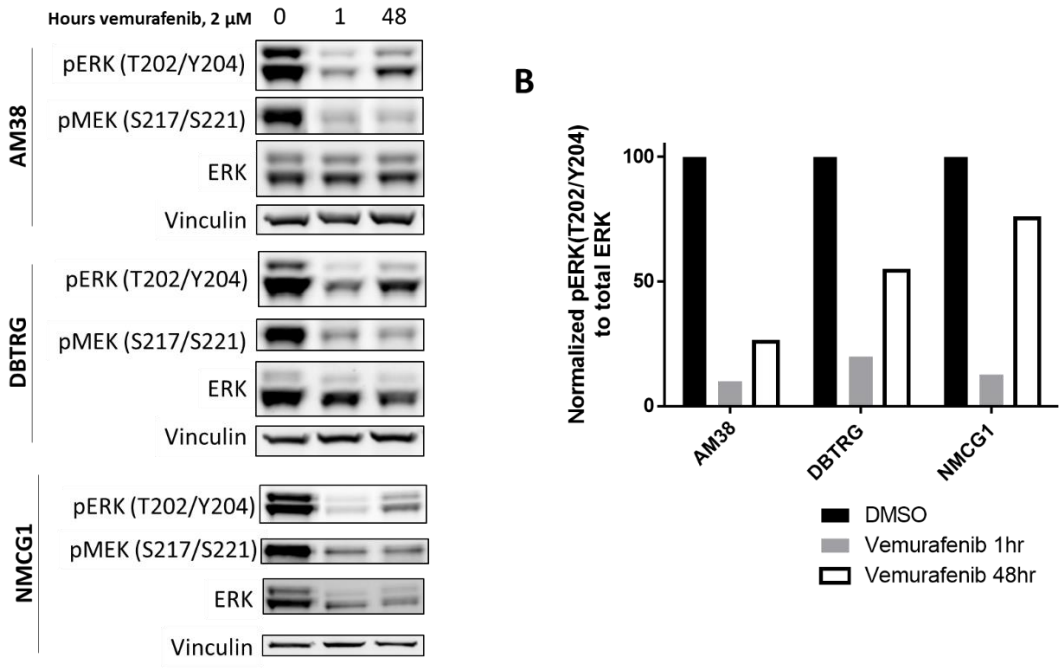

Figure 3-3. Rebound activation of ERK after 48 hours of vemurafenib treatment in BRAF-mutant glioma. (A) Immunoblot of whole cell lysates from BRAF-mutant glioma cells treated with vemurafenib for the indicated times. **(B)** Graph of the relative signal intensity of phosphorylated ERK to total ERK from (2-3A).

Rebound of pERK in the presence of vemurafenib is a well-documented phenomenon and most often is associated with the relief of negative feedback activating CRAF, leading to the formation of vemurafenib-insensitive BRAF/CRAF dimers (Samatar and Poulikakos, 2014). A high magnitude of this negative feedback relief is often associated with a lack of biological response to vemurafenib. However, it has also been shown that BRAF-mutant melanoma cells, which in general are sensitive to vemurafenib can also have some amount of pERK rebound through the same mechanisms.

Therefore, we sought to compare the magnitude of pERK rebound in BRAF-mutant glioma versus BRAF-mutant melanoma. Using the same concentration of vemurafenib, we studied the kinetics of pERK rebound in a panel of BRAF-mutant glioma and BRAF-mutant melanoma cell lines in a time course of vemurafenib treatment, collecting samples at several time points across 48 hours of treatment.

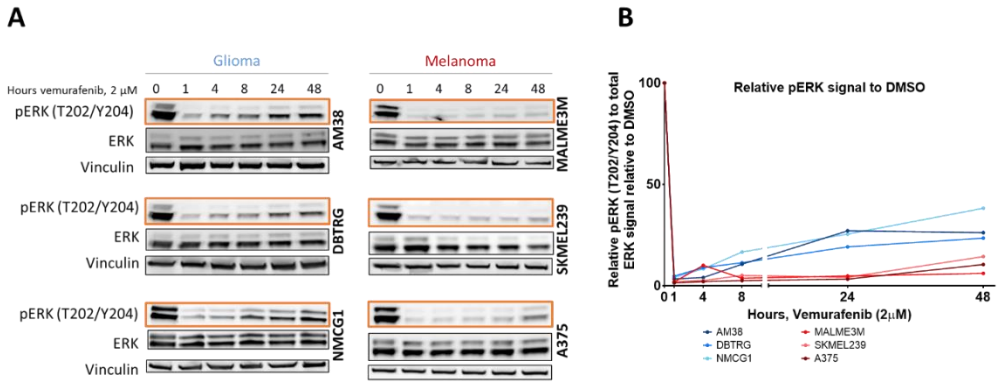

Figure 3-4. Kinetics of ERK reactivation following vemurafenib treatment in BRAF V600E GBM cells. pERK begins to rebound within 24 hours in BRAF-mutant glioma cells, but not in BRAF-mutant melanoma cells. **(A)** Immunoblots of whole cell lysates from BRAF-mutant human cancer cell lines treated with vemurafenib for the indicated times. **(B)** Graph of the ratio of signal intensity of phosphorylated ERK to total ERK relative to DMSO from (2-4A).

As seen before, pERK rebounds in BRAF-mutant glioma within 48 hours (**Figure 3-4A**). In DBTRG, pERK rebound becomes pronounced at 24 hours. In AM38 and NMCG1, pERK rebound begins even sooner, within 8 hours of vemurafenib treatment. Conversely, pERK remains inhibited in a panel of BRAF-mutant melanoma cell lines for up to 48 hours with only a very slight amount of pERK rebound observed. By quantitating the ratio of pERK to total ERK at each time point relative to the initial ratio pf ERK activation, it becomes evident that there is a greater amount of pERK rebound in all three mutant-BRAF glioma lines relative to the three melanoma cell lines (**Figure 3-4B**). This demonstrates that while pERK remains durable inhibited in BRAF-mutant melanoma, pERK does not remain inhibited by vemurafenib in BRAF-mutant glioma, rebounding throughout long term treatment.

Although ERK phosphorylation is required for its activity, it is not a very exact measure of total ERK activity because ERK also regulates its own phosphorylation through upregulating dual specificity phosphatases (DUSPs). Therefore, we wanted to see if rebound in pERK was associated with a rebound in ERK activity.

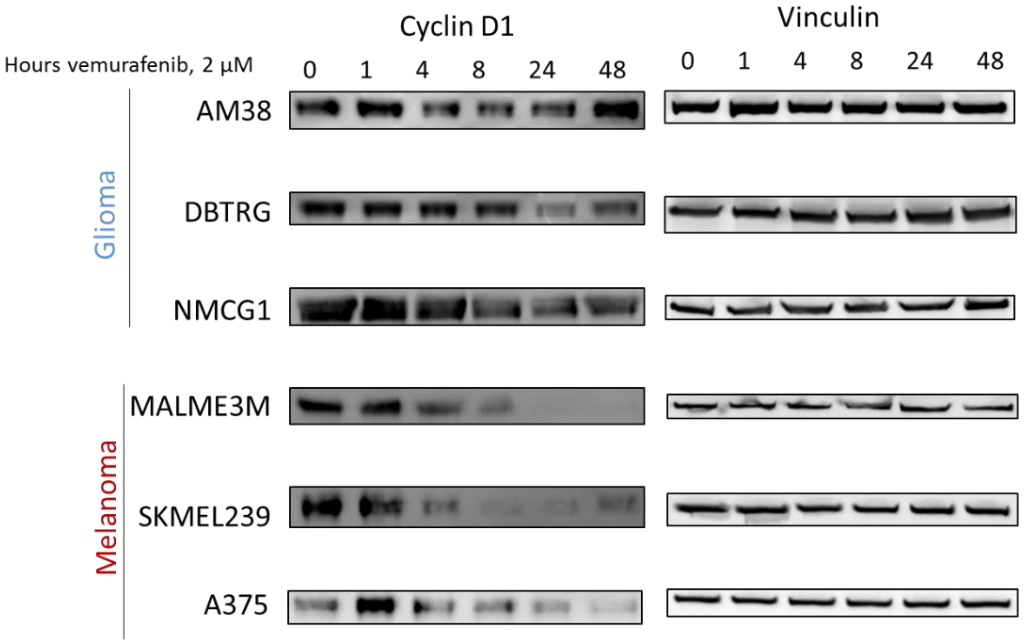

Figure 3-5. Incomplete inhibition of the ERK target gene Cyclin D1 by vemurafenib in BRAF-V600E mutant GBM cells. BRAF-V600E mutant cancer cells were treated with vemurafenib for the indicated times, then whole cell lysates were subjected to immunoblot analysis for the indicated proteins.

We measured the protein expression of the protein Cyclin D1, whose transcription is directly upregulated by activated ERK during a time course of vemurafenib treatment. Cyclin D1 levels remain constant, or initially fall only slightly, after a few hours of vemurafenib treatment in BRAF-mutant glioma (**Figure 3-5**). However, by 24-48 hours, Cyclin D1 expression also rebounds. Conversely, Cyclin D1 expression levels fall towards the threshold of detection in the BRAF-mutant melanoma cell lines. Total levels of remaining Cyclin D1 expression remain much higher in vemurafenib treat BRAF-mutant glioma than BRAF-mutant melanoma.

Cyclin D1 is a cell cycle protein whose expression is necessary for the transition between G1 and S-phase. Growth factor stimulation of ERK activation upregulates expression of this Cyclin D1, ushering the cell forward through the cell

cycle. Blocking expression of Cyclin D1 can growth arrest cells. Because of this, we asked if incomplete Cyclin D1 repression in vemurafenib treated BRAF-mutant glioma cells was also associated with incomplete growth repression by vemurafenib.

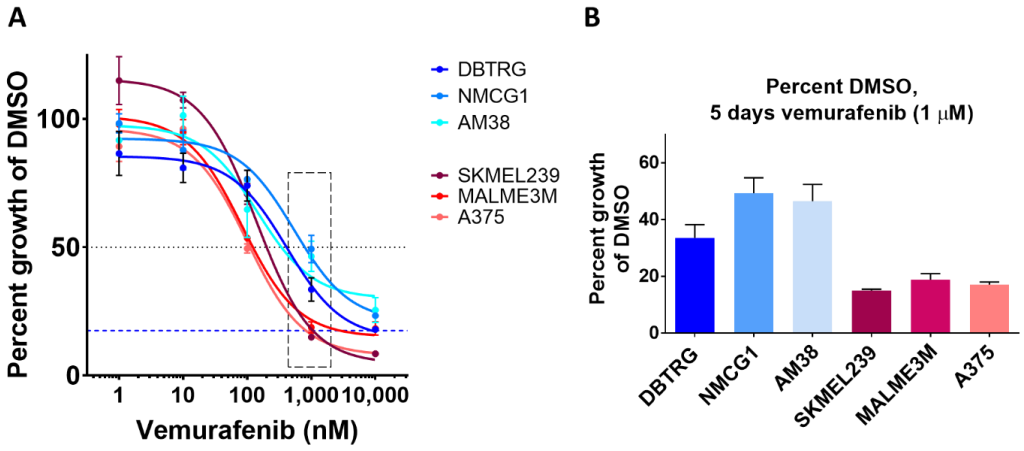

Figure 3-6. BRAF-V600E GBM cells are less sensitive to growth inhibition by vemurafenib than BRAF-V600E melanoma cells. (A) Cells were plated into various concentrations of vemurafenib and grown for 5 days, then counted in a trypan blue exclusion assay. Normalized cell counts were plotted and the resulting growth inhibition curves plotted in Prism Graphpad. Boxed data is reproduced in **(B),** a graph of the number of cells as a percent of the vehicle treated cells for each cell line treated with 1 μM vemurafenib.

We measured the proliferation of a panel of BRAF-mutant glioma and melanoma cell lines in the presence of various doses of vemurafenib for 5 days of growth (**Figure 3-6A**). While the total proliferation of all cell lines was reduced by some amount of vemurafenib treatment, the IC50s for the BRAF-mutant glioma lines were all right shifted relative to those for BRAF-mutant, demonstrating that these lines are intrinsically less sensitive to vemurafenib.

The residual rate of growth in the presence of 1 μM vemurafenib was also much higher in the BRAF-mutant glioma cell lines than in the BRAF-mutant melanoma cell lines (**Figure 3-6B**). The BRAF-mutant melanoma cell lines had, on average, less than 20% growth of the vehicle treated cells, while the BRAF-mutant glioma cell lines had on average about 40% of the growth of the vehicle treated cells, demonstrating that they had less total growth suppression than the BRAF-mutant melanoma cell lines.

Finally, we wanted to compare the sensitivity of BRAF-mutant glioma cells to another BRAF-mutant context which is known to become insensitive to vemurafenib through relief of negative feedback. When treated with vemurafenib, ERK-dependent inhibition of HER3 and its ligand NRG1 are relieved, and pERK rebounds.

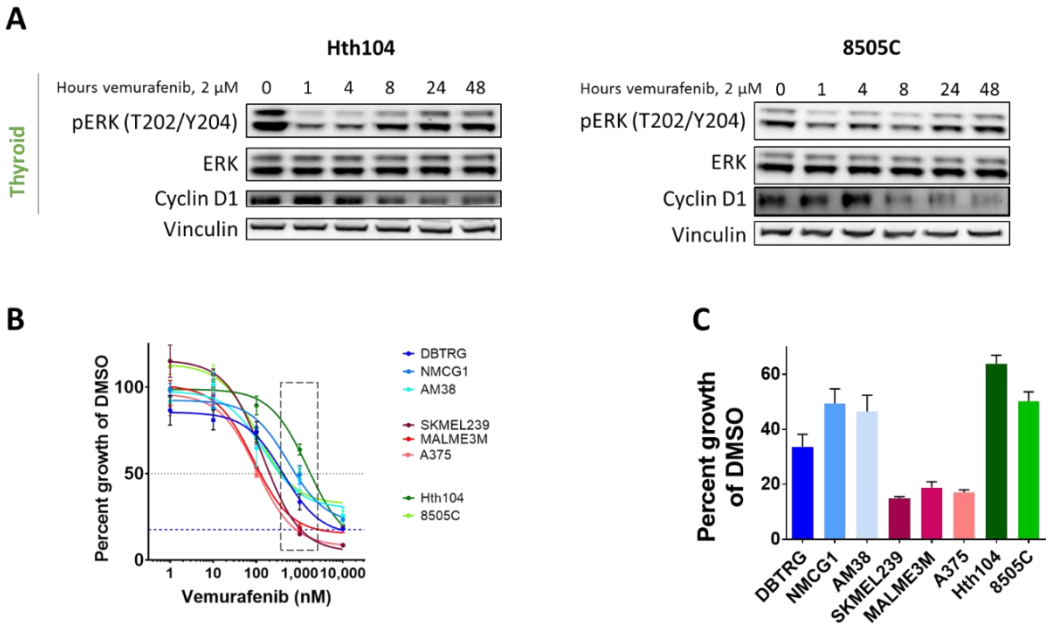

Figure 3-7. BRAF V600E GBM resemble BRAF V600E thyroid cancer cells in the kinetics of ERK rebound activation and incomplete growth inhibition. (A) BRAF-mutant thyroid cells were treated with vemurafenib for the indicated times, then whole cell lysates were subjected to immunoblot analysis for the indicated proteins. **(B)** Cells were plated into various concentrations of vemurafenib and grown for 5 days, then counted in a trypan blue exclusion assay. Normalized cell counts were plotted and the resulting growth inhibition curves plotted in Prism Graphpad. Boxed data is reproduced in **(C)**, a graph of the number of cells as a percent of the vehicle treated cells for each cell line treated with 1 μM vemurafenib.

We treated two thyroid cell lines with 2 μM vemurafenib for the same amounts of time as in **Figure 3-4** and **2-5** and measured the amount of pERK rebound and correlated that with Cyclin D1 repression. As expected, pERK rebounded from being inhibited quickly, though vemurafenib failed to achieve the same amount of inhibition at 1 hour in the BRAF-mutant thyroid lines compared to BRAF-mutant glioma and BRAf-mutant melanoma (**Figure 3-7A**). Furthermore, the amount of pERK rebound

was much more pronounced in the thyroid cell lines, suggesting the relief of negative feedback in BRAF-mutant thyoid cell lines leads to pronounced reactivation of the pathway.

We also measured the growth inhibition of vemurafenib in the BRAF-mutant thyroid cell lines and compared it to the BRAF-mutant glioma and BRAF-mutant melanoma cell lines (**Figure 3-7B**). The IC50 for BRAF-mutant thyroid were further right shifted from those of BRAF-mutant melanoma, indicating that they two were much less sensitive to vemurafenib. This is further represented by the amount of growth suppression in the presence of 1 μM vemurafenib (**Figure 3-7C**). The thyroid cell lines still had on average about 50% of the growth of the vehicle treated samples.

From this we conclude that BRAF-mutant glioma is similar to BRAF-mutant thyroid cells in that both have pronounced reactivation of ERK signaling following vemurafenib treatment and are relatively insensitive to vemurafenib compared to BRAF-mutant melanoma.

Discussion

Interrogating BRAF-mutant glioma with vemurafenib on a short time scale suggests that these tumors might be very similar. Their biochemical IC50s for acute ERK inhibition are nearly identical. However, when looking on a longer time scale, it become more evident that BRAF-mutant glioma is actually quite different from BRAF-mutant melanoma. While vemurafenib quite potently inhibits pERK for 48 hours post treatment in BRAF-mutant melanoma, pERK rebounds within 24 hours, or even sooner, in BRAF-mutant glioma treated with vemurafenib. This pERK rebound is associated with incomplete Cyclin D1 repression and decreased sensitivity to vemurafenib.

These observations further underscore the importance of biochemical pERK rebound and connecting it with a phenotypic outcome. Cell lines with a pronounced rebound in pERK fail to durably inhibit Cyclin D1 transcription and expression. They are also less growth arrested by vemurafenib. Presumably, a lack of Cyclin D1 expression plays a role in the lack of growth arrest by vemurafenib in BRAF-mutant glioma.

Rebound in pERK has very important clinical ramifications. The extent of pERK inhibition in vemurafenib treated patients is highly correlated with clinical response. Preclinical models have demonstrated that BRAF inhibitors require complete ERK inhibition in order to result in tumor regressions (Bollag et al., 2010). Patients whose tumors bear residual pERK relapse sooner than those who do not.

This also explains why tumors may try to upregulate pERK in order to escape the anti-oncogenic effects of BRAF inhibition. The fact that pERK is initially inhibited in BRAF-mutant glioma before rebounding suggests that these cells escape vemurafenib though an adaptive response, rather than an acquired mutation or de novo resistance mechanism.

CHAPTER 4: VEMURAFENIB RELIEVES ERK-DEPENDENT FEEDBACK ON RAS-ERK SIGNALING

Introduction

Not all BRAF-mutant tumors have dramatic responses to BRAF inhibitors like vemurafenib. For instance, in Phase I trials of vemurafenib in BRAF-mutant colorectal (CRC) and thyroid tumors, very few objective tumor responses were recorded (Kopetz et al., 2010). The general unresponsiveness of these tumors turned out to be the result of adaptive responses to mutant-BRAF inhibition. The first of these adaptive responses to be thoroughly described was transient ERK inhibition with vemurafenib in CRC. Phospho-ERK rebounded through EGFR-mediated reactivation of the pathway by inducing the formation of vemurafenib insensitive BRAF/CRAF dimers (Corcoran et al., 2012; Prahallad et al., 2012). Blocking both EGFR and BRAF lead to tumor regressions.

Similarly, in BRAF-mutant thyroid tumors, vemurafenib treatment also results in transient pERK inhibition (as we replicated in Figure 3-**7**). This turned out to be an adaptive response through relief of ERK-dependent negative inhibition of HER3 receptor as well as its ligand NRG1 (Montero-Conde et al., 2013). Blocking HER kinase activity with lapatinib in combination with a BRAF inhibitor was sufficient to block pERK rebound and induce tumor regressions in preclinical models.

Using these findings as a model for candidates of BRAF-inhibitor adapative responses, we sought to determine if any ERBB family members were subject to ERK-dependent feedback activation and might mediate pathway reactivation following BRAF inhibition.

Results

Because most of the adaptive responses to BRAF-inhibition occurred through ERBB family members, we considered them our first candidates for mediating the vemurafenib insensitivity of BRAF-mutant glioma.

The ERBB family is composed of 4 receptors, EGFR, HER2, HER3, and HER4 (summarized in **Figure 4-1**) (Hynes and Lane, 2005). Upon stimulation with an ERBB-ligand, the receptors dimerize and signal through downstream effector pathways. HER2 receptor has no known ligands, so it primarily serves as the preferred co-receptor for all other ERBB family members. HER3 has no intrinsic kinase activity, so it must form heterodimers as well in order to signal.

There are ten ERBB ligands. The first family of ligands—epidermal growth factor (EGF), amphiregulin (AREG) and transforming growth factor-α (TGFα)—bind specifically to EGFR. The second family, composed of betacellulin (BTC), heparin-binding EGF (HB-EGF) and epiregulin (EREG) can bind both EGFR and HER4. Neuregulins (NRG) 1, 2, 3, and 4 comprise the last two families. NRG1 and NRG2 can bind both HER3 and HER4 while NRG3 and NRG4 are specific to only to HER4.

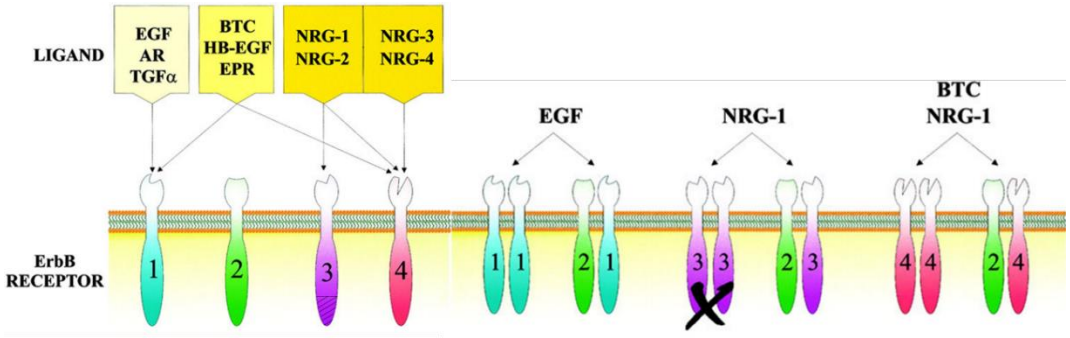

Figure 4-1. The ERBB family of ligands and their receptor specificities. There are 4 family members in the ERBB receptor tyrosine kinase family—EGFR, HER2, HER3, and HER4—as well as 10 ligands with various specificities for those receptors as well as the ability to induce specific dimerization partners. (Adapted from Olayioye, M. et al, *EMBO* 2000).

We first asked if any of the ERBB family member receptors, or their ligands, were transcriptionally activated in response to vemurafenib treatment in BRAF-mutant DBTRG cells. We treated DBTRG cells with vemurafenib for various time points then collected and isolated RNA and quantitated ERBB family member and ligand transcript levels through QPCR.

We first verified that the drug treatment worked by looking at two genes which are directly upregulated by ERK activity (**Figure 4-2A**). The product of these genes, *DUSP6* and *SPRY4*, negatively regulate ERK activity. DUSP6 dephosphorylates and inactivates ERK while SPRY4 disconnects RTK signaling from RAS. Both of these genes serve to limit ERK activation under physiological conditions. However, when mutant-BRAF is inhibited, loss of expression of these genes can serve to augment pERK reactivation.

DUSP6 expression rapidly fell to 25% of its original level after vemurafenib treatment, before falling further to 10% of its original level at 24 hours. The kinetics of

SPRY4 repression were slower, but by 24 hours, SPRY4 had fallen to 25% of its original level. Both of these genes then slowly rebounded over the following 5 days, indicative of the rebound in pERK and its activity seen in the last chapter.

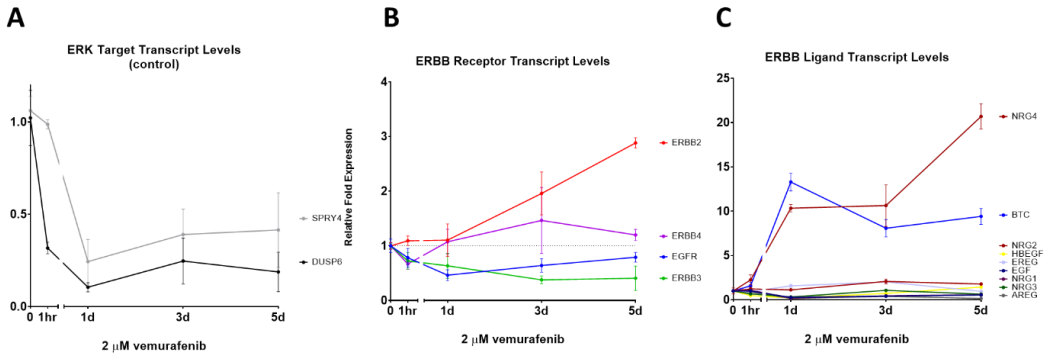

Figure 4-2. Vemurafenib induces transcription of selected ErbB family ligands and receptors in BRAF V600E GBM cells (DBTRG cell line). (A), **(B)**, and **(C)**. Relative expression of the indicated genes was quantified by QPCR from RNA isolated from DBTRG BRAF-mutant glioma cells treated with 2 μM vemurafenib for the amounts of time specified. EGF – epidermal growth factor; AREG - amphiregulin; TGFA - transforming growth factor-α; BTC – betacellulin; HBEGF - heparin-binding EGF; EREG – epiregulin; NRG – neuregulin.

We then looked at the expression of the ERBB receptors *EGFR*, *ERBB2*, *ERBB3* and *ERBB4* (**Figure 4-2B**). Only *ERBB2* was significantly upregulated, rising by 3 fold over the five days of vemurafenib treatment. *ERBB4* and *EGFR* remained relatively constant, while ERBB3 interestingly fell by 50%. From the total receptor analysis, we hypothesize that HER3 may have a role in facilitating the adaptive response leading to vemurafenib insensitivity.

Finally, we looked at the transcription of the EGF family of ligands (**Figure 4-2C**). All of the ligands remained unchanged during the five days of vemurafenib

treatment except for *BTC*, which was upregulated by 10-15 fold, and *NRG4*, which was upregulated 20-fold by the end of the experiment. NRG4, recall, is a specific ligand for only HER4, while BTC activated both EGFR and HER4. From this analysis, we hypothesize that EGFR and HER4 may play a role in facilitating the adaptive response leading to vemurafenib insensitivity.

We next sought to verify if the changes in transcript levels were reflected in changes at the protein level. We collected whole cell lysates from DBTRG cells treated with vemurafenib for various amount of time (**Figure 4-3A**). Total HER2 levels were upregulated 4-fold above DMSO. We also looked at the primary tyrosine autophosphorylation sites of EGFR, HER2, and HER3 which typically indicate that they are being activated (**Figure 4-3B**). All three phosphorylation sites rose relative to DMSO in response to vemurafenib treatment, with them most dramatic changes in EGFR and HER2.

The results in **Figure 4-3** are largely consistent with those from **Figure 4-2**. Total *ERBB2* transcript levels rose, and this was reflected in a rise in total HER2 protein levels. The ligands upregulated suggest that EGFR and HER4 should be the most highly activated of the ERBB family members. Indeed, EGFR-Y1068 (pEGFR) did modestly rise. However, all of the ERBB family member receptors can heterodimerize, so the more dramatic changes in HER2-Y1248 (pHER2) and HER3-Y1289 (pHER3) could possibly be HER4 heterodimers.

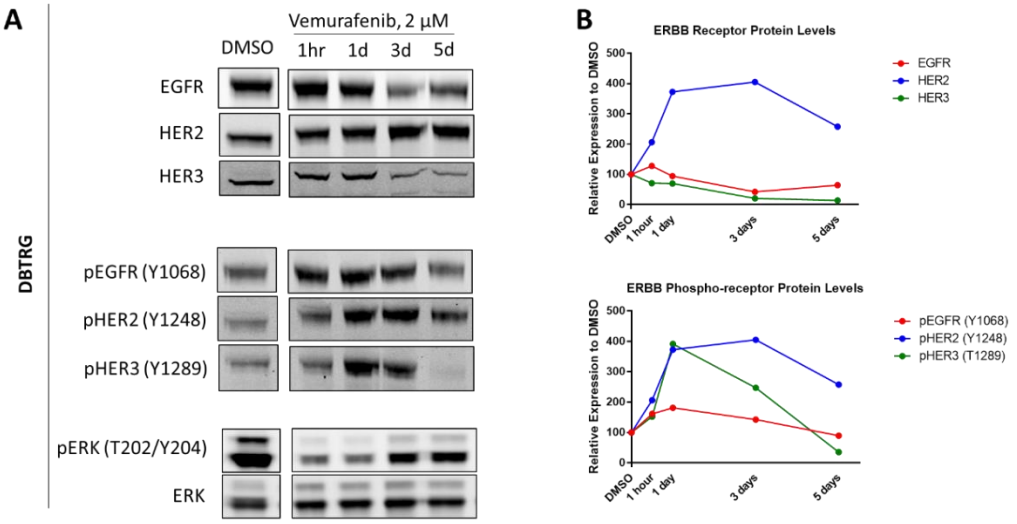

Figure 4-3. Immunoblotting confirms vemurafenib induced upregulation of selected ErbB pathway members in BRAF V600E mutant GBM cells (DBTRG cell line) Long term vemurafenib treatment increases HER2 receptor levels and EGFR, HER2, and HER3 activation. (A) DBTRG cells were treated with 2 μM vemurafenib for the indicated times, then whole cell lysates were subjected to immunoblot analysis for the indicated proteins. **(B)** Graph of the ratio of signal intensity of indicated proteins to total ERK relative to their initial DMSO treated expression from (3-3A).

After observing rises in ERBB receptor and ligand transcript levels, and well as increases in the receptor protein levels and their activation, we then wanted to know if EGFR and/or HER2 kinase acticity were responsible for mediating pERK rebound and vemurafenib resistance. To do this, we employed the highly selective EGFR and HER2 kinase inhibitor lapatinib. We treated DBTRG cells with vemurafenib alone or in combination with lapatinib to see if adding an ERBB kinase inhibitor would blunt the rebound in pERK.

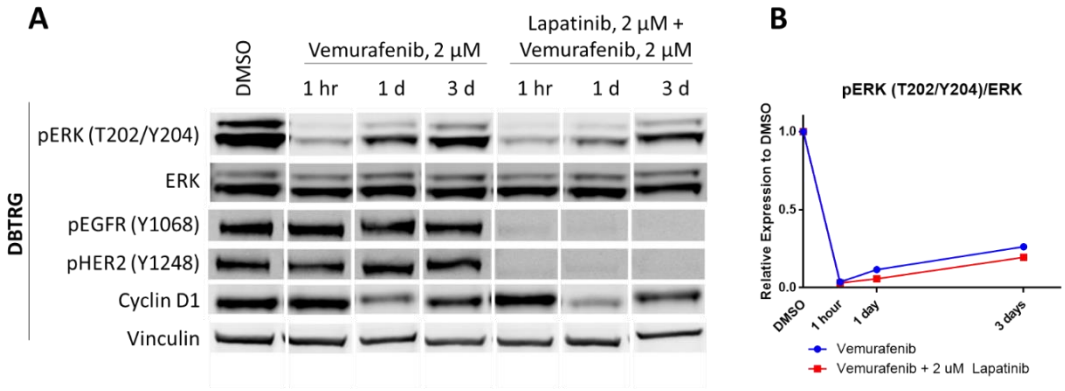

Figure 4-4. Inhibition of EGFR and HER2 kinase activity is not sufficient to blunt vemurafenib-induced feedback activation of ERK in BRAF V600E mutant GBM cells (DBTRG cell line). (A) Whole cell lysates from DBTRG cells treated with 2 μM vemurafenib alone or in combination with 2 μM lapatinib for the indicated amounts of time were subjected to immunoblot analysis for the indicated proteins. **(B)** Graph of the ratio of signal intensity of phosphorylated ERK to total ERK relative to DMSO from (4-4A).

We observed complete absence of pEGFR and pHER2, indicating that lapatinib completely blocked their activity. Nevertheless, we observed a very similar rebound in pERK in both the vemurafenib treated cells as well as those treated with both vemurafenib and lapatinib. This indicated that EGFR and HER2 kinase activity is not required to facilitate a rebound in pERK. Cyclin D1 follows the pERK activity, being initially inihibited and then being incompletely inhibited at 3 days.

This lack of biochemical activity was also reflected in a growth assay in which we grew DBTRG cells in vemurafenib alone or in combination with 2 μM lapatinib. Laptininb along inhibited the growth of DBTRG cells approximately 20%, but failed to provide additional growth inhibition when added to a dose rage of vemurafenib.

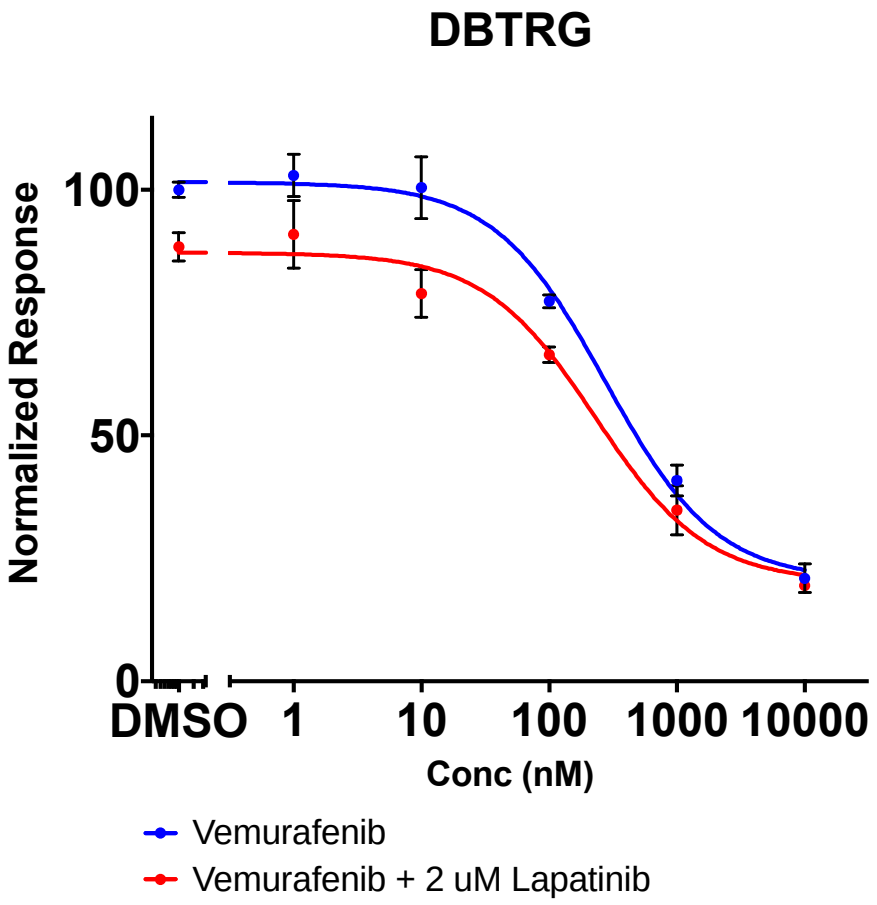

	Vemurafenib	Vemurafenib + 2 uM Lapatinib
IC50	275.3	230.2

Figure 4-5. Lapatinib does not increase the sensitivity of DBTRG cells to vemurafenib. DBTRG cells were plated various doses of vemurafenib alone or in combination with 2 μM lapatinib for 5 days then counted in a trypan blue exclusion assay. Normalized cell counts were plotted and the resulting growth inhibition curves plotted in Prism Graphpad.

Because the growth inhibition curves of vemurafenib with and without lapatinib are almost superimposable and because lapatinib failed to block

vemurafenib-induced pERK rebound, we conclude that EGFR and HER2 kinase activity alone are not responsible for the insensitivity of DBTRG to vemurafenib.

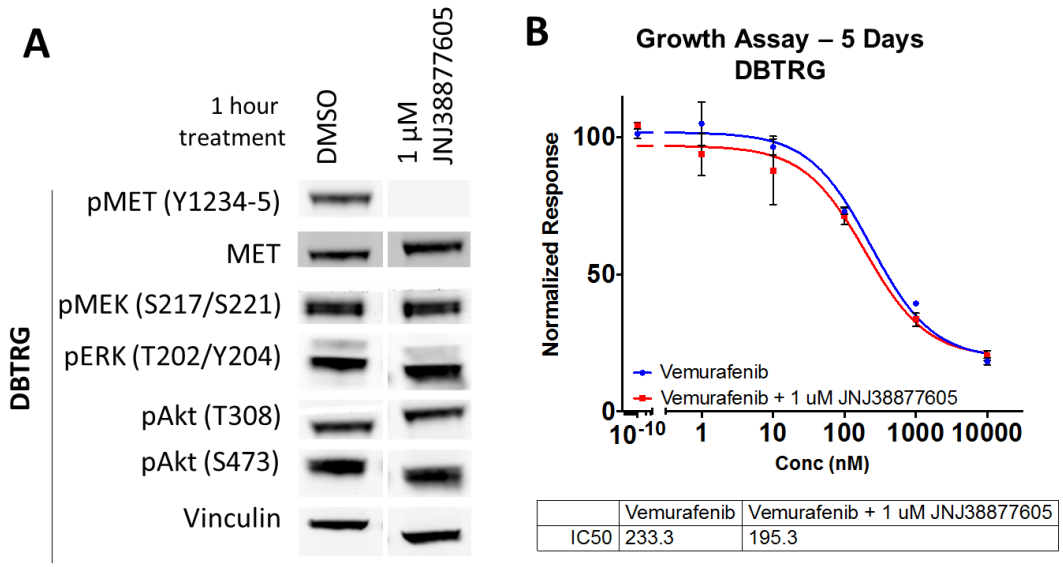

Figure 4-6. The MET kinase inhibitor JNJ38877605 also does not sensitize BRAF V600E mutant GBM cells (DBTRG cell line) to vemurafenib, (A) DBTRG were treated with various doses of vemurafenib for 1 hour or with 1 µM the MET inhibitor JNJ38877605, then whole cell lysates were subjected to immunoblot analysis for the indicated proteins. **(B)** DBTRG cells were plated various doses of vemurafenib alone or in combination with 1 µM JNJ38877606 for 5 days, then counted in a trypan blue exclusion assay. Normalized cell counts were plotted and the resulting growth inhibition curves plotted in Prism Graphpad.

We also noticed that DBTRG express MET receptor (Figure 4-6). MET receptor has also been implicated in feedback reactivation of both MAPK and PI3K pathways following vemurafenib treatment in BRAF mutant thyroid (Byeon et al., 2015). We used the selective MET kinase inhibitor JNJ38877605 to inhibit MET

kinase activity to see if it could sensitive BRAF mutant DBTRG cells to vemurafenib treatment.

Despite effectively inhibiting MET-Y1234-5 (pMET), JNJ38877605 failed to further sensitize DBTRG cells to vemurafenib in a growth assay in which cells were treated with vemurafenib alone or in combination with the JNJ38877605. The vemurafenib IC50s were almost identical as were the growth inhibition curves, suggesting the MET kinase activity does not activate ERK signaling in DBTRG cells, and therefore does not mediate resistance from feedback reactivation of the pathway.

After eliminating the most likely candidates for feedback reactivation of ERK signaling, we wanted to take a more unbiased approach to identifying possible upregulated RTKs that could mediate reactivation of the ERK pathway through relief of negative feedback. To do so, we employed an RTK array which measures over 50 phospho-proteins simultaneously. We compared all three cell lines after being treated with vemurafenib for 72 hours.

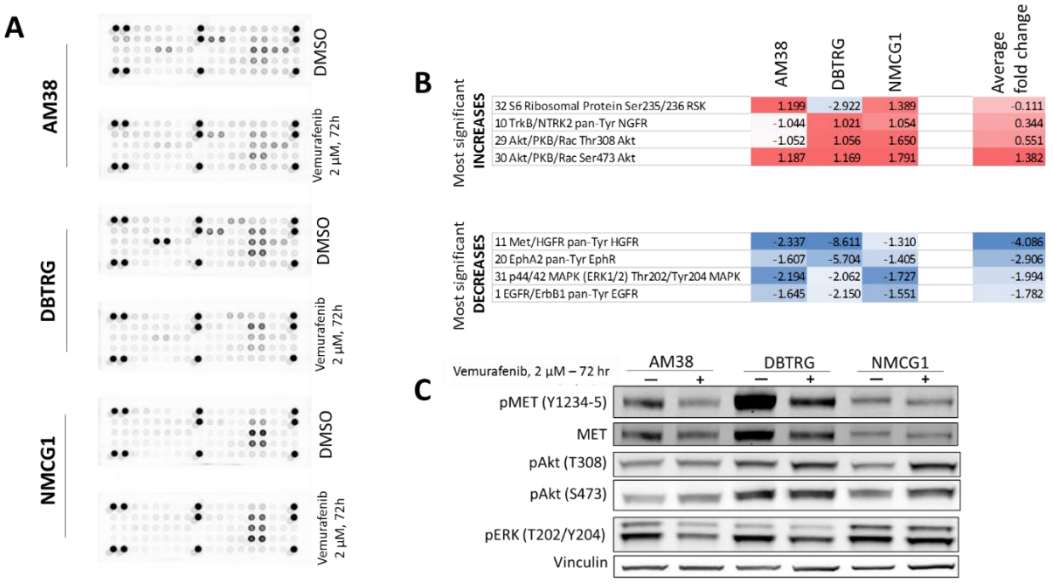

Figure 4-7. Phospho-RTK arrays fail to identify receptor tyrosine kinases that are induced by vemurafenib and might explain ERK rebound reactivation. (A) BRAF-mutant glioma cells were treated with 2 μM vemurafenib for 72 hours, lysed in Cell Signaling Cell Lysis Buffer, and whole cell lysates were incubated with pre-coated RTK array slides. Membranes were stained with infrared dye conjugated secondary antibody and imaged on a Licor Odyssey instrument. **(B)** Signal intensity from slides was quantitated, averaged across duplicate spots, and rank ordered by average fold change across all three cell lines. The most significantly upregulated and downregulated phosphoproteins are listed. **(C)** Whole cell lysates collected in (3-7A) were subjected to immunoblot analysis for the indicated proteins.

Unfortunately, we did not observe any significantly upregulated RTKs on the array. We noted that pERK decreased by 2-fold on average, indicating that vemurafenib inhibited ERK signaling. The most significantly upregulated proteins were Akt-T308 and Akt-S473, although these proteins increased by less than 2-fold. We also recorded the most significantly downregulated proteins. Interestingly, vemurafenib treatment resulted in dramatic decreases in pMET. Very few proteins

included on this RTK array were upregulated by vemurafenib treatment. Among those that were are pAkt-T308 and S473. pMET was dramatically inhibited by vemurafenib treatment in DBTRG and to a lesser extent in AM38, further supporting the finding that MET inhibition would not sensitize DBTRG to vemurafenib.

Interestingly, the RTK array also failed to pick up the more dramatic changes we observed by western blot in pHER2 and pHER3. We suspect that this is because RTKs are inherently less sensitive than immunoblots because they detect any tyrosine phosphorylation instead of using antibodies to the specific phosphorylation events that we surveyed.

Discussion

Is it slightly disappointing that despite observing rather dramatic changes in ERBB receptor and ligand transcript levels that we were still unable to pinpoint the RTK or RTKs primarily responsible for mediating relief of ERK-dependent feedback pathway reactivation. However, there are a few possible explanations for why this might be.

We might hypothesize that feedback on other ERBB family memebrs besides EGFR and HER2 is relieved in order to reactivate pERK signaling. Our experiments do not rule out HER3 or HER4 as heterodimeric partners in reactivating ERK signaling as lapatinib only inhibits EGFR and HER2. This observation is also supposed by the strong activation of pHER3 we observed. We could perform co-IP experiments to determine which ERBB family members are the predominant dimers following relief of ERK-dependent negative feedback. Then, we might be able to useing other inhibitors, such as the antibody pertuzumab, which block the ability of HER2 to dimerize with other receptors.

However, it is also possible that there are no significant RTKs that become upregulated following vemurafenib treatment. Lito has demonstrated that ligand-dependent signaling from RTKS is negatively inhibited in BRAF-mutant cells (Lito et al., 2012). Vemurafenib mediated relief of ERK-dependent feedback occurs on most of these RTKs, and instead of specifically hyper-activating one of them, allows the cell to become permissive to ligand mediated RTK signaling, having lost most of its negative feedback. In melanoma, which have relatively little basal RTK signaling, the rise in ERK from this increase in RTK signaling permissiveness is small, but detectable. Therefore, one might hypothesize that if BRAF-mutant glioma has more basal RTK activity than melanoma, relief of negative feedback on this RTK activity might be sufficient to lead to vemurafenib insensitivity.

Using this dynamic view of feedback, it is also interesting to speculate on the kinetics of BTC transcript level changes (**Figure 4-2**). BTC initially rose 15-fold at 1 day of vemurafenib treatment, before falling to 10-fold upregulated at 3 and 5 days of vemurafenib treatment. This is consistent with BTC restoring some signaling capacity to the ERK pathway which would in turn re-restore some of the ERK-dependent feedback on BTC, lowering its transcript levels somewhat, and reaching a new steady state.

This dynamic process might also explain why pEGFR, pHER2, and pHER3 all initially rise following vemurafenib treatment in DBTRG before falling to somewhat lower levels (**Figure 4-3**). This rise in ERBB activity restore some ERK pathway activity which then restores some ERK-dependent feedback, lowering the amount of ERBB activity.

CHAPTER 5: RELIEF OF NEGATIVE FEEDBACK INDUCES RAS-GTP DEPENDENT RAF DIMERS THAT ARE RESISTANT TO VEMURAFENIB BUT SENSITIVE TO RAF DIMER INHIBITORS

Introduction

While there are several different mechanisms for a tumor to achieve a resistant state, they actually all share a very common etiology based in basic RAF science. Under physiological conditions, RAF molecules must dimerize in order to become signaling competent. This dimerization is induced by the formation of RAS-GTP. Without sufficient levels of RAS-GTP, RAF molecules will remain in a monomeric, signaling incompetent state. Indeed, following pathway stimulation, ERK will exert negative feedback on RTKs and RAS-GTP, serving to limit pathway activation and to return to baseline conditions.

BRAF-V600E, however, has gained the ability to signal as a monomer through an activating mutation in its kinase domain. In fact, the high ERK out of mutant-BRAF places very strong negative feedback on RTK/RAS components, and maintains the cell in a RAS-GDP state (**Figure 5-1**) (Lito et al., 2012, 2013). However, following vemurafenib treatment, this ERK-dependent negative feedback is relieved, and RTKs begin to stimulate activation of RAS-GTP. In the presence of RAS-GTP, mutant-BRAF protein forms dimers. While vemurafenib can still bind the mutant-BRAF protomer of the induced dimers, it will transactivate the other RAF partner, reactivating RAF/ERK signaling, and rendering the RAF dimer insensitive to vemurafenib.

Finally, the restoration of some ERK activity will restore some of its negative feedback as well, lowering signaling from its rebound. This process will oscillate until

the cell reaches a new steady state where ERK signaling remains insensitive to vemurafenib.

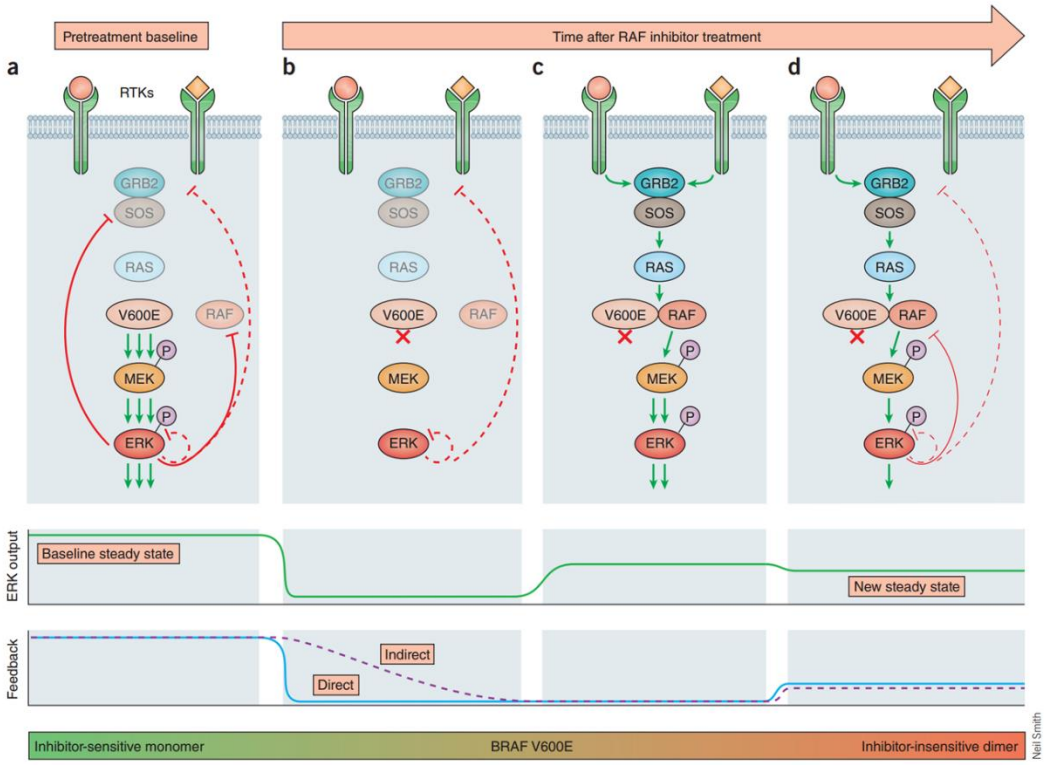

Figure 5-1. Tumor adaptation to BRAF inhibitors. (A) In V600E BRAF tumors, ERK signaling is high, as is ERK feedback inhibition of CRAF, SOS, and RTKs. RAS-GTP levels are therefore low, and BRAF signals as a monomer. **(B)** Following BRAF-V600E inhibitor treatment, ERK signaling and negative feedback rapidly fall. **(C)** In the absence of negative feedback, RTKs are then able to activate RAS, leading to a rise in RAS-GTP levels and the induction of vemurafenib-insensitive RAF dimers. **(D)** As ERK activity rebounds, so does some of its negative feedback. The cells reach a new steady state of ERK signaling which in insensitive to vemurafenib and sensitive to the amount of RTK signaling. Figure from Lito P. et al, *Nature Medicine* 2013.

We sought to determine if the rise in RAS-GTP was responsible for mediating the vemurafenib insensitivity of mutant-BRAF glioma. To do so, we used a RAS-GTP pulldown assay. RAS-GTP pulldowns use the observation that the RAS-Binding Domain (RBD) of CRAF protein binds only RAS-GTP. The RAF-RBD is fused to a GST tag, and the RAS-GTP immunoprecipitated from whole cell lysates.

We compared the basal levels of RAS-GTP in a panel of BRAF-mutant glioma cell lines. We compared these to H1299, an NRAS-mutant cell line, and HCT116, KRAS-mutant cell line as positive controls for RAS-GTP loading since Ras-mutant cell lines have lost the ability to hydrolyze GTP and therefore remain constitutively GTP bound.

As expected H1299 and HCT116 possess high levels of RAS-GTP. We then observed that Ras-GTP levels are almost completely feedback inhibited in BRAF-mutant glioma cell lines, consistent with their elevated ERK output (see **Figure 5-4**). We also measured the amount of activated CRAF by probing for CRAF-S338. The RAS-mutant cell lines have high levels of activated CRAF, consistent with having high levels of CRAF-dimer signaling due to the presence of high levels of RAS-GTP. Conversely, levels of activated in CRAF were much lower in the BRAF-mutant glioma cell lines, consistent with CRAF largely being feedback inhibited.

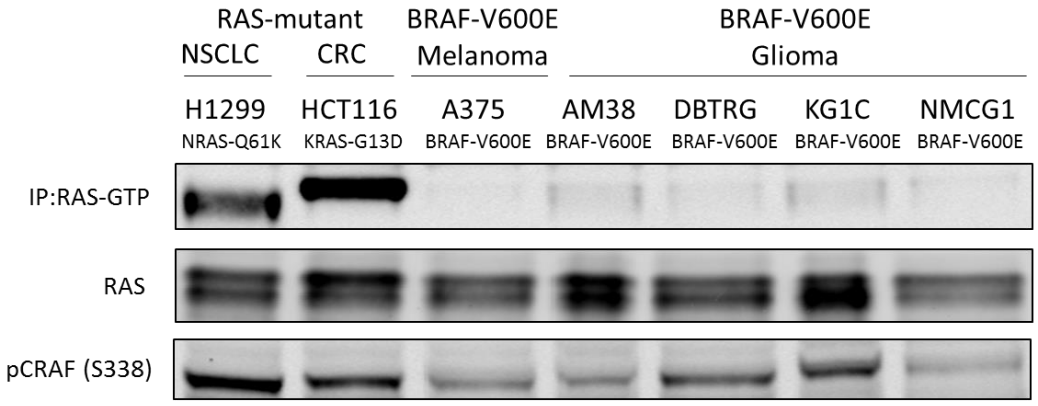

Figure 5-2. Basal RAS-GTP is feedback-inhibited in BRAF-V600E GBM cells. Aliquots of whole cell lysates were immunoprecipitated with a GST-tagged RAS-binding domain of CRAF (GST-CRAF-RBD). The pulldown product (RAS protein bound to RAS-GTP exclusively) was subjected to immunoblot analysis with a RAS antibody to detect RAS-GTP along with whole cell lysates for the indicated proteins.

After observing that Ras-GTP is feedback inhibited in BRAF-mutant glioma cell lines, we next asked if vemurafenib-mediated BRAF inhibition relieved this feedback and resulted in a rise in RAS-GTP. To do so, we measured RAS-GTP levels over a 5-day time course of vemurafenib treatment in BRAF-mutant glioma cell lines (**Figure 5-3A**). Basal levels of RAS-GTP were low in the DMSO treated samples, as before. However, following vemurafenib treatment, we observed a rise in RAS-GTP in all three cell lines. This indicates that relief of negative feedback resulted in a rise in RAS-GTP levels. This rise in RAS-GTP levels is correlated with insensitivity to vemurafenib and an observed rebound in pERK.

We also quantitated the amount of RAS-GTP relative to total RAS and plotted the rise relative to the ratio of RAS-GTP in the DMSO treated samples (**Figure 5-3B**). The rise in RAS-GTP was most dramatic in the AM38 cells, although there was an

observable rise in all three cell lines. This rise in RAS-GTP paralleled in the rebound in pERK, suggesting that they might be correlated. This would be consistent with elevated RAS-GTP levels causing the induction of RAF dimers to which vemurafenib is insensitive, resulting in incomplete mutant-BRAF inhibition and a rebound in pERK signaling.

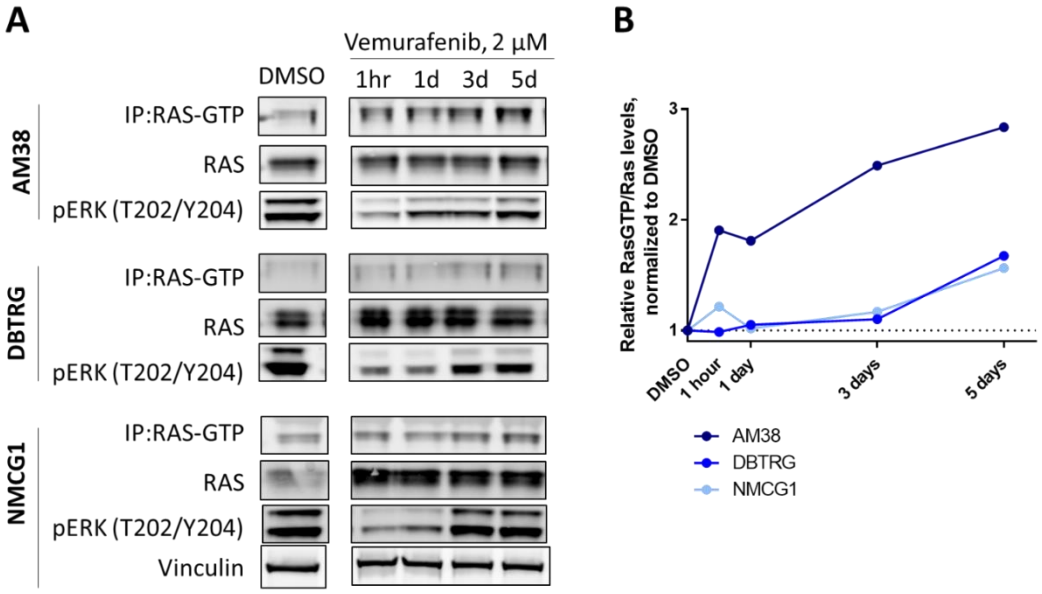

Figure 5-3. Vemurafenib induced RAS-GTP loading in BRAF V600E mutant GBM cells. (A) Aliquots of whole cell lysates from cells treated with 2 μM vemurafenib for the indicated amounts of time were immunoprecipitated with GST-CRAF-RBD. The pulldown product was subjected to immunoblot analysis with a RAS antibody along with whole cell lysates for the indicated proteins. **(B)** Graph of the ratio of signal intensity of RAS-GTP to total RAS (or vinculin for NMCG1).

Under physiological conditions, either RAS-GTP dependent heterodimerization (for example, BRAF/CRAF) or homodimzerization (for example, BRAF/BRAF) of RAF proteins is required for RAF signaling (Lavoie and Therrien, 2015). We therefore wanted to interrogate the constituent members of any RAF dimers

formed in the presence of RAS-GTP from vemurafenib induced relief of negative feedback. We hypothesized that elevated RAS-GTP levels would likely form mutant-BRAF/CRAF dimers. To test this, we knocked down CRAF protein in the BRAF-mutant glioma cell line NMCG1 by generating a stable cell line expressing a doxycycline inducible shRNA to *RAF1* and then measured the magnitude of pERK rebound following a time course of vemurafenib treatment (**Figure 5-4A**). If our hypothesis was correct, we would expect to see that CRAF knockdown would blunt pERK rebound as elevated RAS-GTP levels would be unable to induce mutant-BRAF/CRAF dimers if the cells were depleted of CRAF.

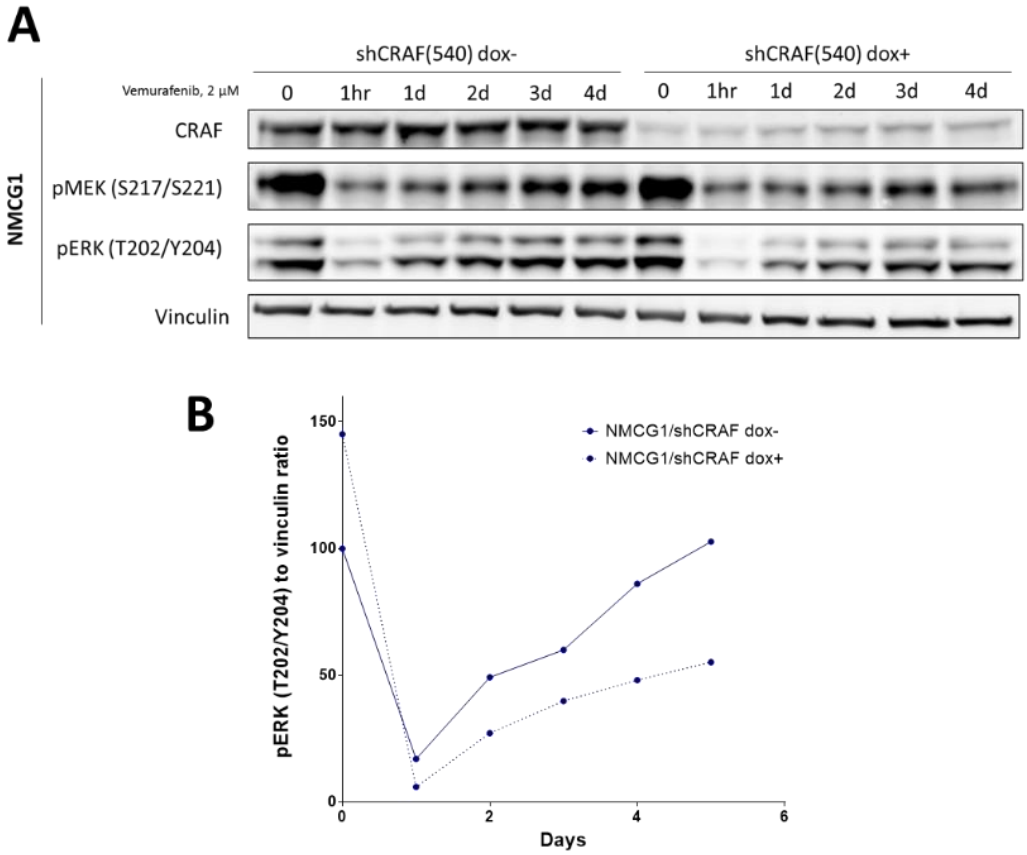

Figure 5-4. Depletion of CRAF protein mitigates vemurafenib-induced ERK rebound in BRAF V600E mutant GBM cells (NMCG1 cell line). (A) BRAF-V600E glioma cell lines stably expressing a doxycycline inducible shRNA cassette to CRAF were treated with 2 μg/ml of doxycycline for three days, then treated with 2 μM vemurafenib for the indicated amounts of time, before being lysed. Whole cell lysates were subjected to immunoblot analysis for the indicated proteins. **(B)** Graph of the normalized ratio of signal intensity of pERK to vinculin.

We observed that with quite potent knockdown of CRAF, we were able to partially blunt the rebound in pMEK and pERK. While pERK rebounded as previously observed in the cells without shCRAF induction, the magnitude of pERK rebound in the cells depleted of CRAF was lower, though there was still a pronounced rebound.

From this we conclude that CRAF is likely a component of RAF dimers formed by vemurafenib-induced, although probably not the predominant member.

Since CRAF seems to play at least a partial role in transmitting RAS-GTP dependent signaling and because vemurafenib is unable to inhibit the signaling of RAF-dimers, we looked for other BRAF inhibitors that would also be able to inhibit RAF dimers. One such compound we identified from the literature is LY3009120 (Peng et al., 2015).

	ARAF		BRAF			CRAF	
	In Vitro	KiNative Whole Cell Assay	Wildtype In Vitro	V600E In vitro	KiNative Whole Cell Assay	In Vitro	KiNative Whole Cell Assay
Vemurafenib (nM)	–	950	32	6.1	310	414	>10,000
LY3009120 (nM)	–	44	9.1	5.8	39	15	42

Figure 5-5. Inhibition of RAF isoforms by vemurafenib and LY3009120. IC50s for ARAF, BRAF, and CRAF as measured in in vitro kinase assays or in KiNativ Whole Cell Assays. Adapted from Ping SB, *Cancer Cell* 2015.

Since CRAF protein seems to play a role in ERK rebound, are there any other inhibitors that can inhibit CRAF protein?

We initially compared the selectivity profiles of vemurafenib and LY3009120. Vemurafenib shows the highest affinity for BRAF-V600E, with lower affinities towards ARAF and CRAF. However, vemurafenib completely fails to inhibit CRAF in the KiNative Whole Cell Assay, which measures the ability of compounds to inhibit their targets under highly physiological conditions, due to paradoxical activation of

BRAF-CRAF heterodimers (Patricelli et al., 2011). In contrast, LY3009120 is able to inhibit all RAF isoforms at less than 50 nM, including in the KiNativ Whole Cell Assay, indicating that it is a pan-isoform RAF inhibitor.

We then wanted to determine if LY3009120 could durably inhibit ERK signaling, even in the presence of elevated RAS-GTP levels. To do so, we plater BRAF-mutant glioma cells side by side into a time of course of vemurafenib and LY3009120 and measured both RAS-GTP elevation and pERK (**Figure 5-6**). While the rise in RAS-GTP in the vemurafenib treated cell line was modest (but measureable), the increase in RAS-GTP from LY3009120 was quite dramatic.

Furthermore, despite causing even more elevated RAS-GTP levels, LY3009120 was able to durably inhibit ERK signaling, suppressing pERK rebound even 5 days after initial treatment. We believe these two observations are completely related. By achieving greater suppression of pERK, even more negative feedback is relieved, and RAS-GTP becomes even more activated. This means that RAS-GTP elevation can be used as a surrogate for pERK suppression. This suggests that drugs

that can inhibit RAF dimers are able to suppress pERK rebound in contexts in which vemurafenib would in fact result in ERK rebound.

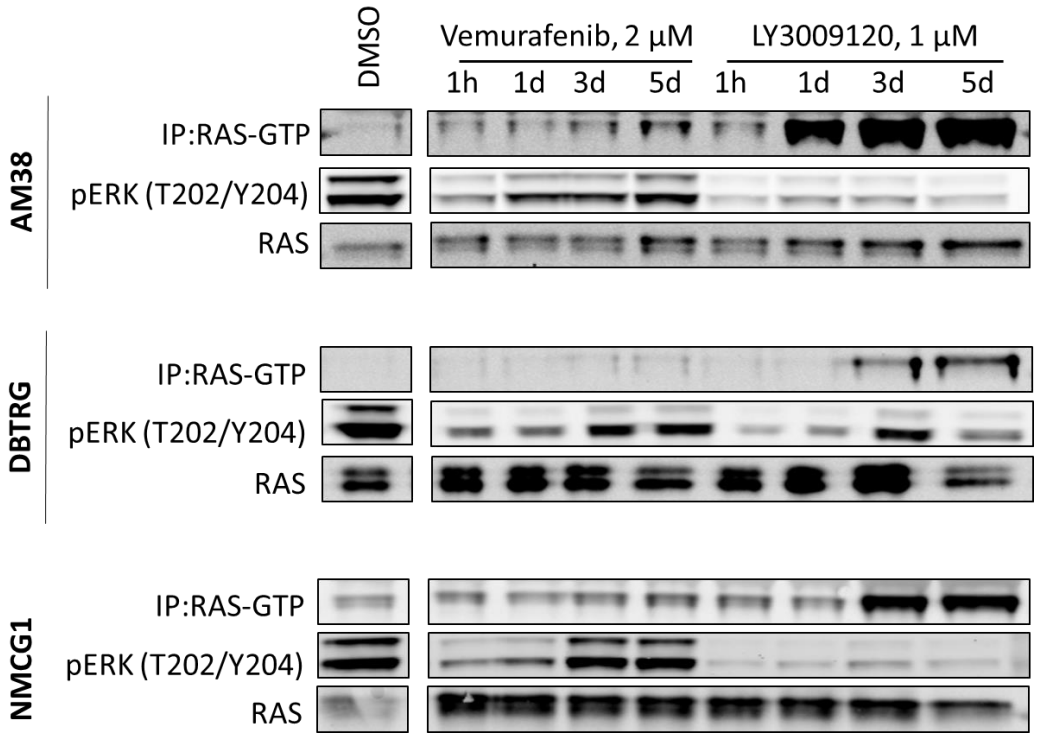

Figure 5-6. LY3009120 induces less ERK rebound than vemurafenib in BRAF V600E GBM cells. Aliquots of whole cell lysates from cells treated with 2 μM vemurafenib or with 1 μM LY3009120 for the indicated amounts of time were immunoprecipitated with GST-CRAF-RBD. The pulldown product was subjected to immunoblot analysis with a RAS antibody along with whole cell lysates for the indicated proteins.

We next wanted to determine if the greater suppression of pERK was correlated with greater suppression of ERK activity. To do so, we measured pERK rebound and Cyclin D1 expression in BRAF-mutant glioma cells treated either with vemurafenib or LY3009120 (**Figure 5-7**). Cyclin D1 is a direct ERL target can be

used to determine the amount of ERK activity in a cell lines. As before, pERK rebounded in the vemurafenib treated cells. This was associated with an incomplete suppression of Cyclin D1 expression. In stark contrast, LY3009210 was able to achieve a much greater suppression of Cyclin D1 expression, even at 5 days after

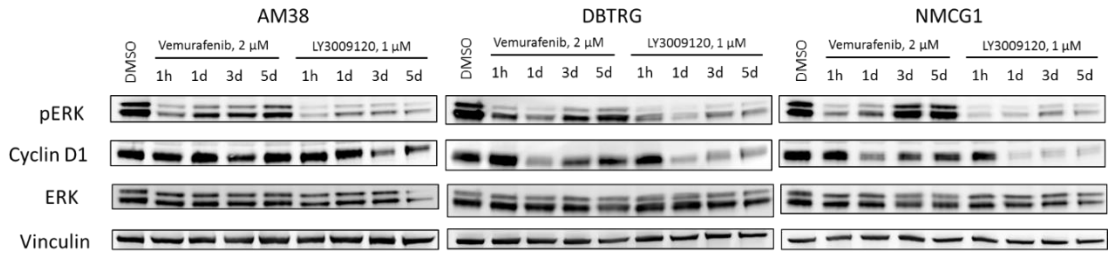

initial treatment.

Figure 5-7. LY3009120 more durably suppresses Cyclin D1 expression than vemurafenib in BRAF V600E mutant GBM cells. Immunoblot of whole cell lysates from BRAF-mutant glioma cells treated with 2 μM vemurafenib or with 1 μM LY3009120 for the indicated amounts of time.

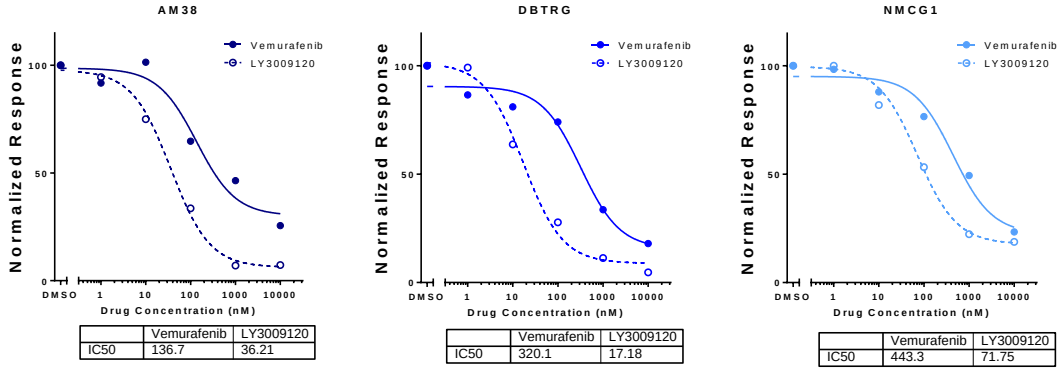

	Vemurafenib	LY3009120
IC50	136.7	36.21

	Vemurafenib	LY3009120
IC50	320.1	17.18

	Vemurafenib	LY3009120
IC50	443.3	71.75

Figure 5-8. LY3009120 more potently suppresses proliferation of BRAF-mutant glioma cells than vemurafenib. BRAF-mutant glioma cells were plated various doses of vemurafenib or LY3009120 for 5 days, then counted in a trypan blue exclusion assay. Normalized cell counts were plotted and the resulting growth inhibition curves plotted in Prism Graphpad

Finally, after determining that LY3009120 was able to potently suppress Cyclin D1 expression, we then wanted to ask if this would translate into greater growth suppression (**Figure 5-8**). We plated a panel of BRAF-mutant cell lines into a dose range of vemurafenib or LY3009120 and then counted the number of viable cells via a trypan blue assay and compared the effectiveness of the two drugs and inhibiting the proliferation of the cell lines.

LY3009120 was significantly more potent in all three cell lines, with IC50s that were approximately 10 fold lower. Furthermore, LY3009120 was also able to achieve much more significant growth suppression in AM38 and DBTRG which were essentially completely arrested at the higher concentrations of drug. Together, these experiments underscore the observation that incomplete pERK suppression is associated with incomplete Cyclin D1 expression and insensitivity to vemurafenib. However, dimer inhibitor LY3009120 was able to inhibit the dimers formed as a result of negative feedback and durably suppress ERK activity.

Because LY3009120 is a relative new drug, we wanted to try to rule out the possibility of off-target effects accounting for the potency we observed. LY3009120 in fact inhibits several other kinases at doses 10-20 fold higher than that of BRAF, several of which are relevant in gliomas (**Figure 5-9A**). The doses used in the previous experiments quite likely inhibit PDGFRα and PDGFRβ. These genes are oncogenes in glioma, so it was important to rule out the possibility that inhibiting them was actually what was responsible for the impressive potency of LY3009210.

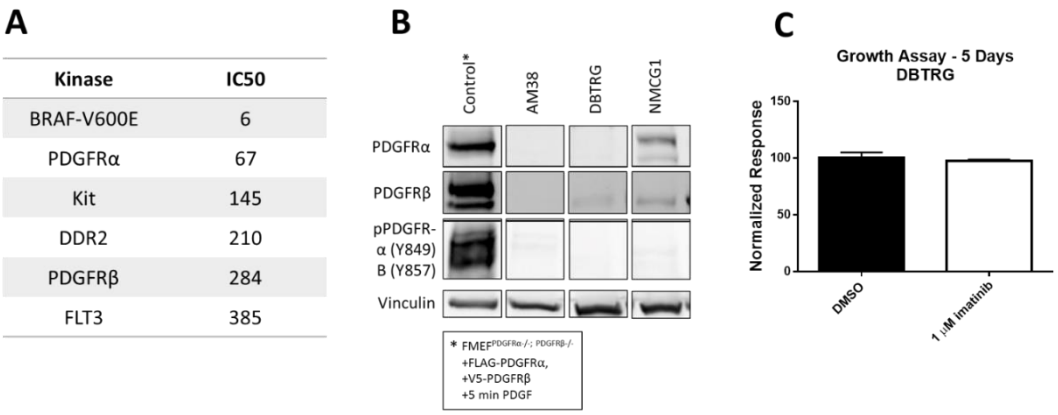

Figure 5-9. Activity of LY3009120 is unlikely due to off-target inhibition on PDGFR. (A) IC50 for various kinases measures in in vitro kinase assays. Adapted from Peng SB, *Cancer Cell* 2015. **(B)** Whole cell lysates from a control cell line and BRAF-mutant glioma cells treated were subjected to immunoblot analysis for the indicated proteins. Control cell lines is PDGFRα and PDGFRβ-null MEFs stably infected with constructs expressing PDGFRα and PDGFRβ and then stimulated with PDGF ligand for 5 minutes. **(C)** DBTRG cells were plated in 1 μM imatinib for 5 days and then counted in a trypan blue exclusion assay. Normalized cell counts were plotted and the resulting growth inhibition curves plotted in Prism Graphpad.

We measured the levels of PDGFRα and PDGFRβ by immunoblot and compared them to a PDGFRα and PDGFRβ null cell engineered to express tagged alleles of PDGFRα and PDGFRβ (**Figure 5-9B**). These cells were then stimulated with PDGF for 5 minutes to activate their receptors. The BRAF-mutant glioma cell lines express very low to undetectable levels of PDGFRα and PDGFRβ and express completely undetectable levels of activated receptor.

Furthermore, the growth of DBTRG cells is not inhibited by the presence of PDGFRα and PDGFRβ inhibitor imatinib. This suggests that any PDGFRα and PDGFRβ present is likely dispensable for proliferation. Therefore, it is unlikely that

the off target effects of LY3009120 are responsible for its potent activity in BRAF-mutant glioma.

In order to provide further evidence for our proof of concept we then asked the question that if the mechanism of action of pan-RAF inhibitors like LY3009120 work by effectively inhibiting RAF dimers (which vemurafenib does not), would other RAF dimer inhibitors also be as effective? To answer his question, we conducted a time course comparing pERK rebound and Cyclin D1 repression of vemurafenib to BGB659, another BRAF inhibitor that binds both sites of BRAF-mutant dimers with equal potency (Yao et al., 2015b).

Although BGB659 this drug appears to be slightly less potent than LY3009120, we still observed a more potent induction of RAS-GTP in the BGB659 treated cells, suggesting that ERK was more strongly inhibited by BGB559 than it was by vemurafenib (**Figure 5-10A**). We also observed lower Cyclin D1 levels in both cell lines, which is also associated with more potent pERK inhibition.

We also measured the effects of BGB659 in a growth assay. A lower dose of dimer inhibitor BGB659 (1 μM) than of vemurafenib (2 μM) was able to more potently block proliferation of both AM38 and NMCG1. AM38 had 50% growth of the DMSO at 5 days while BGB659 had only 35%. NMCG1 was similar lowered from almost 60% to 40%, respectively. Taken together, this suggests that using RAF dimer inhibitors should be able to overcome vemurafenib mediated resistance from relief of ERK dependent negative feedback.

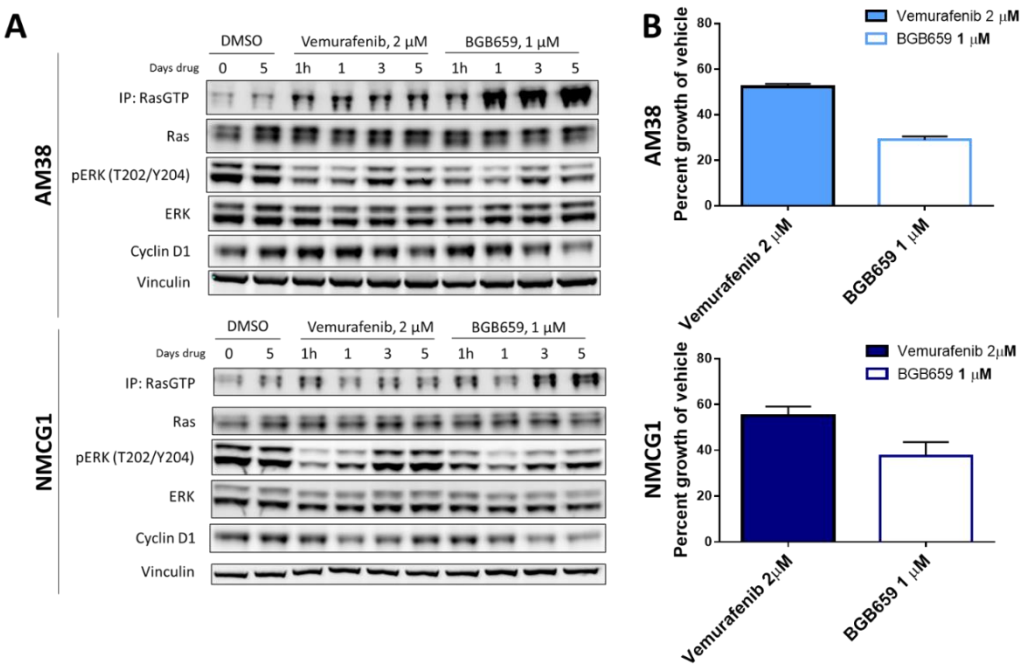

Figure 5-10. BGB659, a drug which binds both sites of mutant BRAF dimers with equal potency, also blocks ERK rebound and more potently suppresses growth of BRAF-mutant glioma. (A) Aliquots of whole cell lysates from cells treated with 2 μM vemurafenib or with 1 μM BGB659 for the indicated amounts of time were immunoprecipitated with GST-CRAF-RBD. The pulldown product was subjected to immunoblot analysis with a RAS antibody along with whole cell lysates for the indicated proteins. **(B)** AM38 and NMCG1 BRAF-mutant glioma cells were plated various doses of vemurafenib or LY3009120 for 5 days, then counted in a trypan blue exclusion assay. Normalized cell counts were plotted and the resulting growth inhibition curves plotted in Prism Graphpad.

Finally, we wanted to try to represent the utility of RAF dimer inhibitor drugs in a more clinical context. Pediatric gliomas often contain BRAF-fusions. However, there are few, if any, available preclinical models for these tumor types.

To establish a preclinical model, we established a collaboration with Weill Cornell, New York Presbyterian, and Memorial Sloan Kettering to receive samples of brain tumors resected from pediatric patients. These patients have an extremely high prevalence of BRAF:KIAA1549 fusions (**Figure 5-1**). These fusions have several breakpoints across BRAF but always maintain the kinase domain and lose the N-terminal regulatory domain. These BRAF fusions then spontaneously dimerize, resulting in constitutive BRAF activity (**Figure 5-11**). We hypothesized that these patients should benefit from a drug that inhibits RAF-dimer activity.

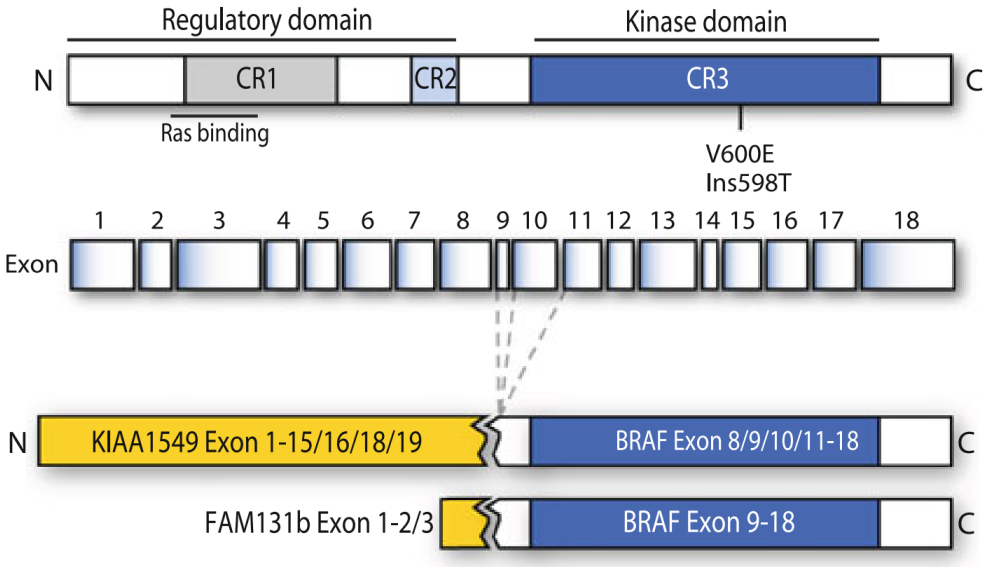

Figure 5-11. Genomic map of breakpoints of BRAF fusions and partners in juvenile pilocytic astrocytoma (JPA). BRAF fusions detected in pilocytic astrocytoma in all cases result in the loss of the regulatory domain of BRAF and constitutive activation of kinase activity. CR – conserved region. Adapted from Gronych J, Cell. Mol. Life Sci. (2011)

When we received these tumor samples in lab, we would then section them into 300 μM sections on a vibratome, and then place these tumor sections into

different drugs to study their biochemical responsiveness (**Figure 5-12A**). We received a tumor from one such patient, whose MRI is shown in **Figure 5-12B**. Tumors are often presented as suspected as containing a BRAF fusion based on patient characteristics like age and tumor location. However, genetic conformation of BRAF fusions often is not done until well after a surgery, which necessitates assuming the mutational status of a tumor and treating the tumor as such.

The tumor we treated in Figure 5-12 ended up being wildtype for BRAF. Consistent with this finding, vemurafenib in fact induced pERK signaling in the tumor slices, consistent with what would be expect in a tumor signaling with wildtype BRAF, which also constitutively signals as a dimer. We also observed that treating the tumor with LY3009120 did not result in pERK induction (consider the pERK to total ERK signal, as total ERK appears to be higher in the LY3009120 sample).

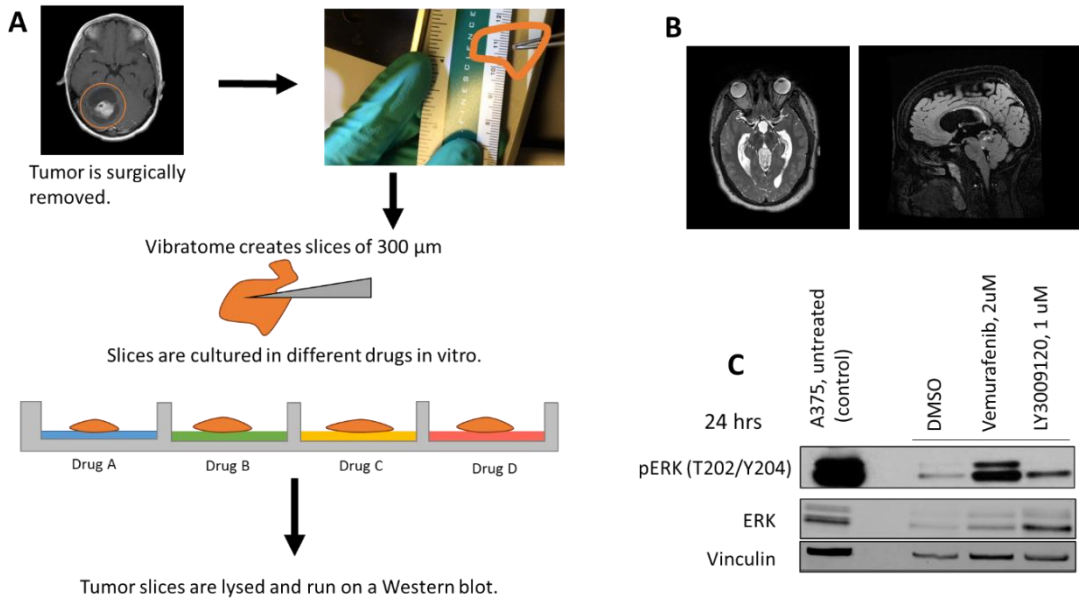

Figure 5-12. Schematic of the ex vivo treatment of surgical JPA tumor samples. (A) Patients with suspected JPA have their tumors surgically removed in the operating room. Tumor samples arrive in the lab and are cut into 300 µM sections on a vibratome. The resulting tumor slices are placed into different drugs for varying amounts of time before being lysed and analyzed by immunoblot. **(B)** MRI of patient's brain tumor. **(C)** Immunoblot of vibratome slices treated with the drugs indicated for 24 hours.

While we have yet to be able to treat a BRAF-fusion containing tumor sample in this way, this experiment serves as a proof of concept that we will be able to analyze BRAF-fusions in their native niche using these tools.

Discussion

The data collected in the earlier experiments establish what has been shown in several other contexts, including that elevated BRAF activity is associated with

feedback inhibition on RTK and RAS signaling, leading to constitutively low RAS-GTP levels that cannot support the formation of significant amounts of RAF dimers. However, following BRAF inhibition, relief of this negative feedback creates a permissive environment for RTK signaling, leading to increased levels of RAS-GTP formation and the induction of vemurafenib insensitive RAF dimers.

However, our data showing that RAF dimer inhibitors can overcome this phenomenon and durably inhibit ERK signaling driven by relief of feedback driven dimer formation is quite novel, and could have therapeutic impact beyond just BRAF-mutant glioma or even beyond tumor adaptation to mutant-BRAF signaling. Indeed, any tumor driven by RAF-dimers would be expected to respond to a RAF dimer inhibitor. For example, pancreatic, lung, ovarian, and thyroid cancers with specific in-frame deletions near the kinase domain shifts BRAF into a conformation that favors spontaneous dimerization have recently been shown to respond to LY3009120 (Chen Peng).

While LY3009120 informs the bulk of the data we've shown, it is quite likely the more RAF dimer inhibitors with better selectivity profiles and potencies will become available. As they are, it will be interesting to compare thier effectiveness and therapeutic indices. LY3009120 inhibits RAF monomers and dimers, but is less potent again RAS-mutant driven RAF actions. On the other hand, BGB659 only inhibits dimers containing mutant-BRAF and actually paradoxically activates wild-type RAF dimers, giving it a wider therapeutic index.

CHAPTER 6: EXPLORING THE MEK DEPENDENCY OF NF1-DEFICIENT GBM

Introduction

The most common and well understand of RAS-activating mutations are the canonical RAS mutations that impair the intrinsic GTPase enzymatic activity of RAS(Cox et al., 2014). These mutations prevent RAS from hydrolyzing bound GTP to GDP. However, RAS can also become activated through loss of its GTPase acting protein (GAP) NF1. The normal function of NF1 is to catalyze the intrinsic enzymatic activity of RAS. However, a certain proportion of tumors have been reported with mutations that either delete NF1 protein or impair its catalytic activity, leading to impaired regulation of RAS activity.

RAS has many effector pathways including the RAF-MEK-ERK pathway as well as the PI3K/Akt/mTOr pathway, as well as several others. However, repeated studies have revealed a MEK dependency in NF1-deficient tumors (Nissan et al., 2014). Why NF1-deficient tumors seem so dependent on RAF-MEK-ERK signaling instead of any of the other RAS effector pathways remains an open question.

Results

In glioma, NF1 mutations occur in the mesenchymal subtype, which are especially aggressive and hard to treat The first TCGA project in GBM found mutations or allelic loss in NF1 in 18% of tumors recorded, suggesting that NF1 loss is a frequent event in GBM (Figure 6-1A). Of almost 1000 tumors in the COSMIC database in which an alteration of NF1 was recorded, only about 12% were a point

mutation. The rest were frameshift or complex genomic events that completely eliminated the allele, or nonsense mutations that prematurely truncated the protein (Figure 6-1B).

Using an inducible NF1 cDNA, we decided to explore the biochemical and biological MEK dependency of NF1-defieicnt GBM.

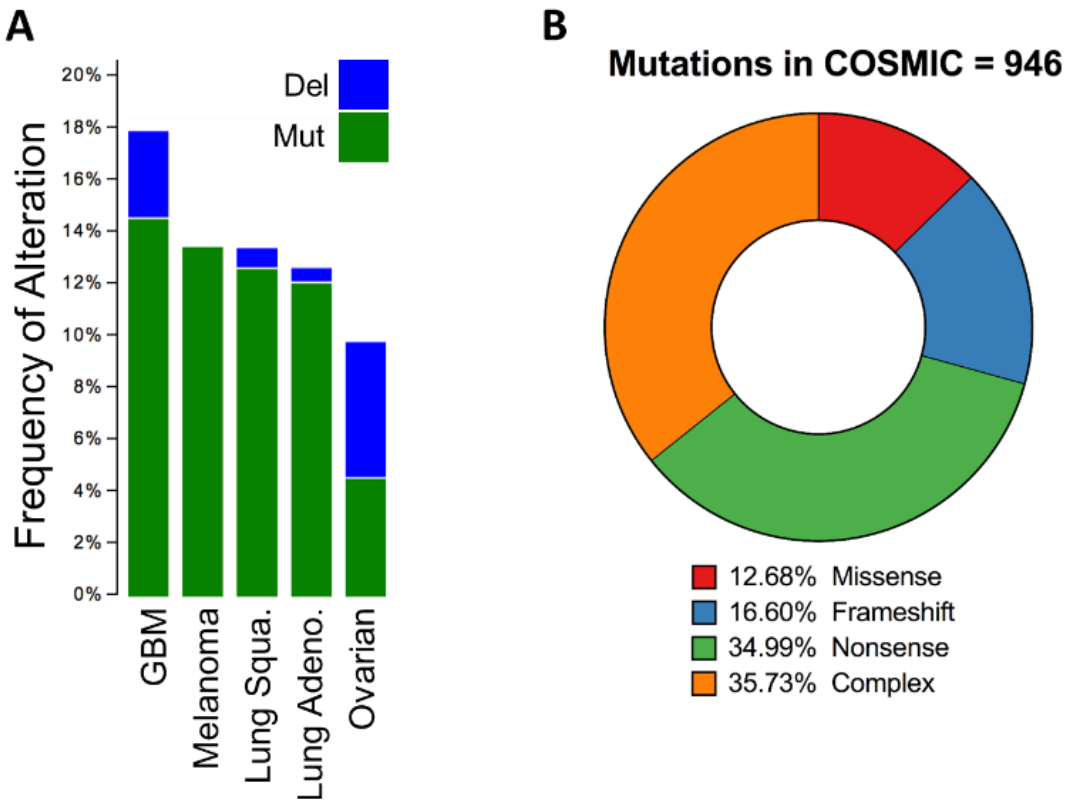

Figure 6-1. NF1 is recurrently mutated in glioblastoma and several other cancers. **(A)** Graph of the frequency of point mutation or copy number loss of NF1 in glioblastoma (GBM) and several other cancers as measured in their respective TCGA analyses. **(B)** Graph of the proportion of types of alterations in NF1 recorded in the COSMIC database.

We first cloned an inducible cDNA of NF1 into the two-vector TET-on T3G system from Clontech. This system puts the Tet-operator under the control of a constitutive promoter on one vector with one selection marker and the NF1 cDNA under the control of the Tet-response element (TRE), allowing for greater size of inserts into viral packaging systems, necessary to accommodate the 8.5 kB coding sequence of the NF1 gene. Treatment of stable cell lines with doxycycline induces expression of the cDNA at the TRE.

We started by validating the construct biochemically by reconstituting NF1 function in a variety on contexts and studying its biochemical functions. We initially chose U251 cells which have a homozygous frame shift in NF1 that genetically would be expected to eliminate the allele. U251 indeed express no detectable NF1 and have detectable RAS-GTP (**Figure 6-2A**, Lane 1). However, after treatment with doxycycline, an NF1 antibody-reactive band appears (**Figure 6-2A**, Lane 2). This is associated with a concomitant decrease in RAS-GTP loading.

We next asked if overexpression of NF1 in a NF1-wildtype cell line would also decrease RAS-GTP loading. T98G cells are wildtype for NF1 (**Figure 6-2B**). Basal expression of endogenous NF1 results in lower expression of RAS-GTP. When treated with doxycycline, NF1 over-expression results in further unloading of RAS-GTP.

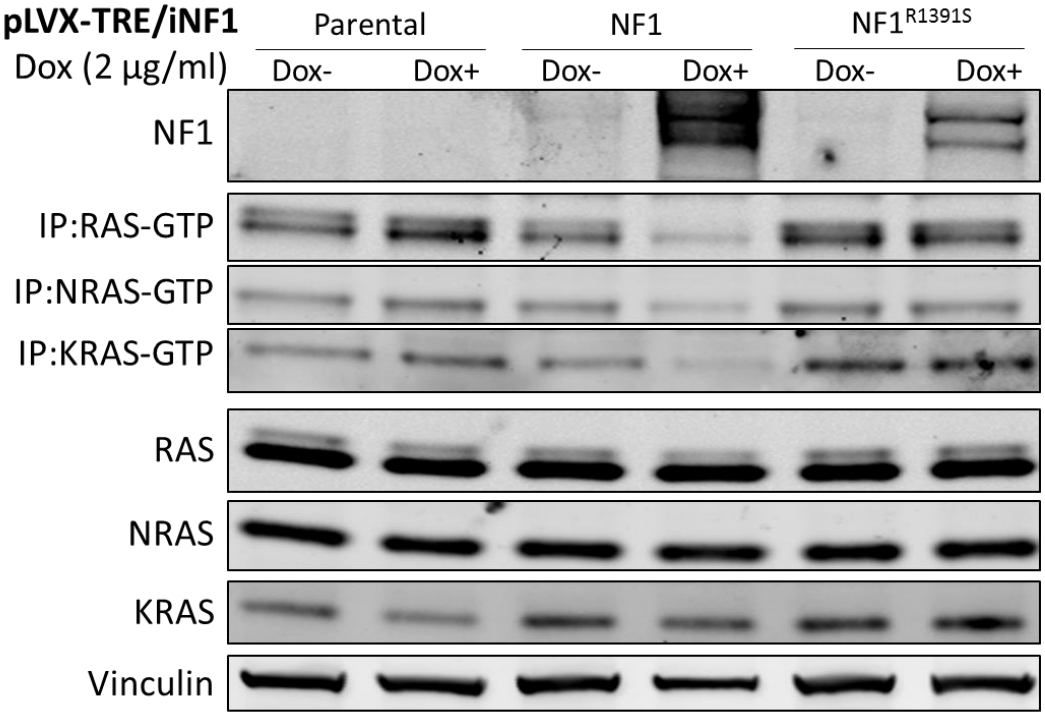

Figure 6-2. A doxycycline inducible cDNA of NF1 restores GTPase activity in cell lines with NF1 loss or wild type NF1, but not RAS mutations. Cells with **(A)** biallelic NF1 loss, **(B)** wild type NF1, or **(C)** NRAS mutation were infected with a doxycycline inducible NF1 expression cassette. Aliquots of whole cell lysates from cells treated with 2 µg/ml doxycycline or vehicle for 3 days were immunoprecipitated with GST-CRAF-RBD. The pulldown product was subjected to immunoblot analysis with a RAS antibody along with whole cell lysates for the indicated proteins. **(D)** NF1 deficient TM31 cells were infected with a doxycycline inducible NF1 expression cassette. Aliquots of whole cell lysates from cells treated with various dilutions doxycycline for 3 days were immunoprecipitated with GST-CRAF-RBD. The pulldown product was subjected to immunoblot analysis with a RAS antibody along with whole cell lysates for the indicated proteins

Finally, to rule out the possibility that the NF1 cDNA could be acting in dominant negative manner, we overexpressed NF1 in H1299 cells which harbor an NRAS mutation (**Figure 6-2C**). Induction of NF1 over-expression with doxycycline failed to reduce RAS-GTP, consistent with the evidence that RAS-mutants lack GTPase catalytic activity that cannot be activated by NF1.

We also titrated NF1 expression using a dilution series of doxycycline (**Figure 6-2D**). Increasing amounts of doxycycline resulted in creased expression levels and corresponding decreases in RAS-GTP loading for concentrations of doxycycline up to between 1 μg/ml and 3 μg/ml. This indicated that the NF1 construct in inducible across a wide range on concentrations of doxycycline. Taken together, NF1 reconstitution and over-expression result in consistently lower levels of RAS-GTP, except in RAS-mutant cells which would not be expect to respond, validating the biochemical activity of the construct.

As a final validation step, we engineered an NF1 mutant with a mutation in the GAP-related domain (GRD) that would render the GTPase activity of NF1 catalytically dead (**Figure 6-3**). When wildtype NF1 was reconstituted in the NF1-deficient cell line, total-RAS-GTP decreased. WE also measured the RAS-GTP levels of NRAS and KRAS isoforms as well, and each of these was individually unloaded by wildtype NF1 reconstituion. When the NF1-R1391S mutation was reconstituted in an NF1-deficient cell line, it failed to reduce RAS-GTP levels, indicating that NF1 mutant was catalytically inactive.

Taken together, NF1 reconstitution and over-expression result in consistently lower levels of RAS-GTP, except in RAS-mutant cells which would not be expect to respond, validating the biochemical activity of the construct.

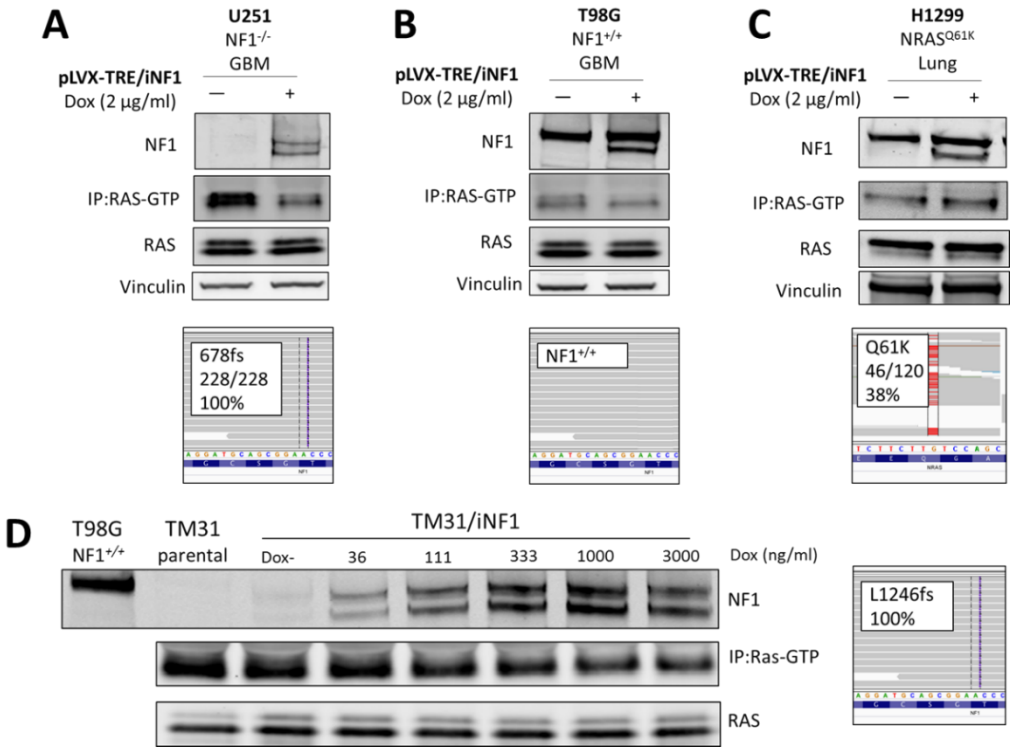

Figure 6-3. Reconstitution of NF1 with inactivating mutations in the RAS-GTPase domain does not decrease RAS-GTP levels. Aliquots of whole cell lysates from NF1 deficient TM31 cells expressing a doxycycline inducible wildtype, R1391S, or K1423E NF1 expression cassette cells treated with 2 µg/ml doxycycline or vehicle for 3 days were immunoprecipitated with GST-CRAF-RBD. The pulldown product was subjected to immunoblot analysis with a RAS antibody along with whole cell lysates for the indicated proteins.

Both mutants are found in GBM while K1423 is also is the catalytic lysine in NF1. Reconstitution of wildtype NF1 unloads RAS-GTP while the two RAS-GTPase

mutant do not. The RAS-GAP mutants are expressed at lower levels, so it's possible that increasing their expression might uncover residual GTPase enzymatic activity.

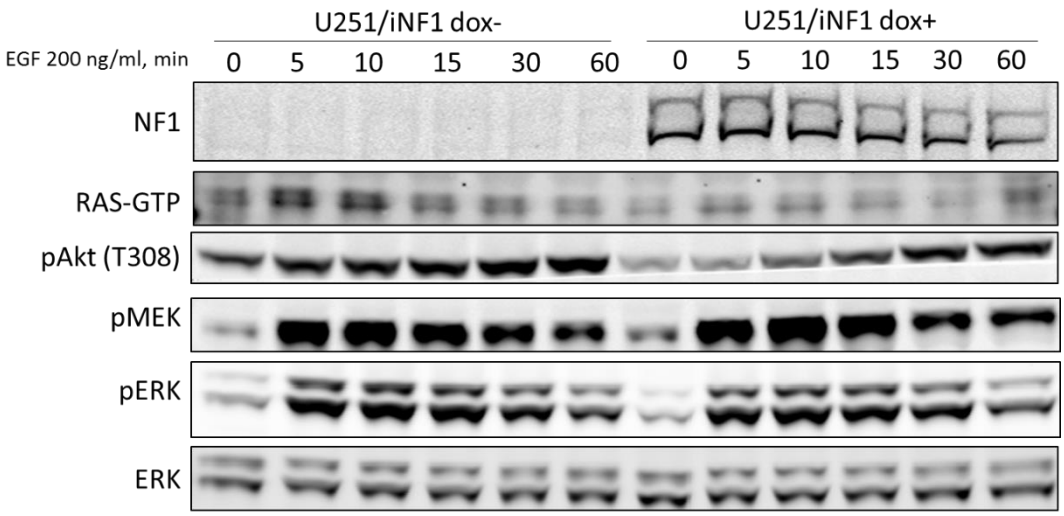

Figure 6-4. Reconstitution of NF1 blunts EGF-induced RAS-GTP loading and Akt activation. Aliquots of whole cell lysates from NF1-deficient U251 cells expressing a doxycycline inducible NF1 expression cassette cells treated with 2 μg/ml doxycycline or vehicle for 3 days, serum starved overnight, and then stimulated with 200 ng/ml EGF for the indicated amounts of time were immunoprecipitated with GST-CRAF-RBD. The pulldown product was subjected to immunoblot analysis with a RAS antibody along with whole cell lysates for the indicated proteins.

We next sought to try to understand the effects of NF1 reconstitution on the RAS-effector pathways RAF-MEK-ERK and PI3K-Akt signaling. We reconstituted NF1 expression in U251 cells, starved them overnight, and then conducted a stimulation time course with EGF (**Figure 6-4**). To the cell not treated with doxycyclin and that lack NF1 reconstitution, , EGF increased the the loading of RAS-GTP at 5 and 10 minutes before tapering off. Phosphorylation of Akt-T308 started high, and increased through the hour of EGF stimulation. EGF also potently

stimulated MEK and ERK signaling with rapidly rose at 5 minutes and then tapered slowly throughout the hour. In stark constrant, NF1 reconstitution blunted RAS-GTP loading and severly retarded and blunted the activation of pAkt-T308. However, MEK and ERK activation appeared to have identical kinetics with and without NF1

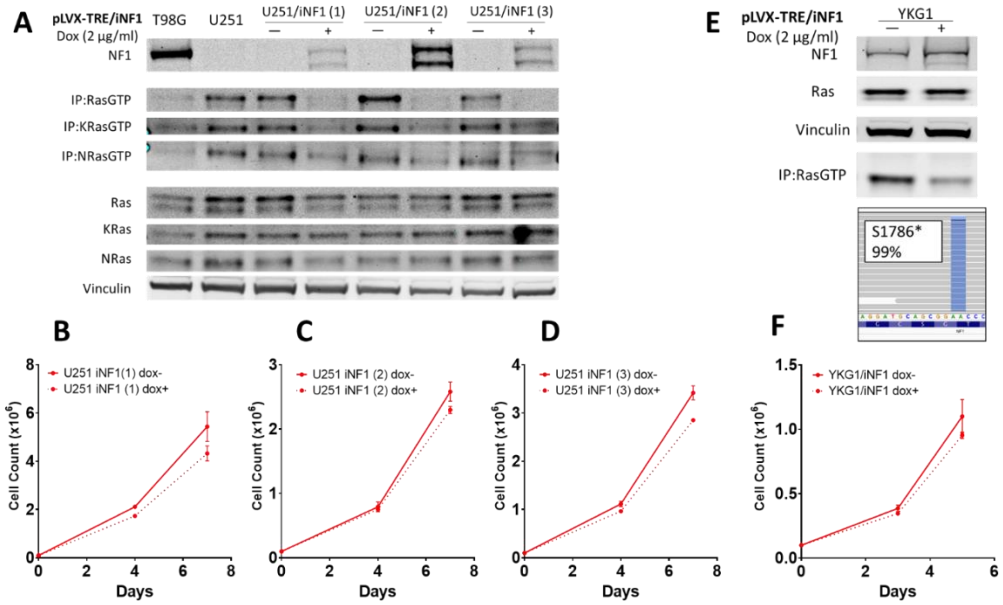

expression. This provides both clear biochemical evidence that NF1 reconsitution is functional and also suggests to us that that in these cells, NF1 is not "wired" to alter MEK-ERK signaling and instead functions to control PI3K/Akt signaling.

Figure 6-5. Reconstitution of NF1 does not significantly slow the proliferation of two NF1-deficient cell lines. (A) NF1-deficient U251 cells were independently infected three times [labeled (1), (2), and (2)] with a doxycycline inducible NF1 expression cassette. Aliquots of whole cell lysates from parental cells and the independently infected cells treated with 2 µg/ml doxycycline or vehicle for 3 days were immunoprecipitated with GST-CRAF-RBD. The pulldown product was subjected to immunoblot analysis with a RAS antibody along with whole cell lysates for the indicated proteins. **(B), (C),** and **(D)** The independently infected cells were plated into 2 µg/ml doxycycline and the number of viable cells counted by trypan blue

exclusion assay at the times indicated. **(E)** and **(F)** NF1-deficient YKG1 cells were treated as above.

With such clear evidence for the biochemical activity of NF1 reconstitution, we next sought to ask if NF1 reconstitution would also have such a profound effect the biology of NF1-deficient cell lines. To test this question, we reconstituted NF1 expression by infecting U251 cells three independent times, resulting in three different levels of reconstituted protein (**Figure 6-5A**, lanes 4, 6, and 8). In all three cases, NF1 reconstitution resulted in an unloading of total RAS-GTP, as well as decreases in KRAS-GTP and NRAS-GTP. However, in all three cases, there was no significant inhibition of proliferation (**Figure 6-5B, C and D**). We also tried to reconstitute NF1 in a different NF1-deficient cell line YKG1. Again, despite clear evidence for unloading RAS-GTP, we observed no inhibition of proliferation.

We also reconstituted NF1 in the NF1-deficient GBM cell line TM31, which was isolated from a patient with neurofibromatosis who was born with a germline mutation in one allele of NF1. Presumably the tumor received a Knudsen "second hit" in NF1 in order to develop a high grade glioma. We reasoned that an NF1-deficient tumor isolated from such a patient would be the most likely to retain a dependency on NF1 for tumor maintenance. Reconstitution of NF1 in TM31 reduced RAS-GTP loading, as in the other NF1-deficient cell lines before. However, NF1 reconstitution had a much more pronounced effect on inhibition of proliferation, reducing it about by at 50% in two separate trials.

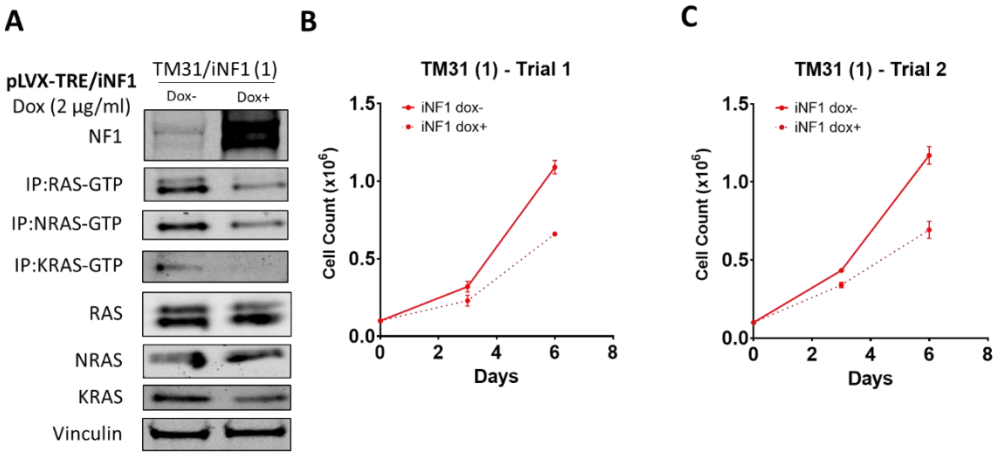

Figure 6-6. Reconstitution of NF1 in a GBM cell line isolated from a patient with neurofibromatosis unloads RAS-GTP and inhibits proliferation. (A) NF1-deficient TM31 cells were infected with a doxycycline inducible NF1 expression cassette. Aliquots of whole cell from cells treated with 2 µg/ml doxycycline or vehicle for 3 days were immunoprecipitated with GST-CRAF-RBD. The pulldown product was subjected to immunoblot analysis with a RAS antibody along with whole cell lysates for the indicated proteins. **(B)** and **(C)** The infected cells were independently plated into 2 µg/ml doxycycline or vehicle and the number of viable cells counted by trypan blue exclusion assay at the times indicated.

From these results, we conclude that some, but not all NF1-deficent tumors maintain their dependence on NF1-deficient signaling. NF1 mutations are thought to be early events in the developments of glioma, so it is possible that NF1-deficient signaling is required for tumor initiation, but not for tumor maintenance in certain cell lines (Zhu et al., 2005). The observation that a GBM cell line isolated from a neurofibromatosis patient retains its NF1-dependency leads us to believe that in certain contexts though, it is very possible to retain an addiction to NF1-deficient signaling.

We also sought to determine what effect NF1 reconstitution had on MEK signaling in NF1 deficient cell lines. In three separate cell lines in which we reconstituted NF1 and successfully unloaded RAS-GTP, we did not see any changes in MEK or ERK signaling (**Figure 6-7**). We found this observation somewhat unexpected, as cell lines that develop with a MEK dependence as a result of loss of a tumor suppressor would be expected to have altered MEK signaling as a result of reconstituting that tumor suppressor.

With that in mind, we then interrogated the MEK kinase dependence of a panel of NF1-deficient cell lines and compared their IC50s to that of BRAF-mutant glioma and a BRAF-mutant melanoma cell line, which have a clearly established dependence on MEK kinase activity. We measured the growth inhibition of the MEK inhibitor trametinib in these cell lines, plotted the growth inhibition curves, and determined their IC50s.

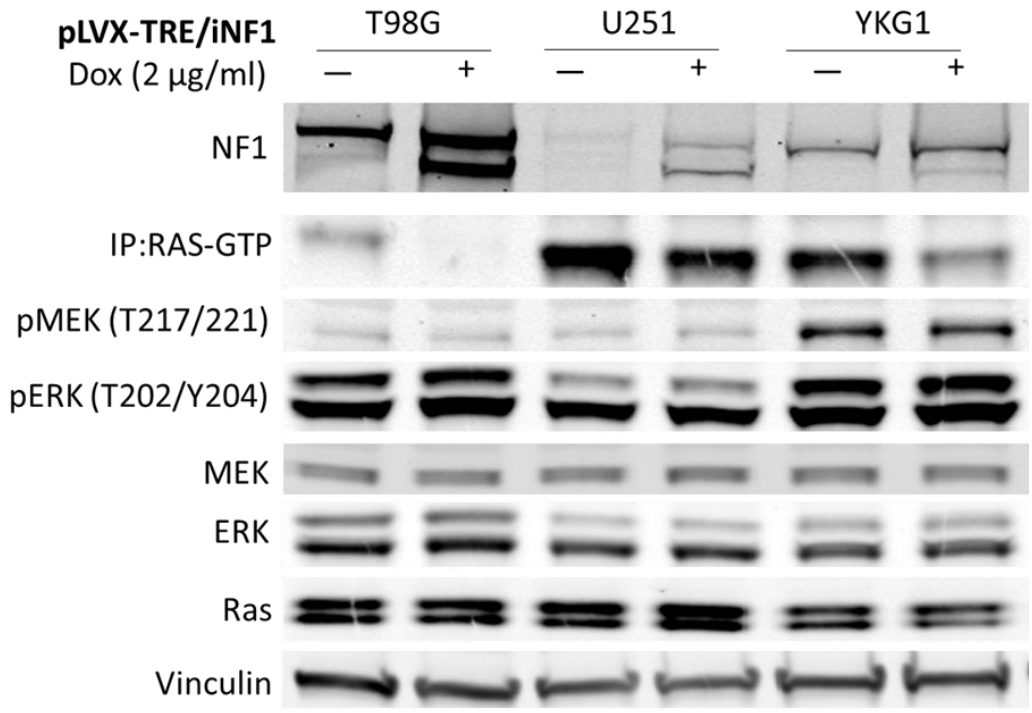

Figure 6-7. Despite unloading RAS-GTP, NF1 reconstitution in NF1 deficient cell lines does effect MEK/ERK signaling. NF1-deficient cell lines were infected with a doxycycline inducible NF1 expression cassette. Aliquots of whole cell from cells treated with 2 µg/ml doxycycline or vehicle for 3 days were immunoprecipitated with GST-CRAF-RBD. The pulldown product was subjected to immunoblot analysis with a RAS antibody along with whole cell lysates for the indicated proteins.

Interestingly, the three NF1-deficient cell lines were all sensitive to trametinib, but at 20 to 50-fold higher concentrations of trametinib (**Figure 6-8A**). The IC50s for th eNF1-deficient cell lines were calculated to be between 10 and 20 nM. This was consistent with the concentration at which ERK appeared to be inhibited in representative acute biochemistry (**Figure 6-8B**). We also looked at the sensitivity of 537 cells which were treated with the allosteric MEK inhibitor AZD6244 (selumetinib) to determine if sensitivity to MEK inhibitors is a universal feature of

cancer cell lines. The cancer cell line encyclopedia ranks cell line based on their sensitivity to drugs (**Figure 6-8C**). The green dots represent cell lines with IC50s that fall below the maximum concentration of drug used in the assay. We conclude that only 15% of the cell line tested showed sensitivity to selumetinib, so it is unlikely that response to MEK inhibitors is a universal feature of cancer cell lines.

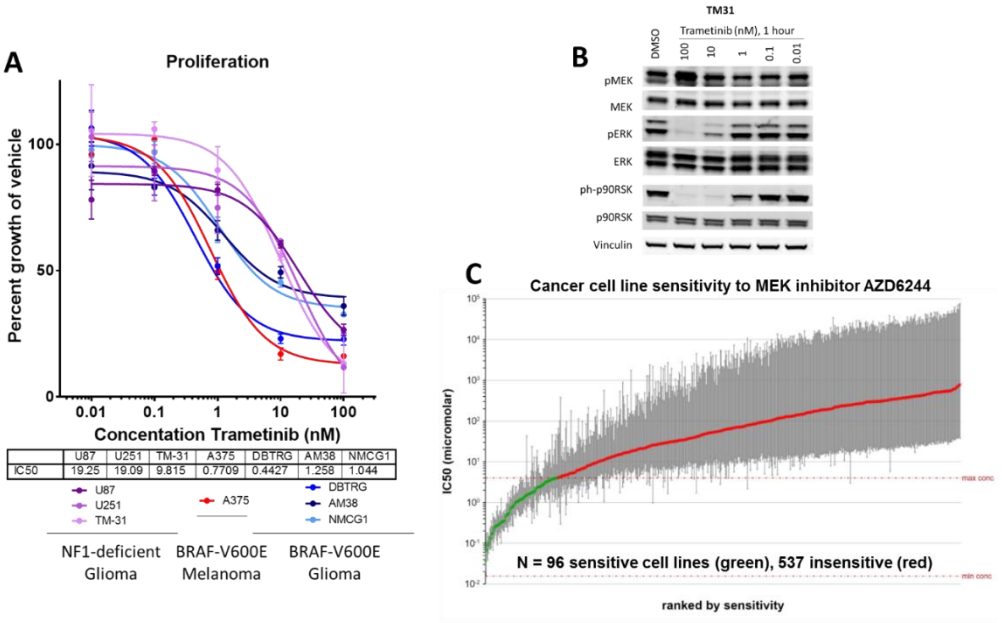

Figure 6-8. Proliferation of NF1-deficient cells is inhibited at higher concentrations of trametinib than is of BRAF-mutant melanoma and glioma. (A) The cell lines indicated were plated in various doses of trametinib for 5 days, then counted in a trypan blue exclusion assay. Normalized cell counts were plotted and the resulting growth inhibition curves plotted in Prism Graphpad. **(B)** Immunoblot of TM31 cells treated with various doses of trametinib for one hour. **(C)** Plot of range of IC50s for allosteric MEK inhibitor AZD6244 for the cancer cell line encyclopedia.

Trametinib is a highly selective allosteric inhibitor. Nevertheless, in order to rule out off target effects, we expressed a drug resistant allele of MEK (MEK1-L115P or MEK2-L119P; collectively referred to as MEK-LP) and compared its ability to

rescue the growth inhibition of trametinib compared to a wild type MEK allele or the parental cells (**Figure 6-9**).

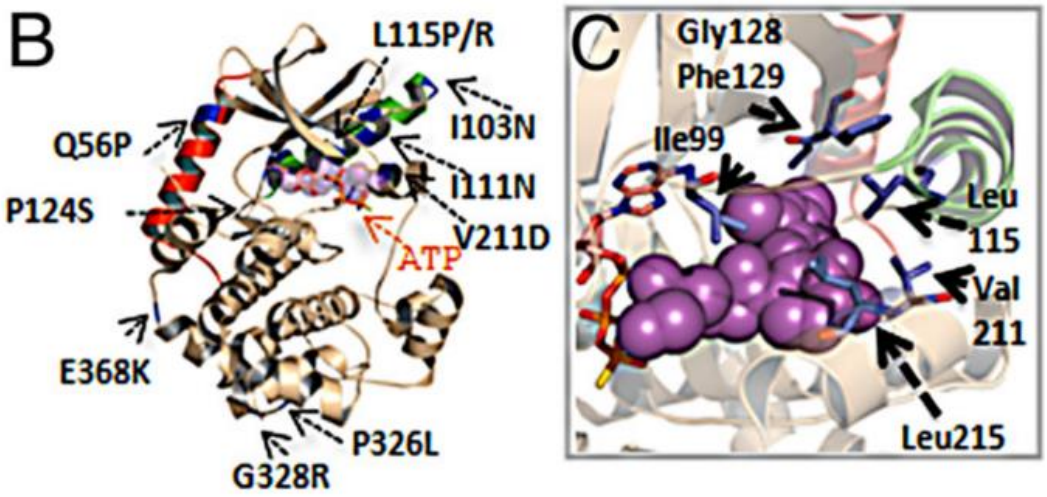

Figure 6-9. Crystallographic depiction of the L119P MEK inhibitor resistant allele. L119 is situated directly within the arylamine pocket to which allosteric MEK inhibitors bind. Shown in purple is the MEK inhibitor PD318088 which has a similar binding mechanism to trametinib. (From Smith et al. 2011)

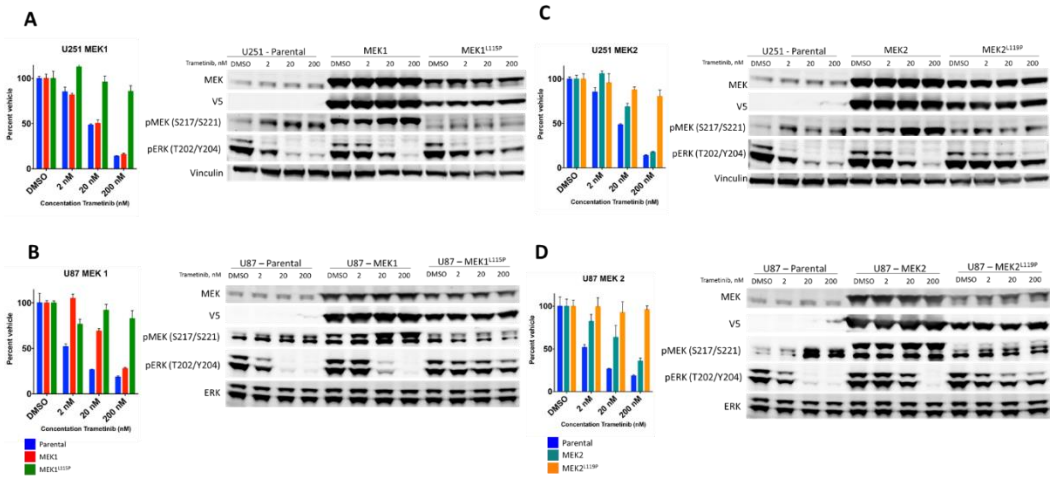

Figure 6-10. Expression of a drug resistant MEK1 or MEK2 allele is sufficient to block trametinib sensitivity in two NF1-deficient cell lines. U251 [**(A)** and **(C)**] or U87 [**(B)** and **(D)**] parental cells where infected with a wild type MEK1 drug resistant MEK1-L115P [**(A)** and **(B)**] or wild type MEK2 or drug resistant MEK2-L119P [**(C)** and **(D)**]. The cell lines were then plated in various doses of trametinib for 5 days, then counted in a trypan blue exclusion assay. Normalized cell counts were plotted and the resulting growth inhibition curves plotted in Prism Graphpad. Immunoblots of each cell line treated with trametinib are shown.

Overexpression of a wild type allele of MEK only provided a very slight rescue (**Figure 6-10**). In contract, expression of a drug resistant MEK1-L115P or MEK2-L119P allele is sufficient to completely rescue trametinib sensitivity in both cell lines at concentrations up to 200 nM trametinib, indicating that the trametinib IC50s for the NF1-deficient cell lines in the 20 nM range is an on target effect.

There is residual pERK signaling in the MEK-LP cells indicated that trametinib binding in inhibed and cannot inhibit pERK remains even at very high doses of trametinib (10 times the IC50 of the NF1-deficient cell lines) and is associated with continued proliferation. In contract, pERK is inhibited in the parental

and wild type MEK expressing cells at 20 nM in most cell lines and at 200 nM in all cell lines. Together, this suggests that NF1-deficient cell lines maintain their MEK sensitivity, but can uncouple it from their NF1-dependency and ability to affect MEK signaling.

Discussion

The canonical roles of NF1 signaling are well established. Guanine exchange factors (GEFs) activate RAS loading while GAPs counterbalance their activity. Activated RAS can then signal to one or more of its effector pathways. However, as with so many other things in cancer, these canonical pathways do not always directly translate to the wiring of oncogenic signal pathways.

We provided direct evidence that NF1 does not alter the biochemical signaling of MEK or ERK by reconstituting NF1 in a variety of NF1-deficient cell lines, including those that are dependent on NF1 for tumor maintenance, and observing that pMEK and pERK do not change. However, we also showed that NF1-deficient cell lines can maintain a dependence on MEK kinase activity and that this dependence is not a universal feature of cancer cell lines. This suggests that NF1-deficient GBM can disconnect their MEK kinase dependency from their biochemical dependency on NF1.

APPENDIX A: MATERIALS AND METHODS

Cell lines and culture conditions

Cell lines were sequenced on an Illumina MiSeq for a panel of genes selected by our laboratory, including *ARAF, BRAF, RAF1, HRAS, NRAS, KRAS, NF1, MAP2K1, MAP2K2, MAP3K1, and MAP3K2* and the MSKCC Integrated Genomics Core.

Cell Line	Reference Cell Line Name	Source	Method of obtaining	Product Number	Culture Media	Ref.
A375	A-375	ATCC	Purchase	CRL-1619	DMEM+10% FBS with antibiotics	(Giard et al., 1973)
AM-38	AM-38	JCRB	Purchase	IFO50492	MEM+10% FBS with antibiotics	(Izumi et al., 1994)
293T	Lenti-X 293T	Clontech	Purchase	632180	IMDM+10% FBS with antibiotics	(n/a)
DBTRG	DBTRG-05MG	ATCC	Purchase	CRL-2020	DMEM+10% FBS with antibiotics	(Kruse et al., 1992)
NMCG1	NMC-G1	JCRB	Purchase	IFO50467	DMEM+10% FBS with antibiotics	(Naruo et al., 1993)
KG1C	KG-1-C	JCRB	Purchase	JCRB0236	DMEM+10% FBS with antibiotics	(Miyake, 1979)
H1299	NCI-H1299	ATCC	Purchase	CRL-5803	RPMI+10% FBS with antibiotics	(Giaccone et al., 1992)

HCT116	HCT 116	ATCC	Purchase	CCL-247	McCoy+10% FBS with antibiotics	(Brattain et al., 1981)
SKMEL239	SKMEL-239	Rosen Lab	Gift	(n/a)	RPMI+10% FBS with antibiotics	(n/a)
MALME3M	Malme-3M	Rosen Lab	Gift	(n/a)	RPMI+10% FBS with antibiotics	(n/a)
SKMEL264	SKMEL-264	Rosen Lab	Gift	(n/a)	RPMI+10% FBS with antibiotics	(n/a)
Hth104	Hth104	Rosen Lab	Gift	(n/a)	RPMI+10% FBS with antibiotics	(n/a)
8505C	8505C	Rosen Lab	Gift	(n/a)	RPMI+10% FBS with antibiotics	(n/a)
HT29	HT-29	Rosen Lab	Gift	(n/a)	McCoy+10% FBS with antibiotics	(n/a)

Cells were maintained under antiseptic conditions in a water jacketed incubator with a 5% CO_2 atmosphere. Media was supplemented with the antibiotics Primocin (100 μg/ml; Invivogen Product #ant-pm-2) and Normocin (100 μg/ml; Invivogen Product #ant-nr-2). All media (except Opti-MEM) was purchased from and made by the MSKCC Media Preparation Facility. Opti-MEM was purchased from ThermoFisher Scientific (Product #31985070). HyClone Fetal Bovine Serum (FBS) (GE Life Sciences; Product #SH30071.03) was added at 10% of the original volume of media. All additives (except drugs) were added and then passed through a sterile 0.22 μM filter (EMD Millipore Product# SCGPU05RE).

Western Blotting

Cell lysates were collected in Phosphate Buffered RIPA (Boston Bioproducts; Product #BP-415) which contains 10 mM Sodium Phosphate, 150 mM NaCl, 1% Triton X-100, 0.5% Sodium deoxycholate, and 0.1% SDS, pH 7.2. Benzonase nuclease (Sigma-Aldrich; Product #E1014-5KU) was added at 1000X Halt Protease and Phosphatase (ThermoFisher Scientific; Product #78440) was added at 100X. Lysates were clarified by spinning in a benchtop centrifuge at maximum speed for 10 minutes at 4˚C. Protein concentration was determined by DC Protein Assay (Bio-Rad; Product# 5000111) with standards diluted in Phosphate Buffered RIPA. Samples were normalized in 4X NuPAGE LDS Sample Buffer (ThermoFisher Scientific; Product #NP0008) to which 8% β-mercaptoethanol (Sigma-Aldrich; Product #M3148-25ML) was added before normalizing or Laemmli SDS-Sample Buffer – Reducing (6X) (Boston Bioproducts; Product #BP-111R). Samples were heated at 70˚C for 10 minutes. Depending on protein concentration, 20-50 μg of protein were loaded onto a NuPAGE Novex 4-12% Bis-Tris Protein Gels and run at 200V constant for 55 minutes. Gels were transferred using a Bio-Rad Trans-Blot wet transfer apparatus for 1 hour at 95 V constant submerged under ice, 2 hours at 65 V constant at 4˚C, or overnight at 35 V constant at 4˚C.

Membranes were blocked in Odyssey Blocking Buffer (Li-Cor; Product #927-40000) for at least one hour. Membranes were incubated in antibodies (cataloged below) diluted 1:250-1:1000 in Odyssey Blocking Buffer with 0.1% Tween-20 for at least one hour at room temperature with shaking, or overnight with shaking. Membranes were washed at least three times in TBS with 0.1% Tween-20 (TBS-T) for

at least 5 minutes per wash. Blots were incubated with IRDye 680RD Goat anti-Mouse IgG (Li-Cor; Product #926-68070) and IRDye 800CW Donkey anti-Rabbit IgG (Li-Cor; Product #926-32213) dilted 1:10,000 in Odyssey Blocking Buffer with 0.1% Tween-20 for at least 30 minutes at room temperature with shaking. Membranes were washed at least three times in TBS-T for at least 5 minutes per wash. Membranes were rinsed in Milli-Q (or equivalent) purified water before being imaged on a Li-Cor Odyssey Infared Imaging Scanner.

Antibodies against ERK1/2 (#9102), phospho-ERK1/2 (#9101), Akt (#2920), phospho-Akt-S473 (#4060), phospho-Akt-T308 (12038) BRAF (#9434), CRAF (#9422), phospho-CRAF S338 (#9427), phospho-CRAF S289, S296, S301 (#9431), phospho-MEK1/2 (#9154), Cyclin D1 (#2978), EGFR (#4267), HER2 (#4290), HER3 (#12708), HER4 (#4795), phospho-EGFR-Y1068 (3777), phospho-HER2-Y1221-Y1222 (#2243), phospho-HER3-Y1289 (#2842), phospho-HER4-Y1284 (#4757), phospho-S6 Ribosomal Protein-S235-S236 (#8207) were purchased from Cell Signaling Technology. Vinculin was purchased form Sigma-Aldrich (#V9131). Ras antibody was obtained in Ras-GTP kit (described below).

Drugs

Vemurafenib (#S1267) and trametinib (#S2673) were obtained from Selleck Chemicals. LY3009120 and BGB-657 were gifts from the Rosen laboratory. Drugs were diluted in anhydrous DMSO to a 10 mM stock (except trametinib which was diluted to a 1 mM stock) before being further diluted in DMSO to 1000X times the concentration to be used in the assay (for a final concentration of 0.1% DMSO in media). Doxycycline (dox) was obtained from Boston Bioproducts (#ABT-265). Puromycin was obtained from Invivogen (#ant-pr-1).

In-Cell Western

In-Cell Western was performed according to manufacturer's instructions. Briefly, cells were plated in a clear bottomed, black-walled plate (BD Falcon; Product #353948) and treated for drugs in the concentrations indicated. Media was removed and cells were fixed in 4% methanol-free paraformaldehyde (ThermoFisher Scientific; Product #28906). Cells were simultaneously permeabilized and washed five times with PBS containing 0.1% Triton X-100 before being blocked in Odyssey Blocking Buffer. Primary antibody incubation, washing, secondary antibody incubation, and imagine were performed as above.

The average and standard error of the mean were plotted in GraphPad Prism. For experiments in which an IC_{50} was to be calculated, data normalized to percent response of vehicle were fit with a log(inhibitor) vs. response (three parameter) non-linear regression for experiments with 5 or fewer doses including vehicle, or a log(inhibitior) vs. response—variable slope (four parameter) for experiments with 6 or more doses.

RAS-GTP Pulldown Assay

RAS-GTP assay was performed according to manufacturer's instructions. Briefly, lysates were collected in 1X Lysis/Binding/Wash Buffer with 100X Halt Protease and Phosphatase inhibitor cocktail added, then clarified, and quantitated. Equal amounts of protein (500-1000 μg) were added to pre-washed glutathione resin with 80 μg GST-Raf-RBD. Samples were incubated at 4˚C with rotation before being

washed three times in 1X Lysis/Binding/Wash Buffer with 100X Halt Protease and Phosphatase inhibitor cocktail added. Bound RAS was eluted with reducing 1.2X Sample Buffer before being heated at 70˚C for 10 minutes. Eluted protein was run as described above in Western Blotting section using kit provided RAS antibody for detection.

Cellular Proliferation Assays

Cells to be plated were trypsinized and counted. Depending on the growth rate of the cell lines, $0.1x10^6$-$0.3x10^6$ cells were plated in a 6cm dish inn at least triplicate. For experiments in which an IC_{50} was to be calculated, cells and their media were trypsinized/collected, spun down, and counted on a Beckman Coulter Vi-Cell XR Cell Viability Analyzer (trypan-blue bases cell viability assay in which live cells exclude the dye outside their cell membranes) after 5 days in drug. For cells in which proliteration over time was measured, cells were collected and counted as above for the indicated amounts of time.

The average and standard error of the mean were plotted in GraphPad Prism. For experiments in which an IC_{50} was to be calculated, data normalized to percent response of vehicle were fit with a log(inhibitor) vs. response (three parameter) non-linear regression for experiments with 5 or fewer doses including vehicle, or a log(inhibitior) vs. response—variable slope (four parameter) for experiments with 6 or more doses.

Generation of cell lines

pTRIPZ constructs contains doxycycline inducible short hairpin RNAs (shRNAs) targeting human BRAF (#V2THS_240239) and CRAF (#V3THS_303540) were purchased from Dharmacon. pENTR-NF1 was a gift from Karen Chichowski at Harvard.

BRAF	Mature Antisense: TAGTGAGCCAGGTAATGAG
CRAF	Mature Antisense: ACTGCAACATCTCCGTGCC

Stable cell lines with dox inducible shRNA to BRAF or CRAF were generated by producting lentivirus in 293T by cotransfecting packaging plasmids pMD2G and pSPAX2 using Lipofectamine 2000 (ThermoFisher Scientific; Product # 11668019) according to manufacturer's protocol in Opti-MEM media. Transfection mixture was added dropwise to 90% confluent 293T cells in Opti-MEM media. Transfection mixture was incubated overnight before media was changed to IMDM + 10% FBS. Cells were incubated for 24 hours before lentivirus containing supernatant was collected and filtered through a 0.44 μM Steriflip vacuum filter (EMD Millipore; Product # SE1M003M00). This collection process was then repeated 24 hours later.

Filtered supernatant was supplemented with 1000X hexamethrine bromide, 1,5-Dimethyl-1,5-diazaundecamethylene polymethobromide (Polybrene from Santa-Cruz Biotech; Product #sc-134220) and added to cells to be infected overnight. The next morning media was changed to normal growth media. Cells were infected

overnight a second time before being selected in 2-10 μg/ml puromycin for 2-5 days, or until uninfected parental cells are completely dead).

Cell cycle analysis

Cells were treated with drugs for the indicated amounts of time before being trypsinized, washed, fixed, and permeabilized with saponin containing BD Cytofix/Cytoperm according to manufacturer's protocol before being stained with Hoechst 33342 (NucBlue from ThermoFisher Scientific; Product #R37605) and analyzed for DNA content/fluorescence on a flow cytometer. Corresponding peaks were analyzed in FlowJo to determine cell cycle phase.

RNA isolation and cDNA library preparation

RNA was isolated from cells in RLT Buffer (RNeasy from Qiagen; Product74104) and run through a QIAshredder column (Qiagen; Product #79654) to shear genomic DNA, and then isolated according to kit instructions. RNA was eluted in water and the concentration determined on a Nanodrop Analyzer.

RNA for RNAseq experiments was processed as described below.

RNA for quantitative PCR was normalized to 1.0 μg per reaction and cDNA libraries generated with iScript cDNA Synthesis Kit (Bio-Rad; Product #1708891) according to kit instructions. cDNA was then diluted 1:5 in nuclease free water before being used in QPCR experiments.

RNAseq

RNAseq was performed by the MSKCC Integrated Genomics Core. Briefly, double stranded cDNA libraries were prepared from submitted RNA, digested by DNase I to form double stranded cDNA fragments, ligated to Illumina adaptors, amplified by PCR, and then high-throughput sequenced with 50 base pair reads for 40 million reads.

Quantitative PCR

cDNA libraries were analyzed on a QuantStudio 6 Flex Real-Time PCR machine using ABsolute Blue QPCR Mix (ThermoFisher Scientific; Product #AB-4139/A) which contains the passive dye ROX. RNAs were quantitated using the ΔΔCt method and normalized to Large Ribosomal Protein (*RPLPO*) using TaqMan chemistry (VIC probe/MGB quencher, primer limited). Primer probe pairs for genes were ordered from ThermoFisher Scientific and are cataloged below.

Gene	Catalog number
NRG4	Hs00945535_m1
EPGN	Hs04334113_m1
HBEGF	Hs00181813_m1
EGF	Hs01099999_m1
TGFA	Hs00608187_m1
AREG	Hs00950669_m1
EREG	Hs00914313_m1
BTC	Hs01101204_m1
NRG1	Hs00247620_m1
NRG2	Hs00171706_m1
NRG3	Hs01377907_m1
NRG4	Hs01076090_m1
EGFR	Hs01001580_m1
ERBB2	Hs00176538_m1
ERBB3	Hs00955525_m1
ERBB4	Hs00955511_m1

APPENDIX B: BIBLIOGRAPHY

Cancer Genome Atlas Research Network 2008. Comprehensive genomic characterization defines human glioblastoma genes and core pathways. *Nature* 455(7216), pp. 1061–1068.

Cloughesy, T.F., Cavenee, W.K. and Mischel, P.S. 2014. Glioblastoma: from molecular pathology to targeted treatment. *Annu Rev Pathol* 9, pp. 1–25.

Daley, G.Q., Van Etten, R.A. and Baltimore, D. 1990. Induction of chronic myelogenous leukemia in mice by the P210bcr/abl gene of the Philadelphia chromosome. *Science* 247(4944), pp. 824–830.

Hanahan, D. and Weinberg, R.A. 2011. Hallmarks of cancer: the next generation. *Cell* 144(5), pp. 646–674.

Hegi, M.E., Diserens, A.C., Gorlia, T., Hamou, M.F., de Tribolet, N., Weller, M., Kros, J.M., Hainfellner, J.A., Mason, W., Mariani, L., Bromberg, J.E., Hau, P., Mirimanoff, R.O., Cairncross, J.G., Janzer, R.C. and Stupp, R. 2005. MGMT gene silencing and benefit from temozolomide in glioblastoma. *N Engl J Med* 352(10), pp. 997–1003.

Louis, D.N., Ohgaki, H., Wiestler, O.D., Cavenee, W.K., Burger, P.C., Jouvet, A., Scheithauer, B.W. and Kleihues, P. 2007. The 2007 WHO classification of tumours of the central nervous system. *Acta Neuropathol* 114(2), pp. 97–109.

O'Brien, S.G., Guilhot, F., Larson, R.A., Gathmann, I., Baccarani, M., Cervantes, F., Cornelissen, J.J., Fischer, T., Hochhaus, A., Hughes, T., Lechner, K., Nielsen, J.L., Rousselot, P., Reiffers, J., Saglio, G., Shepherd, J., Simonsson, B., Gratwohl, A., Goldman, J.M., Kantarjian, H., Taylor, K., Verhoef, G., Bolton, A.E., Capdeville, R., Druker, B.J. and IRIS Investigators 2003. Imatinib compared with interferon and low-dose cytarabine for newly diagnosed chronic-phase chronic myeloid leukemia. *N Engl J Med* 348(11), pp. 994–1004.

Ringertz, N. 1950. Grading of gliomas. *Acta Pathol Microbiol Scand* 27(1), pp. 51–64.

Stupp, R., Mason, W.P., van den Bent, M.J., Weller, M., Fisher, B., Taphoorn, M.J., Belanger, K., Brandes, A.A., Marosi, C., Bogdahn, U., Curschmann, J., Janzer, R.C., Ludwin, S.K., Gorlia, T., Allgeier, A., Lacombe, D., Cairncross, J.G., Eisenhauer, E., Mirimanoff, R.O., European Organisation for Research and Treatment of Cancer Brain Tumor and Radiotherapy Groups and National Cancer Institute of Canada

Clinical Trials Group 2005. Radiotherapy plus concomitant and adjuvant temozolomide for glioblastoma. *N Engl J Med* 352(10), pp. 987–996.

Verhaak, R.G., Hoadley, K.A., Purdom, E., Wang, V., Qi, Y., Wilkerson, M.D., Miller, C.R., Ding, L., Golub, T., Mesirov, J.P., Alexe, G., Lawrence, M., O'Kelly, M., Tamayo, P., Weir, B.A., Gabriel, S., Winckler, W., Gupta, S., Jakkula, L., Feiler, H.S., Hodgson, J.G., James, C.D., Sarkaria, J.N., Brennan, C., Kahn, A., Spellman, P.T., Wilson, R.K., Speed, T.P., Gray, J.W., Meyerson, M., Getz, G., Perou, C.M., Hayes, D.N. and Cancer Genome Atlas Research Network 2010. Integrated genomic analysis identifies clinically relevant subtypes of glioblastoma characterized by abnormalities in PDGFRA, IDH1, EGFR, and NF1. *Cancer Cell* 17(1), pp. 98–110.

Weinstein, I.B. and Joe, A. 2008. Oncogene addiction. *Cancer Res* 68(9), pp. 3077–80; discussion 3080.

Wen, P.Y. and Kesari, S. 2008. Malignant gliomas in adults. *N Engl J Med* 359(5), pp. 492–507.

Zülch, K.J. 1980. Principles of the new World Health Organization (WHO) classification of brain tumors. *Neuroradiology* 19(2), pp. 59–66.

Eiermann, W. (2001). Trastuzumab combined with chemotherapy for the treatment of HER2-positive metastatic breast cancer: pivotal trial data. Ann Oncol *12 Suppl 1*, S57–S62.

Endicott, J.A., Noble, M.E.M., and Johnson, L.N. (2012). The structural basis for control of eukaryotic protein kinases. Annu Rev Biochem *81*, 587–613.

Hendrickson, W.A. (2005). Transduction of biochemical signals across cell membranes. Q Rev Biophys *38*, 321–330.

Lemmon, M.A., and Schlessinger, J. (2010). Cell signaling by receptor tyrosine kinases. Cell *141*, 1117–1134.

Lynch, T.J., Bell, D.W., Sordella, R., Gurubhagavatula, S., Okimoto, R.A., Brannigan, B.W., Harris, P.L., Haserlat, S.M., Supko, J.G., Haluska, F.G., et al. (2004). Activating mutations in the epidermal growth factor receptor underlying responsiveness of non-small-cell lung cancer to gefitinib. N Engl J Med *350*, 2129–2139.

McCormick, K., and Baillie, G.S. (2014). Compartmentalisation of second messenger signalling pathways. Curr Opin Genet Dev *27*, 20–25.

Mellinghoff, I.K., Wang, M.Y., Vivanco, I., Haas-Kogan, D.A., Zhu, S., Dia, E.Q., Lu, K.V., Yoshimoto, K., Huang, J.H.Y., Chute, D.J., et al. (2005). Molecular determinants of the response of glioblastomas to EGFR kinase inhibitors. N Engl J Med *353*, 2012–2024.

Sturm, D., Witt, H., Hovestadt, V., Khuong-Quang, D.-A., Jones, D.T.W., Konermann, C., Pfaff, E., Tönjes, M., Sill, M., Bender, S., et al. (2012). Hotspot mutations in H3F3A and IDH1 define distinct epigenetic and biological subgroups of glioblastoma. Cancer Cell *22*, 425–437.

Vivanco, I., Robins, H.I., Rohle, D., Campos, C., Grommes, C., Nghiemphu, P.L., Kubek, S., Oldrini, B., Chheda, M.G., Yannuzzi, N., et al. (2012). Differential sensitivity of glioma- versus lung cancer-specific EGFR mutations to EGFR kinase inhibitors. Cancer Discov *2*, 458–471.

Ward, C.W., Lawrence, M.C., Streltsov, V.A., Adams, T.E., and McKern, N.M. (2007). The insulin and EGF receptor structures: new insights into ligand-induced receptor activation. Trends Biochem Sci *32*, 129–137.

Zhang, J., Yang, P.L., and Gray, N.S. (2009). Targeting cancer with small molecule kinase inhibitors. Nat Rev Cancer *9*, 28–39.

Arora, R., Di Michele, M., Stes, E., Vandermarliere, E., Martens, L., Gevaert, K., Van Heerde, E., Linders, J.T., Brehmer, D., Jacoby, E., et al. (2015). Structural Investigation of B-Raf Paradox Breaker and Inducer Inhibitors. J Med Chem.

Bollag, G., Hirth, P., Tsai, J., Zhang, J., Ibrahim, P.N., Cho, H., Spevak, W., Zhang, C., Zhang, Y., Habets, G., et al. (2010). Clinical efficacy of a RAF inhibitor needs broad target blockade in BRAF-mutant melanoma. Nature *467*, 596–599.

Bollag, G., Tsai, J., Zhang, J., Zhang, C., Ibrahim, P., Nolop, K., and Hirth, P. (2012). Vemurafenib: the first drug approved for BRAF-mutant cancer. Nat Rev Drug Discov *11*, 873–886.

Brattain, M.G., Fine, W.D., Khaled, F.M., Thompson, J., and Brattain, D.E. (1981). Heterogeneity of malignant cells from a human colonic carcinoma. Cancer Res *41*, 1751–1756.

Brondello, J.M., Brunet, A., Pouysségur, J., and McKenzie, F.R. (1997). The dual specificity mitogen-activated protein kinase phosphatase-1 and -2 are induced by the p42/p44MAPK cascade. J Biol Chem *272*, 1368–1376.

Byeon, H.K., Na, H.J., Yang, Y.J., Kwon, H.J., Chang, J.W., Ban, M.J., Kim, W.S., Shin, D.Y., Lee, E.J., Koh, Y.W., et al. (2015). c-Met-mediated reactivation of PI3K/AKT signaling contributes to insensitivity of BRAF(V600E) mutant thyroid cancer to BRAF inhibition. Mol Carcinog.

Cancer Genome Atlas Network (2012). Comprehensive molecular characterization of human colon and rectal cancer. Nature *487*, 330–337.

Cancer Genome Atlas Research Network (2014). Integrated genomic characterization of papillary thyroid carcinoma. Cell *159*, 676–690.

Cargnello, M., and Roux, P.P. (2011). Activation and function of the MAPKs and their substrates, the MAPK-activated protein kinases. Microbiol Mol Biol Rev *75*, 50–83.

Caunt, C.J., Sale, M.J., Smith, P.D., and Cook, S.J. (2015). MEK1 and MEK2 inhibitors and cancer therapy: the long and winding road. Nat Rev Cancer *15*, 577–592.

Chang, M.T., Asthana, S., Gao, S.P., Lee, B.H., Chapman, J.S., Kandoth, C., Gao, J., Socci, N.D., Solit, D.B., Olshen, A.B., et al. (2016). Identifying recurrent mutations in cancer reveals widespread lineage diversity and mutational specificity. Nat Biotechnol *34*, 155–163.

Chapman, P.B., Hauschild, A., Robert, C., Haanen, J.B., Ascierto, P., Larkin, J., Dummer, R., Garbe, C., Testori, A., Maio, M., et al. (2011). Improved survival with vemurafenib in melanoma with BRAF V600E mutation. N Engl J Med *364*, 2507–2516.

Citri, A., and Yarden, Y. (2006). EGF-ERBB signalling: towards the systems level. Nat Rev Mol Cell Biol *7*, 505–516.

Corcoran, R.B., Ebi, H., Turke, A.B., Coffee, E.M., Nishino, M., Cogdill, A.P., Brown, R.D., Della Pelle, P., Dias-Santagata, D., Hung, K.E., et al. (2012). EGFR-mediated re-activation of MAPK signaling contributes to insensitivity of BRAF mutant colorectal cancers to RAF inhibition with vemurafenib. Cancer Discov *2*, 227–235.

Cox, A.D., Fesik, S.W., Kimmelman, A.C., Luo, J., and Der, C.J. (2014). Drugging the undruggable RAS: Mission possible? Nat Rev Drug Discov *13*, 828–851.
Cutler, R.E., Stephens, R.M., Saracino, M.R., and Morrison, D.K. (1998). Autoregulation of the Raf-1 serine/threonine kinase. Proc Natl Acad Sci U S A *95*, 9214–9219.

Van Cutsem, E., Köhne, C.H., Láng, I., Folprecht, G., Nowacki, M.P., Cascinu, S., Shchepotin, I., Maurel, J., Cunningham, D., Tejpar, S., et al. (2011). Cetuximab plus irinotecan, fluorouracil, and leucovorin as first-line treatment for metastatic colorectal cancer: updated analysis of overall survival according to tumor KRAS and BRAF mutation status. J Clin Oncol *29*, 2011–2019.

Dasgupta, T., Olow, A.K., Yang, X., Hashizume, R., Nicolaides, T.P., Tom, M., Aoki, Y., Berger, M.S., Weiss, W.A., Stalpers, L.J., et al. (2015). Survival advantage combining a BRAF inhibitor and radiation in BRAF V600E-mutant glioma. J Neurooncol.

Davies, H., Bignell, G.R., Cox, C., Stephens, P., Edkins, S., Clegg, S., Teague, J., Woffendin, H., Garnett, M.J., Bottomley, W., et al. (2002). Mutations of the BRAF gene in human cancer. Nature *417*, 949–954.

Downward, J. (2003). Targeting RAS signalling pathways in cancer therapy. Nat Rev Cancer *3*, 11–22.

Eck, M.J., Pluskey, S., Trüb, T., Harrison, S.C., and Shoelson, S.E. (1996). Spatial constraints on the recognition of phosphoproteins by the tandem SH2 domains of the phosphatase SH-PTP2. Nature *379*, 277–280.

Fabian, M.A., Biggs, W.H., Treiber, D.K., Atteridge, C.E., Azimioara, M.D., Benedetti, M.G., Carter, T.A., Ciceri, P., Edeen, P.T., Floyd, M., et al. (2005). A small molecule-kinase interaction map for clinical kinase inhibitors. Nat Biotechnol *23*, 329–336.

Flaherty, K.T., Puzanov, I., Kim, K.B., Ribas, A., McArthur, G.A., Sosman, J.A., O'Dwyer, P.J., Lee, R.J., Grippo, J.F., Nolop, K., et al. (2010). Inhibition of mutated, activated BRAF in metastatic melanoma. N Engl J Med *363*, 809–819.

Forbes, S.A., Bindal, N., Bamford, S., Cole, C., Kok, C.Y., Beare, D., Jia, M., Shepherd, R., Leung, K., Menzies, A., et al. (2011). COSMIC: mining complete cancer genomes in the Catalogue of Somatic Mutations in Cancer. Nucleic Acids Res *39*, D945–D950.

Furukawa, T., Sunamura, M., Motoi, F., Matsuno, S., and Horii, A. (2003). Potential tumor suppressive pathway involving DUSP6/MKP-3 in pancreatic cancer. Am J Pathol *162*, 1807–1815.

Giaccone, G., Battey, J., Gazdar, A.F., Oie, H., Draoui, M., and Moody, T.W. (1992). Neuromedin B is present in lung cancer cell lines. Cancer Res *52*, 2732s–2736s.
Giard, D.J., Aaronson, S.A., Todaro, G.J., Arnstein, P., Kersey, J.H., Dosik, H., and Parks, W.P. (1973). In vitro cultivation of human tumors: establishment of cell lines derived from a series of solid tumors. J Natl Cancer Inst *51*, 1417–1423.

Gould, A.E., Adams, R., Adhikari, S., Aertgeerts, K., Afroze, R., Blackburn, C., Calderwood, E.F., Chau, R., Chouitar, J., Duffey, M.O., et al. (2011). Design and optimization of potent and orally bioavailable tetrahydronaphthalene Raf inhibitors. J Med Chem *54*, 1836–1846.

Hall-Jackson, C.A., Eyers, P.A., Cohen, P., Goedert, M., Boyle, F.T., Hewitt, N., Plant, H., and Hedge, P. (1999). Paradoxical activation of Raf by a novel Raf inhibitor. Chem Biol *6*, 559–568.

Hanafusa, H., Torii, S., Yasunaga, T., and Nishida, E. (2002). Sprouty1 and Sprouty2 provide a control mechanism for the Ras/MAPK signalling pathway. Nat Cell Biol *4*, 850–858.

Harvey, J.J. (1964). An unidentified virus which causes the rapid production of tumours in mice. Nature *204*, 1104–1105.

Hatzivassiliou, G., Song, K., Yen, I., Brandhuber, B.J., Anderson, D.J., Alvarado, R., Ludlam, M.J., Stokoe, D., Gloor, S.L., Vigers, G., et al. (2010). RAF inhibitors prime wild-type RAF to activate the MAPK pathway and enhance growth. Nature *464*, 431–435.

Hauschild, A., Grob, J.J., Demidov, L.V., Jouary, T., Gutzmer, R., Millward, M., Rutkowski, P., Blank, C.U., Miller, W.H., Kaempgen, E., et al. (2012). Dabrafenib in BRAF-mutated metastatic melanoma: a multicentre, open-label, phase 3 randomised controlled trial. The Lancet *380*, 358–365.

Heidorn, S.J., Milagre, C., Whittaker, S., Nourry, A., Niculescu-Duvas, I., Dhomen, N., Hussain, J., Reis-Filho, J.S., Springer, C.J., Pritchard, C., et al. (2010). Kinase-dead BRAF and oncogenic RAS cooperate to drive tumor progression through CRAF. Cell *140*, 209–221.

Hoeflich, K.P., Gray, D.C., Eby, M.T., Tien, J.Y., Wong, L., Bower, J., Gogineni, A., Zha, J., Cole, M.J., Stern, H.M., et al. (2006). Oncogenic BRAF is required for tumor growth and maintenance in melanoma models. Cancer Res *66*, 999–1006.

Horbinski, C. (2013). To BRAF or not to BRAF: is that even a question anymore? J Neuropathol Exp Neurol *72*, 2–7.

Huillard, E., Hashizume, R., Phillips, J.J., Griveau, A., Ihrie, R.A., Aoki, Y., Nicolaides, T., Perry, A., Waldman, T., McMahon, M., et al. (2012). Cooperative interactions of BRAFV600E kinase and CDKN2A locus deficiency in pediatric malignant astrocytoma as a basis for rational therapy. Proc Natl Acad Sci U S A *109*, 8710–8715.

Hyman, D.M., Puzanov, I., Subbiah, V., Faris, J.E., Chau, I., Blay, J.Y., Wolf, J., Raje, N.S., Diamond, E.L., Hollebecque, A., et al. (2015). Vemurafenib in Multiple Nonmelanoma Cancers with BRAF V600 Mutations. N Engl J Med *373*, 726–736.
Hynes, N.E., and Lane, H.A. (2005). ERBB receptors and cancer: the complexity of targeted inhibitors. Nat Rev Cancer *5*, 341–354.

Izumi, I., Mineura, K., Watanabe, K., and Kowada, M. (1994). Establishment of the two glioma cell lines: YH and AM. Hum Cell *7*, 101–105.

Johannessen, C.M., Boehm, J.S., Kim, S.Y., Thomas, S.R., Wardwell, L., Johnson, L.A., Emery, C.M., Stransky, N., Cogdill, A.P., Barretina, J., et al. (2010). COT drives resistance to RAF inhibition through MAP kinase pathway reactivation. Nature *468*, 968–972.

Joseph, E.W., Pratilas, C.A., Poulikakos, P.I., Tadi, M., Wang, W., Taylor, B.S., Halilovic, E., Persaud, Y., Xing, F., Viale, A., et al. (2010). The RAF inhibitor PLX4032 inhibits ERK signaling and tumor cell proliferation in a V600E BRAF-selective manner. Proc Natl Acad Sci U S A *107*, 14903–14908.

Kamata, T., Hussain, J., Giblett, S., Hayward, R., Marais, R., and Pritchard, C. (2010). BRAF inactivation drives aneuploidy by deregulating CRAF. Cancer Res *70*, 8475–8486.

Kidger, A.M., and Keyse, S.M. (2016). The regulation of oncogenic Ras/ERK signalling by dual-specificity mitogen activated protein kinase phosphatases (MKPs). Semin Cell Dev Biol.

Kirsten, W.H., Schauf, V., and McCoy, J. (1970). Properties of a murine sarcoma virus. Bibl Haematol 246–249.

Knobbe, C.B., Reifenberger, J., and Reifenberger, G. (2004). Mutation analysis of the Ras pathway genes NRAS, HRAS, KRAS and BRAF in glioblastomas. Acta Neuropathol *108*, 467–470.

Kolch, W., Halasz, M., Granovskaya, M., and Kholodenko, B.N. (2015). The dynamic control of signal transduction networks in cancer cells. Nat Rev Cancer *15*, 515–527.

Kopetz, Desai, S., Chan, J., Hecht, E., O'Dwyer, R.J., Lee, J.P., Nolop, J.R., Saltz, B.K., and L (2010). PLX4032 in metastatic colorectal cancer patients with mutant BRAF tumors. ASCO Meeting Abstracts.

Kruse, C.A., Mitchell, D.H., Kleinschmidt-DeMasters, B.K., Franklin, W.A., Morse, H.G., Spector, E.B., and Lillehei, K.O. (1992). Characterization of a continuous human glioma cell line DBTRG-05MG: growth kinetics, karyotype, receptor expression, and tumor suppressor gene analyses. In Vitro Cell Dev Biol *28A*, 609–614.
Lavoie, H., and Therrien, M. (2015). Regulation of RAF protein kinases in ERK signalling. Nat Rev Mol Cell Biol *16*, 281–298.

Le, K., Blomain, E.S., Rodeck, U., and Aplin, A.E. (2013). Selective RAF inhibitor impairs ERK1/2 phosphorylation and growth in mutant NRAS, vemurafenib-resistant melanoma cells. Pigment Cell Melanoma Res *26*, 509–517.

Lito, P., Pratilas, C.A., Joseph, E.W., Tadi, M., Halilovic, E., Zubrowski, M., Huang, A., Wong, W.L., Callahan, M.K., Merghoub, T., et al. (2012). Relief of profound feedback inhibition of mitogenic signaling by RAF inhibitors attenuates their activity in BRAFV600E melanomas. Cancer Cell *22*, 668–682.

Lito, P., Rosen, N., and Solit, D.B. (2013). Tumor adaptation and resistance to RAF inhibitors. Nat Med *19*, 1401–1409.

Mercer, K., Giblett, S., Green, S., Lloyd, D., DaRocha Dias, S., Plumb, M., Marais, R., and Pritchard, C. (2005). Expression of endogenous oncogenic V600EB-raf induces proliferation and developmental defects in mice and transformation of primary fibroblasts. Cancer Res *65*, 11493–11500.

Michaloglou, C., Vredeveld, L.C., Soengas, M.S., Denoyelle, C., Kuilman, T., van der Horst, C.M., Majoor, D.M., Shay, J.W., Mooi, W.J., and Peeper, D.S. (2005). BRAFE600-associated senescence-like cell cycle arrest of human naevi. Nature *436*, 720–724.

Miyake, E. (1979). Establishment of a human oligodendroglial cell line. Acta Neuropathol *46*, 51–55.

Montero-Conde, C., Ruiz-Llorente, S., Dominguez, J.M., Knauf, J.A., Viale, A., Sherman, E.J., Ryder, M., Ghossein, R.A., Rosen, N., and Fagin, J.A. (2013). Relief of feedback inhibition of HER3 transcription by RAF and MEK inhibitors attenuates their antitumor effects in BRAF-mutant thyroid carcinomas. Cancer Discov *3*, 520–533.

Moodie, S.A., Paris, M.J., Kolch, W., and Wolfman, A. (1994). Association of MEK1 with p21ras.GMPPNP is dependent on B-Raf. Mol Cell Biol *14*, 7153–7162.

Nakamura, A., Arita, T., Tsuchiya, S., Donelan, J., Chouitar, J., Carideo, E., Galvin, K., Okaniwa, M., Ishikawa, T., and Yoshida, S. (2013). Antitumor activity of the selective pan-RAF inhibitor TAK-632 in BRAF inhibitor-resistant melanoma. Cancer Res *73*, 7043–7055.

Naruo, K., Seko, C., Kuroshima, K., Matsutani, E., Sasada, R., Kondo, T., and Kurokawa, T. (1993). Novel secretory heparin-binding factors from human glioma cells (glia-activating factors) involved in glial cell growth. Purification and biological properties. J Biol Chem *268*, 2857–2864.

Nguyen, L.K., and Kholodenko, B.N. (2015). Feedback regulation in cell signalling: Lessons for cancer therapeutics. Semin Cell Dev Biol.

Nicolaides, T.P., Li, H., Solomon, D.A., Hariono, S., Hashizume, R., Barkovich, K., Baker, S.J., Paugh, B.S., Jones, C., Forshew, T., et al. (2011). Targeted therapy for BRAFV600E malignant astrocytoma. Clin Cancer Res *17*, 7595–7604.

Nissan, M.H., Pratilas, C.A., Jones, A.M., Ramirez, R., Won, H., Liu, C., Tiwari, S., Kong, L., Hanrahan, A.J., Yao, Z., et al. (2014). Loss of NF1 in cutaneous melanoma is associated with RAS activation and MEK dependence. Cancer Res *74*, 2340–2350.

Okudela, K., Yazawa, T., Woo, T., Sakaeda, M., Ishii, J., Mitsui, H., Shimoyamada, H., Sato, H., Tajiri, M., Ogawa, N., et al. (2009). Down-regulation of DUSP6 expression in lung cancer: its mechanism and potential role in carcinogenesis. Am J Pathol *175*, 867–881.

Patricelli, M.P., Nomanbhoy, T.K., Wu, J., Brown, H., Zhou, D., Zhang, J., Jagannathan, S., Aban, A., Okerberg, E., Herring, C., et al. (2011). In situ kinase profiling reveals functionally relevant properties of native kinases. Chem Biol *18*, 699–710.

Patton, E.E., Widlund, H.R., Kutok, J.L., Kopani, K.R., Amatruda, J.F., Murphey, R.D., Berghmans, S., Mayhall, E.A., Traver, D., Fletcher, C.D., et al. (2005). BRAF mutations are sufficient to promote nevi formation and cooperate with p53 in the genesis of melanoma. Curr Biol *15*, 249–254.

Peng, S.B., Henry, J.R., Kaufman, M.D., Lu, W.P., Smith, B.D., Vogeti, S., Rutkoski, T.J., Wise, S., Chun, L., Zhang, Y., et al. (2015). Inhibition of RAF Isoforms and Active Dimers by LY3009120 Leads to Anti-tumor Activities in RAS or BRAF Mutant Cancers. Cancer Cell *28*, 384–398.

Poulikakos, P.I., Zhang, C., Bollag, G., Shokat, K.M., and Rosen, N. (2010). RAF inhibitors transactivate RAF dimers and ERK signalling in cells with wild-type BRAF. Nature *464*, 427–430.

Poulikakos, P.I., Persaud, Y., Janakiraman, M., Kong, X., Ng, C., Moriceau, G., Shi, H., Atefi, M., Titz, B., Gabay, M.T., et al. (2011). RAF inhibitor resistance is mediated by dimerization of aberrantly spliced BRAF(V600E). Nature *480*, 387–390.

Prahallad, A., Sun, C., Huang, S., Di Nicolantonio, F., Salazar, R., Zecchin, D., Beijersbergen, R.L., Bardelli, A., and Bernards, R. (2012). Unresponsiveness of colon cancer to BRAF(V600E) inhibition through feedback activation of EGFR. Nature *483*, 100–103.

Pratilas, C.A., Taylor, B.S., Ye, Q., Viale, A., Sander, C., Solit, D.B., and Rosen, N. (2009). (V600E)BRAF is associated with disabled feedback inhibition of RAF-MEK signaling and elevated transcriptional output of the pathway. Proc Natl Acad Sci U S A 106, 4519–4524.

Straussman, R., Morikawa, T., Shee, K., Barzily-Rokni, M., Qian, Z.R., Du, J., Davis, A., Mongare, M.M., Gould, J., Frederick, D.T., et al. (2012). Tumour micro-environment elicits innate resistance to RAF inhibitors through HGF secretion. Nature *487*, 500–504.

Su, F., Viros, A., Milagre, C., Trunzer, K., Bollag, G., Spleiss, O., Reis-Filho, J.S., Kong, X., Koya, R.C., Flaherty, K.T., et al. (2012). RAS mutations in cutaneous

squamous-cell carcinomas in patients treated with BRAF inhibitors. N Engl J Med *3*66, 207–215.

Takashima, A., and Faller, D.V. (2013). Targeting the RAS oncogene. Expert Opin Ther Targets *17*, 507–531.

Tsai, J., Lee, J.T., Wang, W., Zhang, J., Cho, H., Mamo, S., Bremer, R., Gillette, S., Kong, J., Haass, N.K., et al. (2008). Discovery of a selective inhibitor of oncogenic B-Raf kinase with potent antimelanoma activity. Proc Natl Acad Sci U S A *10*5, 3041–3046.

Tuveson, D.A., Weber, B.L., and Herlyn, M. (2003). BRAF as a potential therapeutic target in melanoma and other malignancies. Cancer Cell *4*, 95–98.

Uehling, D.E., and Harris, P.A. (2015). Recent progress on MAP kinase pathway inhibitors. Bioorg Med Chem Lett *25*, 4047–4056.

Wainstein, E., and Seger, R. (2016). The dynamic subcellular localization of ERK: mechanisms of translocation and role in various organelles. Curr Opin Cell Biol *39*, 15–20.

Wan, P.T., Garnett, M.J., Roe, S.M., Lee, S., Niculescu-Duvaz, D., Good, V.M., Jones, C.M., Marshall, C.J., Springer, C.J., Barford, D., et al. (2004). Mechanism of activation of the RAF-ERK signaling pathway by oncogenic mutations of B-RAF. Cell *116*, 855–867.

Wellbrock, C., Karasarides, M., and Marais, R. (2004). The RAF proteins take centre stage. Nat Rev Mol Cell Biol *5*, 875–885.

Wilson, T.R., Fridlyand, J., Yan, Y., Penuel, E., Burton, L., Chan, E., Peng, J., Lin, E., Wang, Y., Sosman, J., et al. (2012). Widespread potential for growth-factor-driven resistance to anticancer kinase inhibitors. Nature *487*, 505–509.

Yang, H., Higgins, B., Kolinsky, K., Packman, K., Bradley, W.D., Lee, R.J., Schostack, K., Simcox, M.E., Kopetz, S., Heimbrook, D., et al. (2012). Antitumor activity of BRAF inhibitor vemurafenib in preclinical models of BRAF-mutant colorectal cancer. Cancer Res *72*, 779–789.

Yao, Z., Torres, N.M., Tao, A., Gao, Y., Luo, L., Li, Q., de Stanchina, E., Abdel-Wahab, O., Solit, D.B., Poulikakos, P.I., et al. (2015). BRAF Mutants Evade ERK-

Dependent Feedback by Different Mechanisms that Determine Their Sensitivity to Pharmacologic Inhibition. Cancer Cell *28*, 370–383.

Zhang, W., and Liu, H.T. (2002). MAPK signal pathways in the regulation of cell proliferation in mammalian cells. Cell Res *12*, 9–18.

Zhang, C., Spevak, W., Zhang, Y., Burton, E.A., Ma, Y., Habets, G., Zhang, J., Lin, J., Ewing, T., Matusow, B., et al. (2015). RAF inhibitors that evade paradoxical MAPK pathway activation. Nature *526*, 583–586.

Sosman, J.A., Kim, K.B., Schuchter, L., Gonzalez, R., Pavlick, A.C., Weber, J.S., McArthur, G.A., Hutson, T.E., Moschos, S.J., Flaherty, K.T., et al. (2012). Survival in BRAF V600-mutant advanced melanoma treated with vemurafenib. N Engl J Med *366*, 707–714.

Stanton, V.P., Nichols, D.W., Laudano, A.P., and Cooper, G.M. (1989). Definition of the human raf amino-terminal regulatory region by deletion mutagenesis. Mol Cell Biol *9*, 639–647.

Stowe, I.B., Mercado, E.L., Stowe, T.R., Bell, E.L., Oses-Prieto, J.A., Hernández, H., Burlingame, A.L., and McCormick, F. (2012). A shared molecular mechanism underlies the human rasopathies Legius syndrome and Neurofibromatosis-1. Genes Dev *26*, 1421–1426.

Straussman, R., Morikawa, T., Shee, K., Barzily-Rokni, M., Qian, Z.R., Du, J., Davis, A., Mongare, M.M., Gould, J., Frederick, D.T., et al. (2012). Tumour micro-environment elicits innate resistance to RAF inhibitors through HGF secretion. Nature *487*, 500–504.

Su, F., Viros, A., Milagre, C., Trunzer, K., Bollag, G., Spleiss, O., Reis-Filho, J.S., Kong, X., Koya, R.C., Flaherty, K.T., et al. (2012). RAS mutations in cutaneous squamous-cell carcinomas in patients treated with BRAF inhibitors. N Engl J Med *366*, 207–215.

Takashima, A., and Faller, D.V. (2013). Targeting the RAS oncogene. Expert Opin Ther Targets *17*, 507–531.

Tsai, J., Lee, J.T., Wang, W., Zhang, J., Cho, H., Mamo, S., Bremer, R., Gillette, S., Kong, J., Haass, N.K., et al. (2008). Discovery of a selective inhibitor of oncogenic B-

Raf kinase with potent antimelanoma activity. Proc Natl Acad Sci U S A *105*, 3041–3046.

Tuveson, D.A., Weber, B.L., and Herlyn, M. (2003). BRAF as a potential therapeutic target in melanoma and other malignancies. Cancer Cell *4*, 95–98.
Wainstein, E., and Seger, R. (2016). The dynamic subcellular localization of ERK: mechanisms of translocation and role in various organelles. Curr Opin Cell Biol *39*, 15–20.

Wan, P.T., Garnett, M.J., Roe, S.M., Lee, S., Niculescu-Duvaz, D., Good, V.M., Jones, C.M., Marshall, C.J., Springer, C.J., Barford, D., et al. (2004). Mechanism of activation of the RAF-ERK signaling pathway by oncogenic mutations of B-RAF. Cell *116*, 855–867.

Wellbrock, C., Karasarides, M., and Marais, R. (2004). The RAF proteins take centre stage. Nat Rev Mol Cell Biol *5*, 875–885.

Wilson, T.R., Fridlyand, J., Yan, Y., Penuel, E., Burton, L., Chan, E., Peng, J., Lin, E., Wang, Y., Sosman, J., et al. (2012). Widespread potential for growth-factor-driven resistance to anticancer kinase inhibitors. Nature *487*, 505–509.

Yang, H., Higgins, B., Kolinsky, K., Packman, K., Bradley, W.D., Lee, R.J., Schostack, K., Simcox, M.E., Kopetz, S., Heimbrook, D., et al. (2012). Antitumor activity of BRAF inhibitor vemurafenib in preclinical models of BRAF-mutant colorectal cancer. Cancer Res *72*, 779–789.

Yao, Z., Torres, N.M., Tao, A., Gao, Y., Luo, L., Li, Q., de Stanchina, E., Abdel-Wahab, O., Solit, D.B., Poulikakos, P.I., et al. (2015). BRAF Mutants Evade ERK-Dependent Feedback by Different Mechanisms that Determine Their Sensitivity to Pharmacologic Inhibition. Cancer Cell 2*8*, 370–383.

Zhang, W., and Liu, H.T. (2002). MAPK signal pathways in the regulation of cell proliferation in mammalian cells. Cell Res *12*, 9–18.